FutureWater

TA-6787 UZB: Power Sector Reform Support Program

Climate Risk and Adaptation Assessment for the Electricity Distribution Infrastructure in Uzbekistan

REPORT 254

CLIENT **Asian Development Bank**

AUTHORS **Sonu Khanal**
Tania Imran
Corjan Nolet

DATE **May 2023**

Climate Risk and Adaptation Assessment for the Electricity Distribution Infrastructure in Uzbekistan

TA-6787 UZB: Distribution Network Digital Transformation and Resiliency Project

Client
Asian Development Bank

Author
Sonu Khanal – Senior Hydrologist and Climate Change Expert (s.khanal@futurewater.nl)

Date
May 2023

How to cite
Khanal, S., Imran, T., Nolet, C. 2023. Climate Risk and Adaptation Assessment for the Electricity Distribution Infrastructure in Uzbekistan. FutureWater Report 254.

Executive Summary

The Asian Development Bank (ADB) is assisting the Government of Uzbekistan through the "Distribution Network Digital Transformation and Resiliency Project" to improve the current status of the electric grid system considering future climate change. The project will support the low-carbon transition and green economy development agenda of the country. It aims to improve the power transmission network capacity and reliability in Uzbekistan, reduce transmission and distribution losses, and increase the operational efficiency of the power sector.

To inform the project feasibility study, a Climate Risk and Adaptation (CRA) assessment is carried out to assess the climate vulnerability of the 26 substations (out of a total of 158 substations) subject to rehabilitation and modernization. A detailed CRA is conducted to assess historic trends in relevant climate-related variables and analyse climate projections in the region. Adaptation measures are identified based on this analysis that will help enhance the climate resilience of the proposed project interventions.

An analysis of the historical climate patterns and trends in the last 40 years (1981–2020) shows that the mean temperature has consistently increased by 0.04 ºC per year on average across the project locations which span over 14 provinces in Uzbekistan. Trends in precipitation showed a variable trend, as Fergana, Andizhan and Namangan provinces observed an increase of 0.37 mm/year on average where as the other regions show a decline in trends with the highest decline observed in the Karakalpakstan and Khorezem regions (-0.82 mm/year).

Similarly, a state-of-the-art downscaled multi-model ensemble (CMIP6-NASA-NEX) was used to analyze future climate projections under 2 SSP emissions scenarios and 3 future time horizons (2030, 2050 and 2070). Future trends in precipitation and temperature were obtained and analyzed to identify potential climate risks in the country. All climate models predicted a warmer future across the project locations, with most of the models predicting an increase of more than 4ºC for the 2070 horizon. For precipitation, all the models were not in agreement as most projected a slightly wet condition in the future where as some projected a drier future. For SSP2-45 and the short-term horizon, precipitation will increase to about 3–9% whereas 5–11% and 4–13% for the medium and long-term horizons. On the other hand, the precipitation will increase to about 2–7%, 5–12%, and 7–17% for the SSP5-85 scenario for the short, medium and long-term horizons.

In terms of seasonality, the climate model ensemble projects a general consistent increase in mean temperatures for all months for all project locations. A greater increase in temperatures is predicted in the long-term future horizon and under the higher SSP 5 scenario. The GCM ensemble results show an increase in precipitation, especially in the winter season from October-May for all locations. On the other hand, the summer months (June-September) precipitation decreases in the future compared to the reference for all the time horizons and scenarios by 7%.

An analysis of the climate extreme indices indicates that the climate will be more extreme in the future for the project locations. While the extreme temperature changes remain fairly similar, the changes in the number of continuous dry days in the future are comparatively higher in magnitude in the Fergana, Andizhan and Namangan provinces. This may have serious implications for the heat wave and drought hazards in the future. The annual maximum 1-day precipitation is expected to increase by more than 50% for SSP2 and double for SSP5 by the end of century. The increase in occurrence and magnitude of such extreme events in the future may increase the likelihood of hazards, for instance erosion, floods, and sedimentation.

Next, the potential impacts were assessed to categorize relevant climate risks and identify priorities for adaptation. Through a combination of literature-based information, quantitative analysis, and expert judgement, the extent to which the key climate risks pose a threat to the project were assessed. Floods were identified as a medium to high climate risk in the project locations, exposing the electric grid infrastructure to erosion, short-circuits and subsequent blackouts. Similarly, heatwaves and droughts were also classified as high climate risks, potentially causing higher losses through the transmission lines and extensive dust damage. With respect to dust storms and wind erosion, most of the project locations are at a medium risk and may suffer from structural instability in case of an extreme event. The risk of landslides and mudflows in the region were also analyzed and classified as medium, except in the eastern and southern parts of the country which are mountainous and hence at a higher risk. Given the increasing mean temperatures, wildfire was also investigated as a potential risk; however, the risk remains low in the project locations.

Based on the potential impacts, adaptation options were presented for each climate risk. The adaptation measures comprise of both engineering and non-engineering interventions. Among others, installation of monitoring systems such as supervisory control and data acquisition (SCADA) can significantly improve transmission operation reliability. Similarly, capacity building of the authority managing the regional electric grid (JSC REPN) can lead to effective management of risks and recovery. An analysis of the existing hydrometeorological network, covering the project locations, was also conducted which revealed that there is a dire need to install additional monitoring stations, particularly in the mountainous regions, for improved surveillance and development of data-driven adaptation interventions.

Lastly, a GHG account was drawn to determine the project's contribution towards assisting Uzbekistan actualize its second Nationally Determined Contribution (NDC) agenda which seeks to reduce its GHG emissions per unit of GDP by 35% (compared to the level in 2010), by the year 2030. The reduction in greenhouse gas emissions was estimated as 17,757 tCO_2e/year since the modernization of 26 substations would lead to energy savings of 33,316 MWh per year.

Content

Tables

Figures

1 Introduction

1.1 Background

Uzbekistan is not only the most populous country in Central Asia but also the fastest-growing economy in the region. The economy has sustained a high growth rate, with a reported GDP of 7.4% for the year 2021[1]. Such rapid socioeconomic development calls for adequate, uninterrupted, and reliable power supply. However, with over 1,850 km of 500kV lines, 6,200 km of 220kV lines and 15,300 km of 110kV lines, the power transmission system in Uzbekistan is currently facing challenges with respect to deteriorating infrastructure and power outages. Earlier this summer, the country suffered from occasional blackouts owing to high temperatures and increased demand. The power transmission grids, particularly those subject to direct sunlight, were adversely affected and to reduce the pressure on the national gird, the trains had been running slow on two lines of the Tashkent metro[2]. The impacts of climate change are growing fast in the region; with water scarcity, heat waves and increased number of high heat days (max temperature >39°C) becoming more frequent and intense[3].

To improve the national electric grid system of Uzbekistan, a joint-stock company (JSC) was established in March 2019 to further develop and reform the existing network system. The JSC-National Electric Grid Uzbekistan (JSC NEGU) falls under the jurisdiction of the Ministry of Energy and is responsible for the operation and development of the main electrical networks (as shown in Figure 1), as well as implementation and cooperation with internal and external electric power systems. At the moment, it consists of 14 regional backbone electric networks, 84 substations of 220-500 kV, a central relay protection, automatic service and functional branches[4].

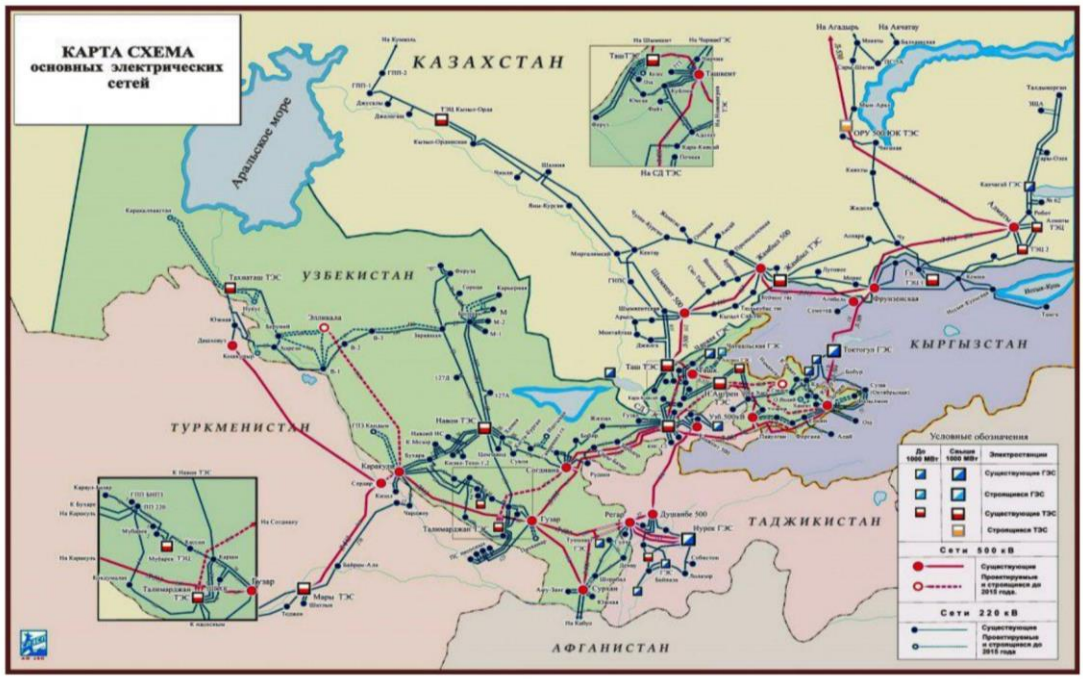

Figure 1. Map of main electrical network (Source: JSC NEGU).

[1] http://wdi.worldbank.org/table/WV.1
[2] https://eurasianet.org/uzbekistan-electricity-grid-strained-by-heat
[3] https://climateknowledgeportal.worldbank.org/country/uzbekistan/climate-data-projections
[4] https://www.uzbekistonmet.uz/en/lists/view/79

The power transmission network was mainly developed in the Soviet era, making the existing transmission lines and substations 30-50 years old. Replacement of any protection and monitoring equipment for the substations is a challenge since spare parts are no longer available. This has resulted in increased power outages, losses, and failure to meet the energy requirements. Compromised substations also impede the process of acquiring and delivering power from renewable power plants. In addition to a fragile and an aging electric grid infrastructure, operational management practices are also obsolete. Hourly records measuring the load of transformers and transmission lines are maintained manually using analog instruments, thus making the process as well as the resulting database extremely vulnerable to errors and losses. Lack of use of modern technology makes the process of fault detection and repair time intensive.

In addition to a weakening power transmission network, Uzbekistan's energy sector is also currently struggling with a surge in electricity demands owing to the rapidly growing population. It is reported that since mid-half of 2010, the demand has grown by 4-5% per annum and will increase by 6-7% per annum till 2030. With a target to increase the gross domestic product from $70 billion in 2021 to $160 billion by 2030, the Government of Uzbekistan is taking steps to ensure that it will be able to meet the spike in electricity demand which is expected to double by 2030. Initiatives include installing an additional 17 gigawatts capacity to the existing available capacity of 12.9 GW, out of which 8 GW will be from renewable energy projects. Currently, the distribution system in Uzbekistan comprises of more than 260,000 kilometers of 0.4-110 kV networks, 1,655 substations and more than 86,000 transformer points. However, more than 50% of the lines have been operational for 30 years and 30% of the substation transformers are in dire need of rehabilitation[1].

Therefore, there is an urgent need to upgrade the existing transmission infrastructure to fulfil the energy demands and ensure steady socioeconomic development in the country. Moreover, increased efficiency will lead to reduced carbon emissions and help Uzbekistan actualize its second Nationally Determined Contribution (NDC) agenda which seeks to reduce greenhouse gas emissions per unit of GDP by 35% (compared to the level in 2010), by the year 2030.

1.2 Project description

Considering the current status of the electric grid system, the growing energy demands and the increasing impacts of climate change, the Asian Development Bank (ADB) is assisting the Government of Uzbekistan through the "Distribution Network Digital Transformation and Resiliency" project. The project aims to rehabilitate medium voltage distribution substations and associated overhead lines along with modernizing the distribution system operations. With an overall goal to strengthen and enhance the existing capacity of the power transmission and distribution system, ADB is closely working with the Joint Stock Company Regional Electric Power Networks (JSC REPN) to:

- **Output 1:** Rehabilitate and modernize 158 distribution substations of 35 kV to 110kV through replacing old transformers, cables, switchgears and control systems. This also includes installing the modern disbution supervisory control and data acquisition (SCADA) system and distribution automation systems to digitalize the network operations, and developing a long-term road map for digitalization and smart grid.

- **Output 2:** Rehabilitate associated distribution lines which extend over 750 kilometers. To reduce variation and ensure better asset management, the cable sizes will be standardized and the voltage will be upgraded. Certified materials fit for higher temperatures and effective cooling

[1] Concept Paper: Distribution Network Digital Transformation and Resiliency Project, September 2022, Asian Development Bank.

systems will be installed. Improvement of waste management practices and occupational health and safety is also a key outcome to help elevate corporate standards to international levels.

- **Output 3**: Enhance the institutional capacity of JSC REPN for financial sustainability and climate resiliency. This includes introducing modern simulation software to conduct load flow analysis, development and adoption of distribution codes, and building knowledge partnership programs to foster sector experts in system planning.

The scope of the project also aligns with ADB's country partnership strategy for Uzbekistan (2019-2023) as well as its internal 2030 strategy which aims to alleviate poverty and inequalities, tackle climate change, build climate and disaster resilience, enhance environmental sustainability, and strengthen institutional capacity.

For the first phase, 26 substations (out of a total of 158 substations) will be subjected to rehabilitation. The distribution and modernization parameters for these substations are shown in Figure 2 and Table 1, respectively.

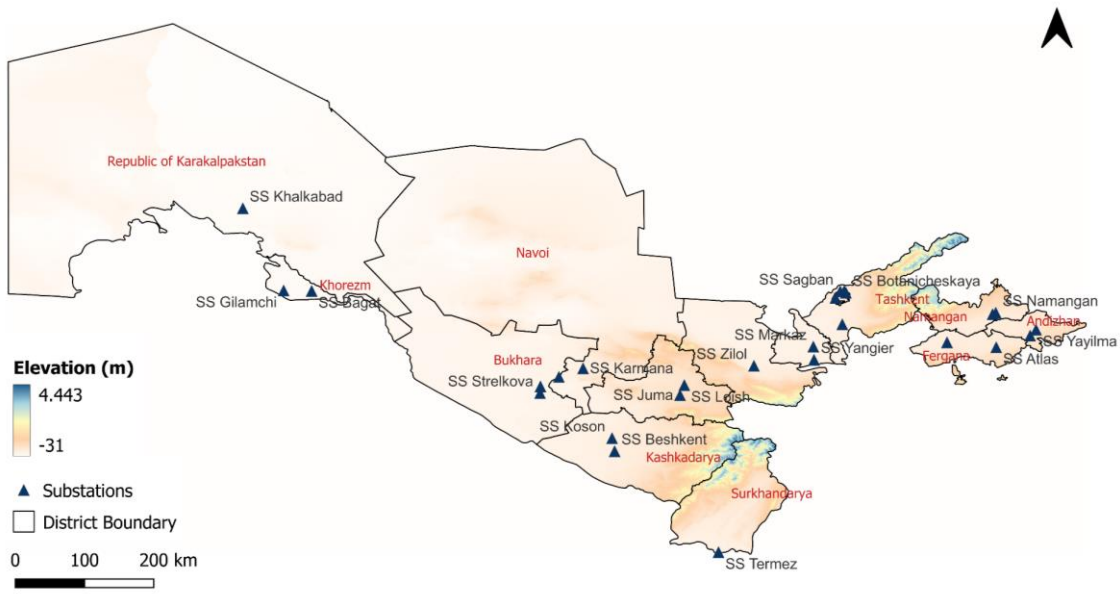

Figure 2. Target substations subject to improvements as part of the " Distribution Network Digital Transformation and Resiliency Project" by ADB.

Table 1. Specifications of substations subject to improvements.

No.	Substation	Region	Main modernization parameters
1	SS Yangier	Sirdarya	Full, 110/35/10kV, 32 MVA to 80 MVA
2	SS Galaosiyo	Bukhara	Full, 110/35/10kV, 20 MVA to 50 MVA
3	SS Strelkova	Bukhara	Full, 110/35/10kV, 126 MVA to 160 MVA
4	SS Sagban	Tashkent	Full, 110/35/10kV, 50 MVA to 126 MVA
5	SS Dungkurgon	Tashkent	Full, 110/35/6kV, 80 MVA to 126 MVA
6	SS Charkhi	Fergana	Full, 110/6/6kV, 41 MVA to 80 MVA
7	SS Khalkabad	Karakalpakstan	Full, 110/35/10kV, 20 MVA to 32 MVA
8	SS Namangan	Namangan	Full, 110/35/6kV, 31 MVA to 126 MVA
9	SS Malikchul	Navoi	Full, 110/35/10kV, 32 MVA to 50 MVA

10	SS Beshkent	Kashkadarya	Full, 110/35/10kV, 20 MVA to 50 MVA
11	SS Vokzal	Namangan	Full, 110/6kV, 32 MVA to 80 MVA
12	SS Yunusabad	Tashkent	Full, 110/35/10kV, 80 MVA to 126 MVA
13	SS Zilol	Dzhizak	Full, 110/35/10kV, 8 MVA to 32 MVA
14	SS Atlas	Fergana	Full, 110/35/6kV, 32 MVA to 126 MVA
15	SS Yayilma	Andizhan	Full, 110/35/6kV, 51.5 MVA to 126 MVA
16	SS Botanicheskaya	Tashkent	Full, 110/35/6kV, 103 MVA to 126 MVA
17	SS Koson	Kashkadarya	Full, 110/35/10kV, 26 MVA to 80 MVA
18	SS Markaz	Sirdarya	Full, 110/35/10kV, 41 MVA to 80 MVA
19	SS Juma	Samarkand	Full, 110/35/10kV, 32 MVA to 80 MVA
20	SS Gilamchi	Khorezm	Full, 110/10kV, 20 MVA to 32 MVA
21	SS Loish	Samarkand	Full, 110/35/10kV, 32 MVA to 80 MVA
22	SS Bagat	Khorezm	Full, 110/35/10kV, 32 MVA to 80 MVA
23	SS Termez	Surkhandarya	Partial, 110/35/6kV, add. 40 MVA, bays
24	SS Asaka	Andizhan	Full, 110/35/6kV, 30 MVA to 80 MVA
25	SS Eshonguzaar	Tashkent	Full, 35/6kV, 26.3 MVA to 50 MVA
26	SS Karmana	Navoi	Full, 110/35/10kV, 20 MVA to 32 MVA

To enhance the climate resilience of the electric grid infrastructure and inform the project design, a detailed climate risk and adaptation assessment (CRA) is performed. Insights from the CRA will be used to devise adaptation strategies and costs to promote climate financing. Through this project, ADB will be supporting Uzbekistan's Green Economy Transition Program and the revised Nationally Determined Contributions by investing in climate mitigation and adaptation measures. Moreover, an efficient and modern power transmission infrastructure will also serve as an incentive for the private sector involved in harnessing renewable energy resources to increase their production and subsequent supply to the national electric grid of Uzbekistan.

1.3 Scope of work

The project aims to modernize the current power transmission and distribution infrastructure and strengthen the institutional capacity of JSC REPN to efficiently operate the network. In addition to addressing the fragility of the substations, their limited capacities with respect to the growing demand, and associated power losses, the project also accounts for the current and future impacts of climate change on the substations.

To ensure that the proposed project interventions are climate resilient, an in-depth assessment of climate risks is needed. A detailed climate risk and adaptation assessment (CRA) is carried out to identify and quantify the risks posed by climate change. Downscaled Coupled Model Intercomparison Project Phase 6 (CMIP6) ensembles will be used, along with other relevant hazards and local information, to develop the CRA. The results from this CRA will be used to identify adaptation measures and provide initial cost estimations to promote climate financing in the energy sector. The existing meteorological monitoring network is reviewed as part of the assignment, so the project can potentially integrate a component that aims at improving the monitoring and surveillance in the project areas.

Lastly, the reduction in GHG emissions from the upgraded transmission lines and substations are quantified to secure climate financing and highlight the potential impact of the project with respect to Uzbekistan's revised NDC ambition.

2 Methodology

2.1 Climate risk assessment guidelines

Since 2014, ADB requires that all investment projects consider climate and disaster risk and incorporate adaptation measures to make the projects more climate resilient. This is consistent with ADB's commitment to scale up support for adaptation and climate resilience in project design and implementation, articulated in the Midterm Review of Strategy 2020: Meeting the Challenges of a Transforming Asia and Pacific (ADB, 2014a), in the Climate Change Operational Framework 2017–2030: Enhancing Actions for Low Greenhouse Gas Emissions and Climate-Resilient Development (ADB, 2017), and in the Climate Risk Management in ADB Projects guidelines (2014).

Climate risk management (CRM) is a mandatory part of project development. Climate risk screening is applied to all ADB investments, with a more detailed assessment undertaken for projects that are assessed to be at medium or high risk. The principal objective of a Climate Risk and Adaptation (CRA) assessment is to identify those components of the project that may be at risk of failure, damage and/or deterioration, reduction, interruption, and/or decreased reliability of service delivery from natural hazards, extreme climatic events or significant changes to baseline climate design values (ADB, 2011, 2014 and 2017). Adaptation measures consistent with the risk assessment serve to improve the resilience of the infrastructure to the impacts of climate change and geo-physical hazards, to protect communities, and provide a safeguard so that infrastructure services are available when they are needed most (Figure 3). As part of this process, the nature and relative levels of risk are evaluated and determined to establish appropriate actions for each proposed investment to help minimize climate change-associated risk.

Earlier the terminology "Climate Risk and Vulnerability Assessment (CRVA)" was used. However, since vulnerability is part of the risk, ADB now recommends using the term "Climate Risk and Adaptation Assessment (CRA)". The CRA process embodies the recognition that many of the future impacts of climate change are fundamentally uncertain and that project risk management procedures must be robust to a range of uncertainty. The CRA, therefore, includes a technical and economic appraisal of adaptation options for the project design.

ADB has developed specific guidelines regarding CRAs. These guidelines mentioned that the main characteristics of a CRA are (i) to characterize climate risks to a project by identifying both the nature and likely magnitude of climate change impacts on the project, and the specific features of the project that make it vulnerable to these impacts. (ii) To identify the underlying causes of a system's vulnerability to climate change, and (iii) to ensure that adaptation measures are locally beneficial, sustainable, and economically efficient.

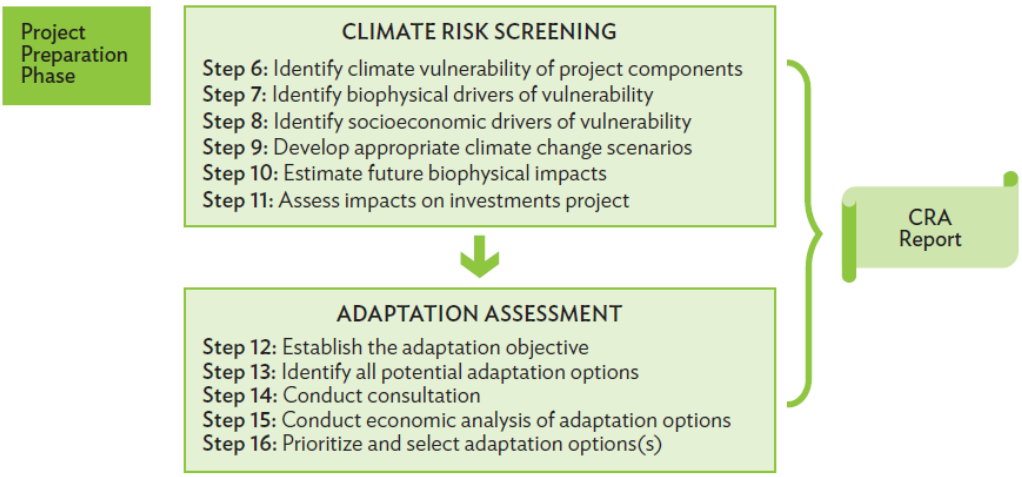

Figure 3. Climate Risk and Adaptation Assessment components (Source: ADB, 2015).

CRAs use a variety of definitions relating to risk and climate change. In this study the following definitions are used (adapted from IPCC, 2014):

- **Hazard:** A process, phenomenon or human activity that may cause loss of life, injury or other health impacts, property damage, social and economic disruption or environmental degradation[1]
- **Exposure:** The presence of people, livelihoods, species or ecosystems, environmental functions, services, and resources, infrastructure, or economic, social, or cultural assets in places and settings that could be adversely affected by climate change and variability.
- **Sensitivity:** The degree to which a system, asset, or species may be affected, either adversely or beneficially, when exposed to climate change and variability.
- **Potential impact:** The potential effects of hazards on human or natural assets and systems. These potential effects, which are determined by both exposure and sensitivity, may be beneficial or harmful.
- **Adaptive capacity:** The ability of systems, institutions, humans, and other organisms to adjust to potential damage, to take advantage of opportunities, or to respond to consequences of hazards.
- **Vulnerability:** The extent to which a system is susceptible to, or unable to cope with, adverse effects of climate change, including climate variability and extremes. It depends not only on a system's exposure and sensitivity but also on its adaptive capacity.
- **Likelihood:** A general concept relating to the chance of an event occurring. Generally expressed as a probability or frequency.
- **Confidence:** A general concept relating to the agreement among the different data and model sources, and the available evidence.
- **Risk:** A combination of the chance or probability of an event occurring, and the impact or consequence associated with that event if it occurs.

The risks originating from climate hazards to individual project activities or outputs can be derived based on the AR6 IPCC risk framework formulation, which considers risk as a combination of hazard (H), exposure (E), and vulnerability (V):

$$R = f(H, E, V)$$

Vulnerability, as earlier defined in the definitions, is a combination of the sensitivity of a project activity to a climate hazard, and the adaptative capacity of the activity (or the project or project context as a

[1] United Nations General Assembly. 2016. Report of the open-ended intergovernmental expert working group on indicators and terminology relating to disaster risk reduction. New York.

whole). Climate risk scores can be calculated quantitatively in case accurate spatial data is available on these risk components. While quantitative hazard data is typically available (for historic conditions based on observations, for future conditions based on model projections), data on sensitivity and adaptive capacity is often more qualitative. In that case, an expert-based judgement on the risk score for the project activities is recommendable.

For this CRA, the risk inputs (exposure to hazard, vulnerability) and the outputs (risk) are classified using a simple qualitative rating scheme comprising four classes, as shown in Table 2.

Table 2. Qualitative classes used to rank hazard.

Classes	Rating	Colour
No data	0	
Low	1	
Moderate	2	
High	3	

2.2 Approach to CRA

The approach towards the development of the CRA is described in this section, while the specific details regarding methodologies and results are presented in the subsequent chapters. Overall, the CRA will consist of the following steps:

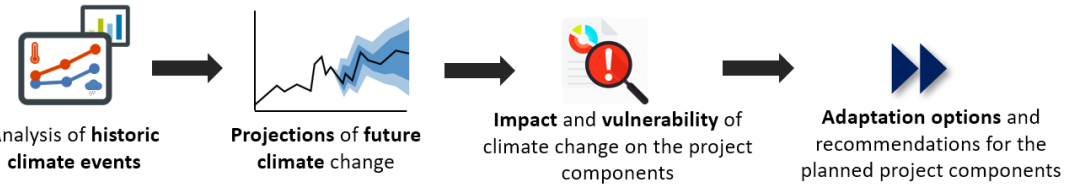

Figure 4. Steps to develop a climate risk and adaptation assessment.

2.2.1 Analysis of historic climate events

A credible and acceptable CRA assessment starts with analyzing historic observations of climate-related events and performing trend analysis. Obviously, trends, or the absence of trends, do not imply that future changes will follow those historic trends. Any statistical trend analysis should be accompanied by an understanding of the underlying physical processes. Analysis of historic climate events should go beyond looking at weather parameters (e.g., temperature and precipitation) and should include parameters that might have been influenced by historic weather conditions. Given the climate risks and vulnerabilities associated to components of the energy sector in general and specific to this project (energy transmission in the desert and mountains), the following long-term climate change processes and hazards were prioritized:

1. Extreme precipitation, related to extreme runoff and flooding events including flash floods, and landslide, erosion.
2. Extreme temperature, related to wildfires, snow and glacier melt runoff floods.
3. Drought hazards
4. Heatwave hazards
5. Wind-related hazards

Climate change-related hazards which are not included as they are not considered relevant for the project area are: cyclonic activities, sea level rise, and are not included in this report as the risk level is insignificant for the scope of this report[1].

2.2.2 Projections of future climates

Projections of future climates are provided by GCMs (Global Circulation Models). An important source of the climate projections to date is the results from the Coupled Model Intercomparison Project Phase 6 (CMIP) activities. CMIP6 has led to a standard set of model simulations and a (more or less) uniform output. Since the downscaling and local adjustment of GCMs are needed, NASA has developed the so-called NEX-GDDP (NASA Earth Exchange Global Daily Downscaled Projections) (Thrasher et al., 2022). The dataset is provided to assist in conducting studies of climate change impacts at local to regional scales and to enhance public understanding of possible future global climate patterns at the spatial scale of individual towns, cities, and watersheds.

The NASA-NEX-GDDP consists of 35 GCM outputs for two SSPs (2 and 5) for a historic period (1950-2014) and the future (2015-2100). For the CRA these data are used for two purposes. First, the projections are analyzed using a set of indicators ranging from more direct ones (e.g., change in temperature) to more meaningful integrated and advanced indicators (e.g., monthly maximum consecutive 5-day precipitation). Second, the NASA-NEX-GDDP is used in the bottom-up approach of the impact and vulnerability assessment. As described later in this report, the projections of future climate vary strongly per climate model, forming one important dimension of future climate uncertainty. It is key to consider this uncertainty by including an ensemble of climate models in the analysis. Based on the range (uncertainty) in the projections, a confidence threshold can be used to benchmark infrastructural developments in the context of future climate change. A similar approach was used in the 'Digitize to Decarbonize – Power Transmission Grid Enhancement' project in Uzbekistan[2].

2.2.3 Impact and vulnerability of climate change

A standardized approach to climate change impact and vulnerability assessment does not exist. There is however a clear trend in CRAs to move from climate projections (GCM) focus to a vulnerability-oriented approach. This change started by the often-non-consistent projections of GCMs (especially in precipitation) and at the same time the desire to put stakeholders' perspectives back into the analysis. This distinction between climate scenario-driven impact assessment approaches is often referred to as "top-down", while the vulnerability-oriented approach is referred to as "bottom-up." The ADB guidelines are less restrictive and recognize that both approaches are complementary and can even be conducted in parallel. In this CRA we combine the approaches and present the full scope of possible futures in terms of climate change, but for the final chapters on vulnerability and adaptation options, we take the perspective from the project design to come up with actionable recommendations.

2.2.4 Adaptation options and recommendations for design

The identification of adaptation options requires the consideration of project specifics and needs, project socio-economic context, and should cover both "hard" measures, for example modifications in the design that make an infrastructure less sensitive to a hazard, or "soft" measures, which relate to capacity building, institutional strengthening, etc. Estimates of the adaptation cost need to be provided, which can be done in relative terms if the project is yet in a concept phase, and in absolute terms if the project is in a feasibility or design phase.

[1] https://thinkhazard.org/en/report/261-uzbekistan/CY
[2] Khanal, S., Imran, T., Nolet, C., 2023. Climate Risk and Adaptation Assessment for Digitize to Decarbonize – Power Transmission Grid Enhancement Project – Uzbekistan. FutureWater Report 243

For this project, some potential climate adaptation options are outlined. These options are based on the detailed risk assessment and the information so far available on the project. When the project is further designed, a more specific list of recommendations for adaptation can be prepared.

ADB has developed some specific guidelines regarding CRAs that are used as source:

- Climate risk management in ADB projects (ADB, 2014)
- Climate Risk and Adaptation in the Electric Power Sector (ADB, 2012)
- Guidelines for Climate Proofing Investment in the Energy Sector (ADB, 2013)
- Guidelines for Climate Proofing Investment in the Transport Sector: Road Infrastructure Projects
- Guidelines for Climate Proofing Investment in the Water Sector: Water Supply and Sanitation (ADB, 2016)

3 Historic Climate Trends

The first step in developing a detailed Climate Risk and Adaptation assessment (CRA) is to analyze historic observations of climate and to perform trend analyses. This can reveal whether trends in climate variables can already be observed based on historic data. Trends, or the absence of trends, do not imply that future changes will follow historic patterns. Any statistical trend analysis should be accompanied by an understanding of the underlying physical processes and future projections using GCMs.

3.1 Dataset used

Reanalysis of past weather (model) data provides a clear picture of past weather. Through a variety of methods of observations from various instruments (in situ, remote sensing, models) are assimilated onto a regularly spaced grid of data. Placing all instrument observations onto a regularly spaced grid makes comparing the actual observations with other gridded datasets easier. In addition to putting observations onto a grid, reanalysis also holds the gridding model constant keeping the historical record uninfluenced by artificial factors. Reanalysis helps ensure a level playing field for all instruments throughout the historical record.

ERA5 Reanalysis Data

ERA5 is the fifth generation European Centre for Medium-Range Weather Forecasts (ECMWF) reanalysis for the global climate and weather for the past 4 to 7 decades. Currently data is available from 1950 until near-present. Reanalysis combines observations from different sources into globally complete fields using the laws of physics with the method of data assimilation (4D-Var in the case of ERA5). ERA5 provides hourly estimates for many atmospheric, ocean-wave and land-surface quantities and fluxes.

ERA5-land is a reanalysis dataset at an enhanced resolution compared to ERA5. ERA5-land has been produced by replaying the land component of the ECMWF ERA5 climate reanalysis. Currently data is available from 1981 until near-present. Reanalysis combines model data with observations from across the world into a globally complete and consistent dataset using the laws of physics. Reanalysis produces data that goes several decades back in time, providing a uniform and accurate description of the climate of the past.

Source: ECMWF

To this end, the ERA5-land reanalysis product from the ECMWF is used to analyze historical trends in temperature and precipitation, and derived indicators, for the project area. This product is used as it provides a global, spatially gridded time series of several climate variables at resolutions of 9km and sub-daily (3hr) timescales. The dataset is fully operational (updated every month) and runs from 1981 to the near present. From this dataset, spatially averaged time series of precipitation and temperature are extracted for the project area at daily, weekly, and yearly timescales for the entire period that the dataset covers. This allows the analysis of annual and seasonal trends in historical climate alongside extremes.

To understand the historical climate patterns and trends, the project infrastructure is clustered into 5 regions (see Figure 5 and Table 3). Since Uzbekistan has a high variability in climate conditions, we chose to use 5 boxes rather than the whole country for the historical climate patterns. The historical data is aggregated for the region covered by the boxes and analyzed in the following sections. In order to avoid repetitiveness, the main report only displays trends and patterns for the 'FerAndNam' box. Nevertheless, the report still discusses these trends and patterns if they differ from one another. Plots for the remaining boxes are provided in the annex of the main report.

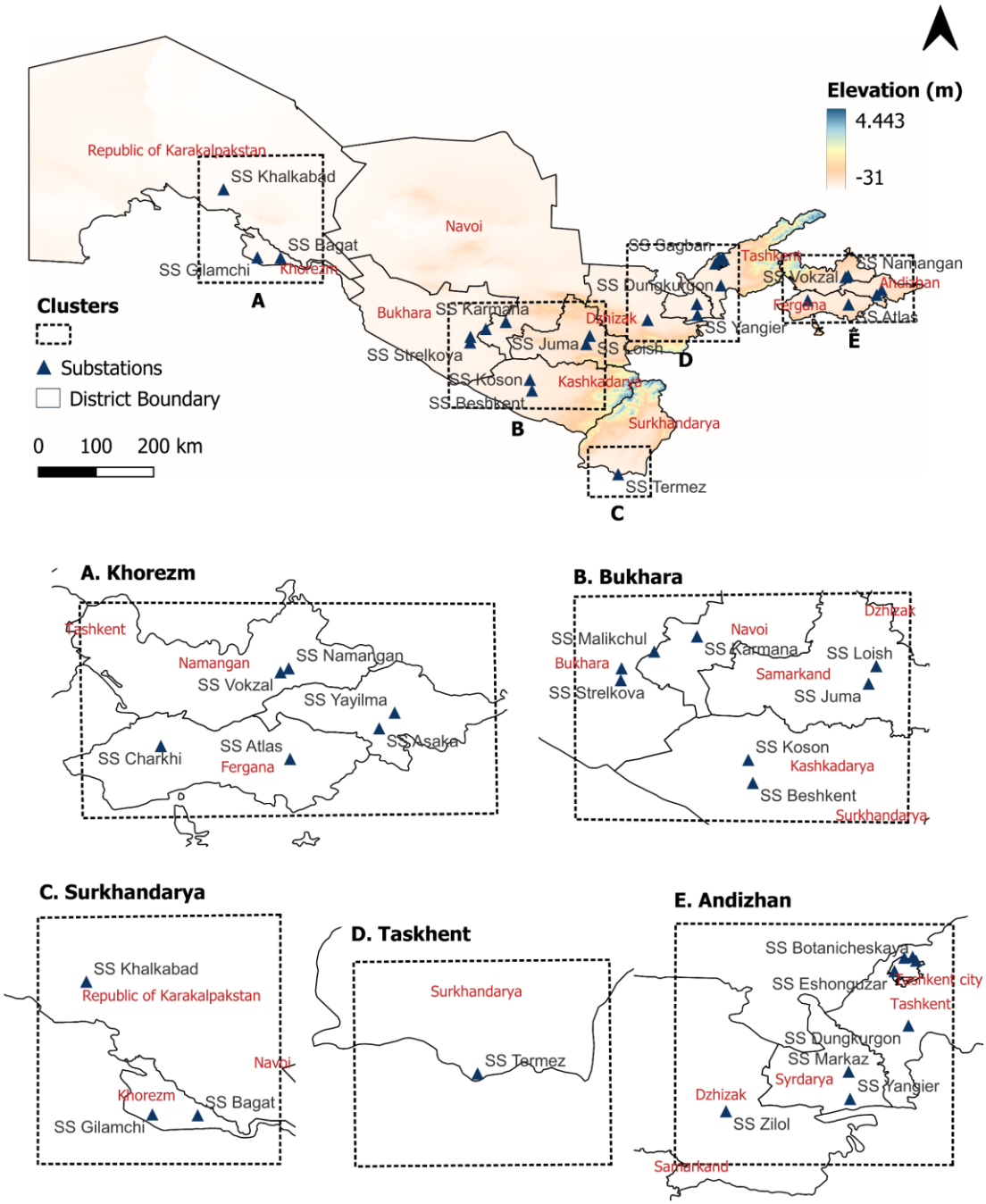

Figure 5. The distribution of the substations and the climate extraction clusters.

Table 3. Description of the boxes and the project components.

Name ID of the boxes	Regions	Project components
FerAndNam	Fergana, Andizhan Namangan	SS Yayilma (Andizhan) SS Asaka (Andizhan) SS Charkhi (Fergana) SS Atlas (Fergana)

		SS Namangan (Namangan) SS Vokzal (Namangan)
TasSyrDhz	Tashkent Syrdarya Dzhizak	SS Eshonguzar (Tashkent) SS Sagban (Tashkent) SS Botanicheskaya (Tashkent) SS Yunusabad (Tashkent) SS Dungkurgon (Tashkent) SS Yangier (Syrdarya) SS Markaz (Syrdarya) SS Zilol (Dzhizak)
Sur	Surkhandarya	SS Termez (Surkhandarya)
BukSamKas	Bukhara, Samarkand, Kashkadarya, Navoi	SS Strelkova (Bukhara) SS Galaosiyo (Bukhara) SS Malikchul (Bukhara) SS Karmana (Navoi) SS Loish (Samarkand) SS Juma (Samarkand) SS Beshkent (Kashkadarya) SS Koson (Kashkadarya)
KarKho	Karakalpakstan Khorezm	SS Khalkabad (Karakalpakstan) SS Bagat (Khorezm) SS Gilamchi (Khorezm)

Note: - The climate extraction cluster names are based on the first three characters of the region names that are covered by each cluster. The BukSamKas cluster also covers 1 substation located in Navoi (SS Karmana).

3.2 Analysis

3.2.1 Climate summary

The physical environment of Uzbekistan is diverse, ranging from the flat, desert topography that comprises almost 80% of the country's territory to mountain peaks in the east reaching about 4,500 meters above sea level. Uzbekistan has a generally arid and continental dry climate with long, warm-to-hot summers and moderate to cold winters. The country is prone to large fluctuations in temperature, both seasonally and from day to day (WB & ADB, 2020).

The country can be broadly divided into two climatic zones: (a) a desert and steppe climate in the western two-thirds of the country and (b) a temperate climate characterized by dry summers and humid winters in the eastern areas. The desert plains, which includes the province of Bukhara, receive only around 80-200 millimeters (mm) of precipitation annually, while the foothills (Samarkand province) can get as much as 300-400 mm, and mountainous regions up to 600-800 mm per year (Figure 6). Due to these prevailing climate conditions, agricultural output is almost fully dependent on irrigation. The main sources of water are transboundary rivers; Amu Darya and Syr Darya.

Uzbekistan receives 52% of the total water available in the region, 92% of which is consumed by the agricultural sector (FutureWater, 2020). Rainfall occurs mostly in late autumn through early spring, dropping off significantly during the summer months. The average monthly temperature for the country is highest in July, at 27°C, and lowest in January, at -3°C. However, temperature ranges vary across the country (Figure 6). Western areas of the country experience relatively colder winter temperatures, whereas temperatures are highest in the south, near the borders of Turkmenistan and Afghanistan (WB

& ADB, 2020). Uzbekistan's desert regions can reach maximum temperatures of 45 – 49°C, while minimum temperatures in the southern parts of the country can drop as low as -25°C.

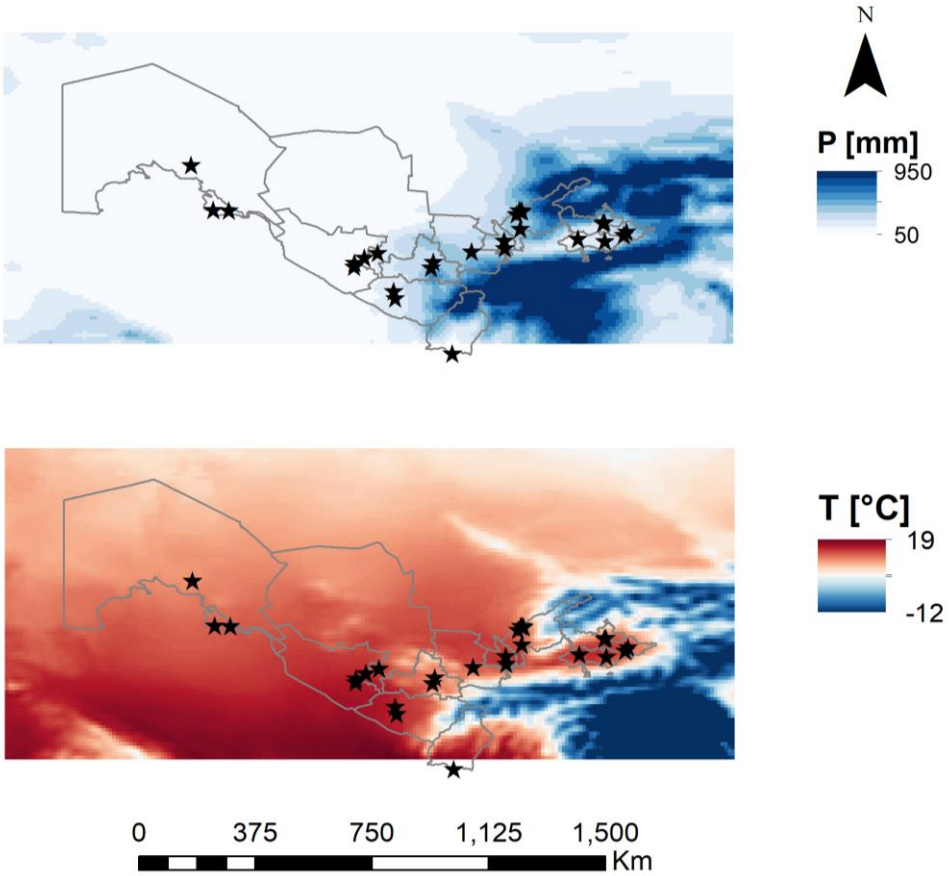

Figure 6. Mean annual precipitation (top) and temperature (bottom) for 1981–2020 across Uzbekistan (Source: own elaboration based on ERA5 dataset).

3.2.2 Temperature and precipitation trends

Historical temperature shows that the average annual temperature is lowest (11.9°C) for box FerAndNam which includes parts of eastern regions such as Andizhan, Fergana, and Namangan, and highest (18.5°C) for box Sur, which covers the lower elevation floodplain of the Amu Darya river around the city of Termez in Surkhandarya province (see Figure 7 and Figure A1 to Figure A4). Extreme variations in temperature are evident as average daily temperatures range from around -16 to 33 ºC for box FerAndNam, -17 to 35 ºC for box TasSyrDhz, -14 to 38 ºC for box Sur, -16 to 37 ºC for box BukSamKas and -20 to 39ºC for box KarKho over 1981–2020. Analysis of temperature data shows that the mean temperature has increased approximately to about 1.2 ºC for box FerAndNam, 1.6 ºC for box Sur, BukSamKas, and KarKho, and 2 ºC for box TasSyrDhz in 40 years in the period 1981–2020 (see Figure 7 and Figure A1 to Figure A4). This supports the fact that the temperature extremes have increased in recent years and may have significant impacts on energy loss from the distribution network.

Historical ERA5 precipitation reveals that the average total annual precipitation exhibits spatial and temporal variability. Western regions receive less than 100 millimeters (mm) of precipitation per year, whereas parts of the east and south-east around the high mountains forming part of the Tien-Shan and Gissar-Alai Ranges can receive up to 800–900 mm per year (Figure 6). The annual average precipitation ranges from 475–800 mm (mean around 603 mm) for box FerAndNam, 330–660 mm (mean around 458

mm) for box TasSyrDhz, 115–330 mm (mean around 215 mm) for box Sur,190–430 mm (mean around 308 mm) for box BukSamKas, and 65–205 mm (mean around 113 mm) for box KarKho (Figure 8 and Figure A5 to Figure A7). The precipitation consistently decreases in all the regions except for the FerAndNam box where it increases at the rate of +0.37 mm per year. The 10-daily maximum cumulative precipitation for individual years, which is an indicator of extreme precipitation, indicates a weak increasing trend of +0.19 mm per year (Figure 8 and
Figure A5 to Figure A7). As shown in Figure 8, Mann Kendall Tau value indicates the strength of the monotonic trend of increase or decrease in a time series, with a value of 1 indicating a strong significant trend and -1 indicating no trend. The 10-day maximum cumulative precipitation is increasing for all the boxes except the box KarKho. This is mainly attributed to the unprecedented high precipitation in the year 1981 which dominates the trend calculation.

There is a large annual precipitation variability in the region. However, the exact figures may have some uncertainty due to possible biases in the precipitation data of ERA5 compared to stations over High Mountain Asia (Khanal et al., 2021). The true amounts of precipitation over the High Mountains of Asia are highly uncertain in general (Immerzeel et al., 2015). Rain gauges are usually situated in the valleys because of accessibility, whereas most of the precipitation falls at high altitudes due to orographic effects. Besides, precipitation gauges usually under catch snowfall. Remote sensing precipitation products on the other hand underestimate snowfalls. Work analyzing glacier mass balances and observed discharge in the upper Indus in the western Himalayas and Karakoram indicates that station-based precipitation products may underestimate the total amount of precipitation by up to 50% (Immerzeel et al., 2015; Immerzeel et al., 2012). The use of a numerical weather model-based reanalysis product, like ERA5, which takes the orographic effect into account, could provide a better alternative (Khanal et al., 2023).

Again, the boxes show variable signs and trends in precipitation. A trend (~0.5 mm per year) of increasing total annual rainfall is evident for the historical period for box FerAndNam which covers the mountains in the East, but with significant interannual variability (Table 4). In contrast, the precipitation decreases (~- 1 mm per year) for box KarKho which covers the dry central and western part of Uzbekistan. This decreasing trend in precipitation is also observed for other boxes TasSyrDhz, Sur, and BukSamKas.

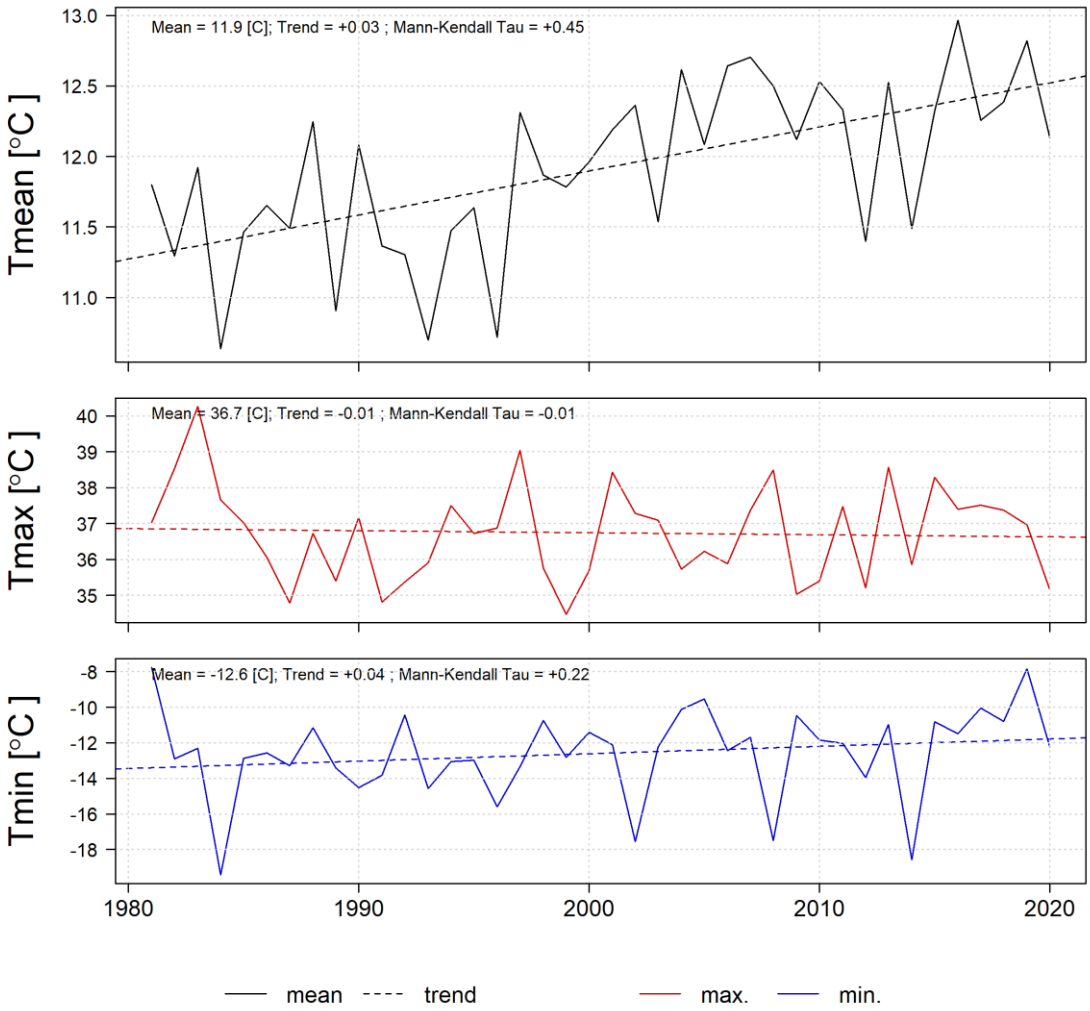

Figure 7. Average, maximum and minimum yearly temperatures from ERA-5 dataset with trendline for box FerAndNam.

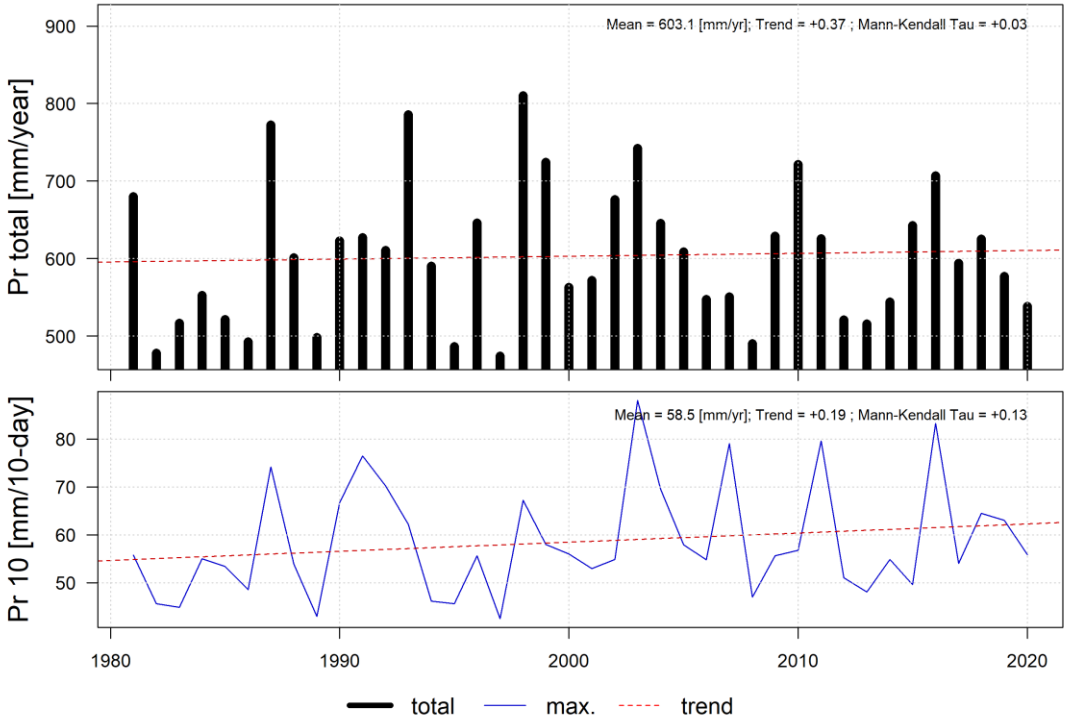

Figure 8. Total yearly and 10-day maximum cumulative precipitation with a trendline for box FerAndNam.

3.2.3 Seasonality

A clear seasonality is evident, with high average monthly temperatures (around 25ºC for box FerAndNam and around 30ºC for box BukSamKas) prevailing during April – September (Figure 9 and Figure A9). Most of the rainfall occurs during the winter and early spring periods in December, January, February, March, and April. The interannual variation is high, as there is high precipitation in the winter season and low precipitation in the summer season (Figure 10 and Figure A10).

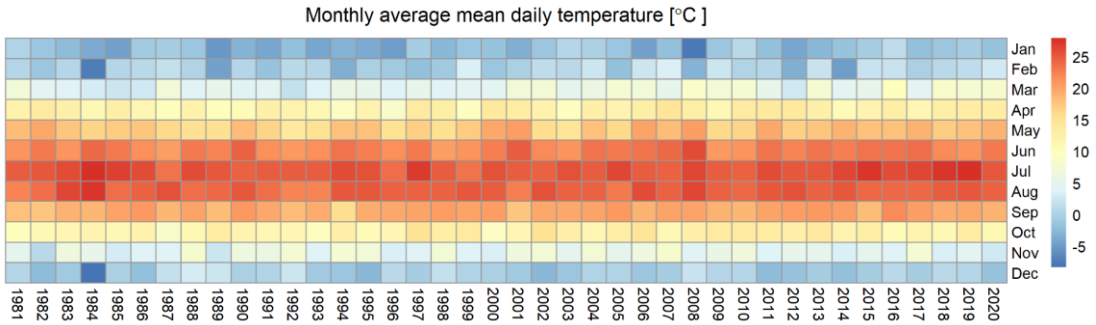

Figure 9. Seasonality in temperature from ERA-5 dataset for box FerAndNam.

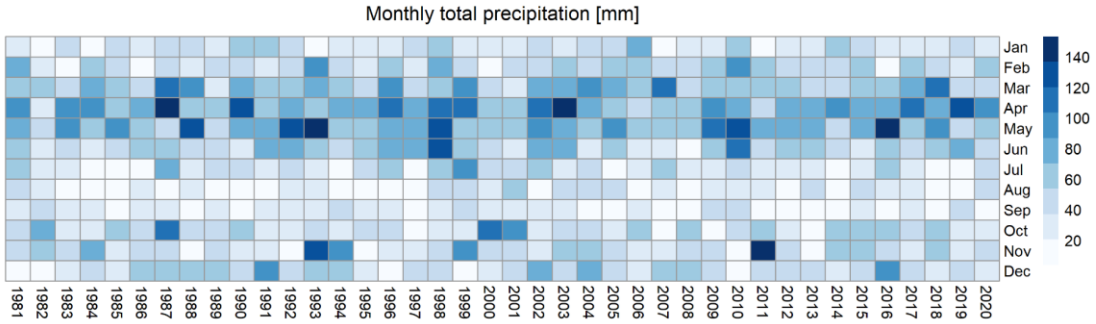

Figure 10. Seasonality of precipitation from ERA-5 dataset for box FerAndNam.

3.3 Summary tables

Summary tables of the mean temperature and precipitation, including trends, are presented in Table 4**.**

Table 4. Summary tables for the box selected.

Box	Precipitation		Temperature	
	Mean (mm)	Trend (mm/yr)	Mean (°C)	Trend (°C/yr)
FerAndNam	603	+0.37	11.9	+0.03
TasSyrDhz	458	-0.60	14.2	+0.05
Sur	215	-0.53	18.5	+0.04
BukSamKas	308	-0.62	15.4	+0.04
KarKho	113	-0.82	13.8	+0.04

4 Future Climate Projections

4.1 Methodology

4.1.1 Climate Model Ensemble

For this CRA, the NEX-GDDP-CMIP6 (Thrasher et al., 2022) data is used to analyze future climate trends. This dataset contains extended sets of variables and is used to provide an analysis of trends in terms of temperature and precipitation, and derived climate change indicators. This product is used as it provides spatially gridded time series including temperature and precipitation derived from an ensemble of 35 General Circulation Models with global coverage (see Table 5 for descriptions of models and units). The data is available at downscaled resolutions of ~25 km and daily time series, covering “historical” (1950 – 2014) and “future” (2015 – 2100) periods and varying emissions scenarios or across two of the four "Tier 1" greenhouse gas emissions scenarios known as Shared Socioeconomic Pathways (SSPs), which are sufficient for the scale of the project.

From this dataset, spatially averaged time series of precipitation and temperature are extracted for the project area at daily, weekly, and yearly timescales for the entire period that the dataset covers. This allows for the analysis of annual and seasonal trends in the future for climatic means and extremes. A similar approach was used in the ‘Digitize to Decarbonize – Power Transmission Grid Enhancement’ project in Uzbekistan[1].

4.1.2 Scenarios and future horizons

Two SSP scenarios (SSP2-4.5 and SSP5-8.5) are analyzed to provide a range of future climate projections. SSP2-4.5 represents a “stabilization scenario”, in which greenhouse gas emissions peak around 2040 and are then reduced. Although often used as ‘business as usual’, the SSP5-8.5 is above the business-as-usual emission scenarios and designed as a worst-case scenario. We include this scenario as an upper limit to the possible future climate. These scenarios are selected as they represent an envelope of likely climate changes and hence cover a plausible range of possible future changes in temperature and precipitation relating to project implementation.

Alongside the two SSP scenarios, projections are evaluated at the following time horizons:

- Reference period [2005]: 1995 – 2014
- Short (T1) [2030]: 2020 – 2039
- Mid-future (T2) [2050]: 2040 – 2059
- Distant-future (T3) [2070]: 2060 – 2079

These periods were selected for the project as they are relevant to the lifetime of the project infrastructure, and therefore cover a realistic range of climate changes that are likely to affect project functioning. A 20-year window was selected as appropriate for deriving average climate changes, effectively considering interannual variations in temperature and precipitation, and robust comparison (see Table 6).

The lifetime of energy transmission and distribution projects is typically in the order of **60 years**.[2] This means that also the distant-future horizon (T3) can be considered relevant for this CRA.

[1] Khanal, S., Imran, T., Nolet, C., 2023. Climate Risk and Adaptation Assessment for Digitize to Decarbonize – Power Transmission Grid Enhancement Project – Uzbekistan. FutureWater Report 243

[2] Salazar and Mendoza. 2008. Life prediction of electrical power transmission towers. Proceedings of the 9th Biennial ASME Conference on Engineering Systems Design and Analysis ESDA08.

Table 5. Climate models included in NASA-NEX dataset.

Model	hurs	huss	pr	rlds	rsds	sfcWind	tas	tasmax	tasmin
unit	%	kg/kg	mm/day	W/m^2	W/m2	m/s	degC	degC	degC
ACCESS-CM2									
ACCESS-ESM1-5									
BCC-CSM2-MR									
CanESM5									
CESM2									
CESM2-WACCM									
CMCC-CM2-SR5									
CMCC-ESM2									
CNRM-CM6-1									
CNRM-ESM2-1									
EC-Earth3									
EC-Earth3-Veg-LR									
FGOALS-g3									
GFDL-CM4 (gr1)									
GFDL-CM4 (gr2)									
GFDL-ESM4									
GISS-E2-1-G									
HadGEM3-GC31-LL	360	360	360	360	360	360	360	360	360
HadGEM3-GC31-MM	360	360	360	360	360	360	360	360	360
IITM-ESM	2099	2099	2099	2099	2099	2099	2099		
INM-CM4-8									
INM-CM5-0									
IPSL-CM6A-LR									
KACE-1-0-G	360	360	360	360	360	360	360	360	360
KIOST-ESM	2058								
MIROC-ES2L									
MIROC6									
MPI-ESM1-2-HR									
MPI-ESM1-2-LR									
MRI-ESM2-0									
NESM3									
NorESM2-LM									
NorESM2-MM									
TaiESM1									
UKESM1-0-LL	360	360	360	360	360	360	360	360	360

Green	historical, SSP245, SSP585 available	360	360 days / year available
yellow	historical & one SSP available;	2099	Timeseries until 2099
Red	No data available	2058	Year 2058 not avaialable

Table 6. Summary of RCP scenarios and future time horizons used in this CRA.

RCP Scenarios	Time horizons	Model projections
Historical	2005 (1995 – 2014)	35
SSP2-4.5	2030 (2020-2039) T1	35
	2050 (2040-2059) T2	35
	2080 (2070-2089) T3	35
SSP5-8.5	2030 (2020-2039) T1	35

	2050 (2040-2059) T2	35
	2080 (2070-2089) T3	35

4.1.3 Climate Extremes Indices

To determine future trends in extreme climate events, CLIMDEX[1] indicators are used. These represent a standardized, peer-reviewed way of representing extremes in climate data and are widely used in climate analyses. They are derived from daily temperature and precipitation data. These are produced through processing the NASA-NEX dataset with Climate Data Operator (CDO) software[2]. This takes as input spatially gridded daily time series and returns yearly series of CLIMDEX indices. This process is useful as it effectively reduces the amount of data analysis needed whilst retaining the ability to represent extremes within data in a comparable way.

To this end, the indices described here are considered the most relevant out of the 27 available. The Rx1day (annual maximum 1-day precipitation) and Rx5day (annual maximum 5-day precipitation) indexes are indicative of future trends in extreme precipitation and therefore likely to be a good measure of potential impacts related to flooding, slope instability, water-induced erosion, mudflow, and extreme snowfall on project components (see Table 7). CDD (consecutive dry days) is important as it provides a useful indication of trends in meteorological drought, which may impact energy transmission via distribution lines. TX_X (annual maximum of daily maximum temperature), a good predictor of extreme temperature, which may have negative effects on project components through extreme heat events, dust storms, snow, and glacier melt-related flooding events.

Table 7. CLIMDEX Precipitation Indices used in the project.

Index name	Description	Unit
RX1 day	Annual maximum 1-day precipitation	mm
RX5 day	Annual maximum 5-day precipitation sums	mm
CDD	Annual maximum consecutive dry days: annual maximum length of dry spells, sequences of days where daily precipitation is less than 1mm per day.	days
TXx	Annual maximum of daily maximum temperature	Celsius

4.2 Climate projections for the project area

4.2.1 Average trends in temperature and precipitation

In terms of average climate trends, the climate model ensemble predicts a clear increase in mean temperature for the FerAndNam in the future for all time horizons (Figure 11). It is also clear that under the higher SSP5-8.5 scenario, a larger increase in temperature is expected compared to the SSP2-4.5 scenario for the boxes (Figure 11 and Figure A11 to Figure A14). For the short-term (T1), changes in temperature around 0.8–1°C are predicted by the climate model ensemble, for the mid and long-term horizons T2 and T3 this increases to around 1.6–2.3°C and 2.4–3.9°C for the FerAndNam box (see Table 8 and Table 9). Changes of a similar order of magnitude are projected for the other boxes (Table A1 to Table A8).

[1] https://www.climdex.org/learn/
[2] https://code.mpimet.mpg.de/projects/cdo

The future trend for precipitation is less clear but, overall, the climate model ensemble projects a slight increase in mean precipitation for all the boxes till the end of the century (Figure 12 and Figure A15 to Figure A18). A large spread in model predictions is evident, with some models predicting (much) higher future increases in precipitation than others. For the short-term horizon (T1), changes in precipitation in the range of around 5–6% are projected by the climate model ensemble, for the mid and long-term horizons T2 and T3, this increases to around 10–12% and 12–17%, with a larger spread in model projections and higher divergence between emissions pathway SSP2-4.5 and SSP5-8.5 for the FerAndNam box (Figure 12 and Figure A15 to Figure A18). Changes of a similar order of magnitude are projected for the other boxes (Table A1 to Table A8).

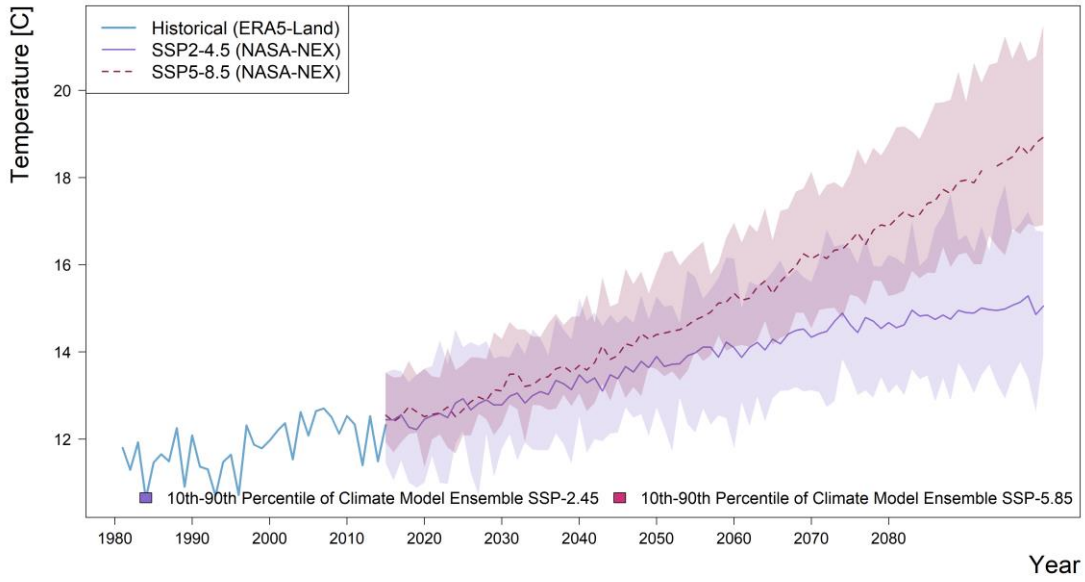

Figure 11. Time series of mean yearly ERA5-Land temperature for the box FerAndNam for the historical period (1981–2020), and NASA NEX (per model bias-corrected) for the future period. Shaded areas show the 10th and 90th percentiles in the spread of model predictions.

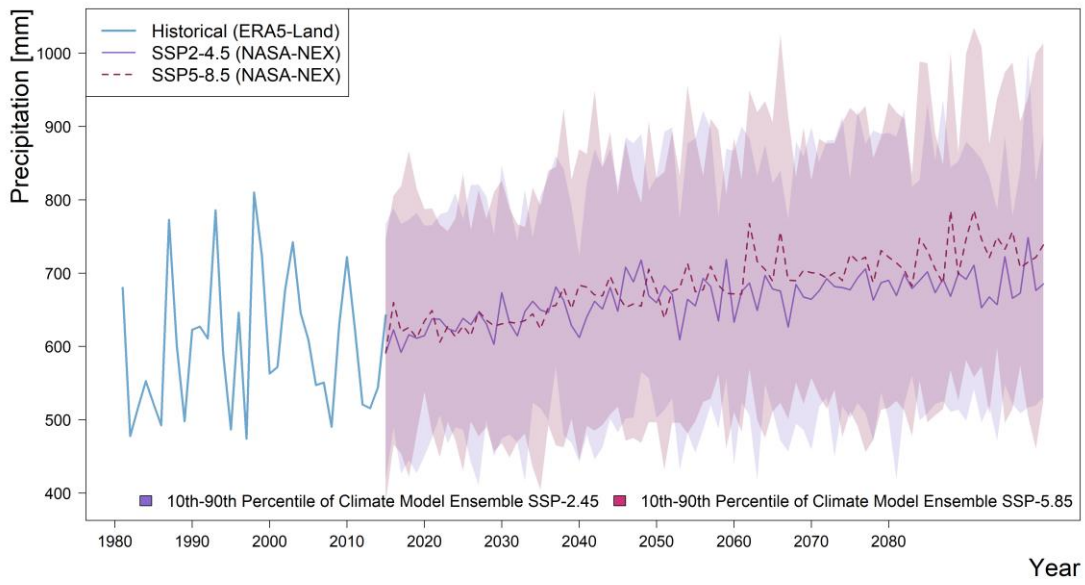

Figure 12. Time series of the yearly ERA5-Land precipitation for the box FerAndNam for the historical period (1981–2020), and NASA NEX (per model bias-corrected) for the future period. Shaded areas show the 10th and 90th percentiles in the spread of model predictions.

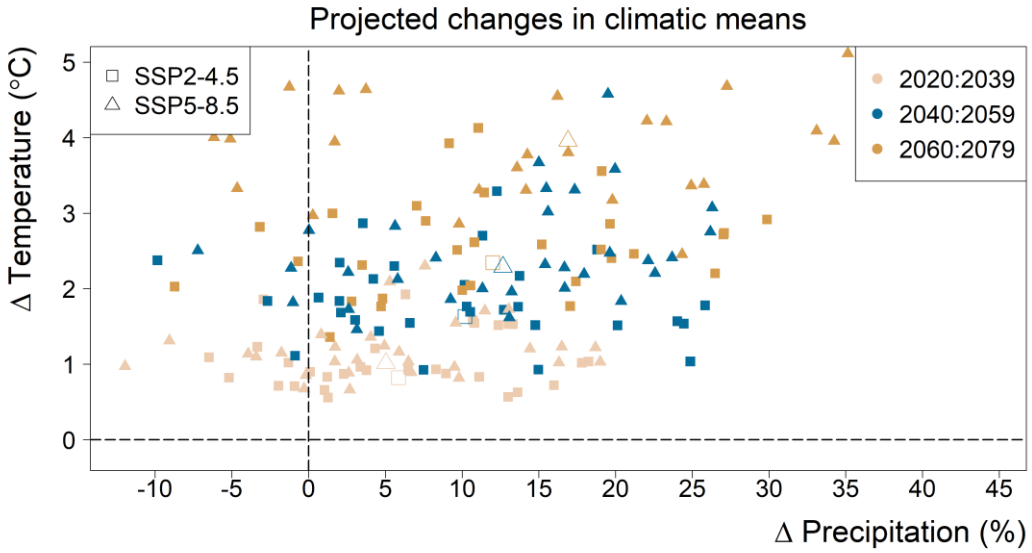

Figure 13. Average temperature and precipitation change for the box FerAndNam region. These indicate the difference (Δ) between historical (1995–2014) and future (2020–2039; 2040–2059; 2060–2079) time horizons for the two SSP scenarios.

4.2.2 Seasonality

In terms of seasonality, the climate model ensemble projects a general consistent increase in mean temperatures for all months for all boxes (Figure 14 and Figure A19 to Figure A22). A greater increase in temperatures is predicted in the long-term future (T3) timescale and under the higher SSP5-8.5 scenario. The GCM ensemble results suggest an increase in precipitation, especially in the winter season from October-May for all the boxes (Figure 15 and Figure A23 to Figure A26). This trend is more extreme under the SSP5-8.5 scenario compared to SSP2-4.5. Interestingly, the summer months (June–September) precipitation decreases in the future compared to the reference for all the time horizons and scenarios.

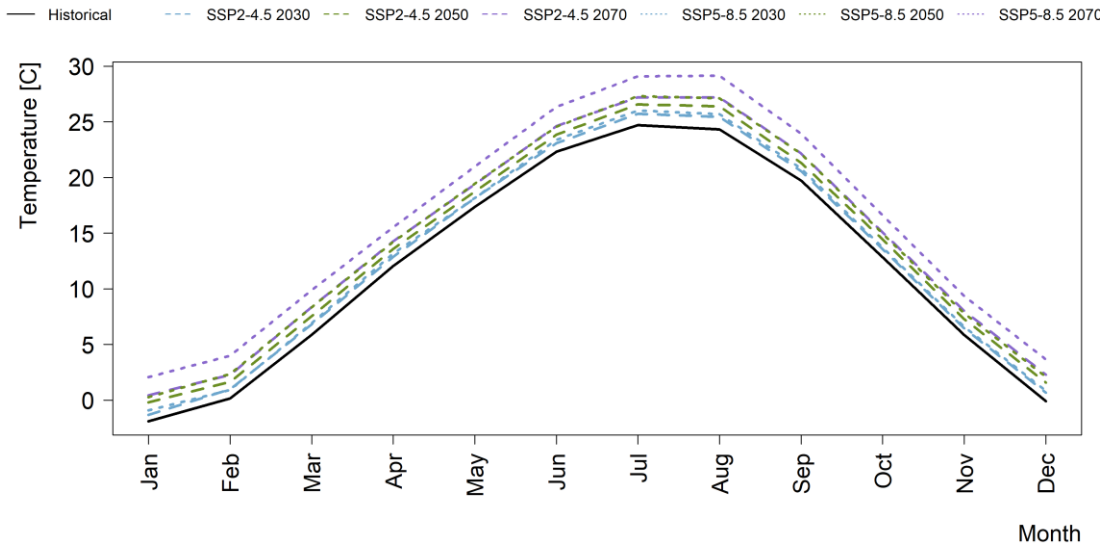

Figure 14. Average monthly temperature for historical (1995–2014) and future (time horizons under the two SSP scenarios for the box FerAndNam.

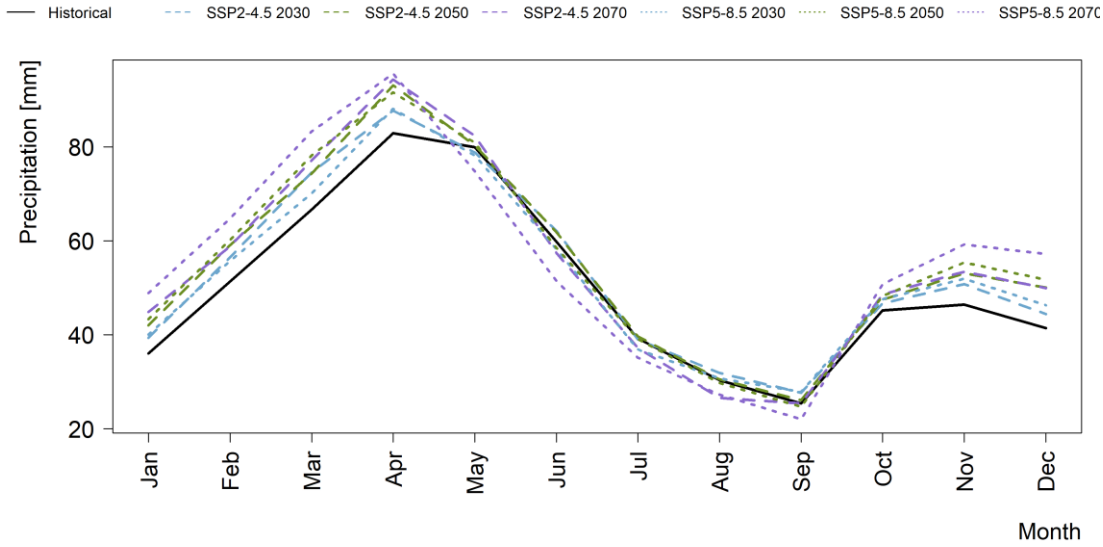

Figure 15. Average monthly precipitation for historical (1995–2014) and future time horizons under the two SSP scenarios for the box FerAndNam.

4.2.3 Trends in Climate Extremes

Temperature-related extremes

When extreme trends are considered, a large level of variation is evident in climate model projections. The uncertainty is higher in predicting extreme trends due to the stochastic nature of these events. The annual daily maximum temperature is expected to increase in the future (Figure 16 and Figure A27 to Figure A30). The climate model ensemble does, however, show a clear trend of increasing extreme temperatures under both SSP scenarios and time horizons, suggesting an increase in the likelihood of heatwaves and wildfires in all the boxes.

These processes are certain to affect seasonal water storage and seasonal patterns of discharge, particularly in the high-elevation sections of river basins where snow and glacier contribution is dominant. The consecutive dry days (CDD) will increase in the future for all the boxes across all the time horizons

and scenarios (Figure 17 and Figure A31 to Figure A34). The mean CDD for SSP5-8.5 scenario is higher compared to the SSP2-4.5 scenarios. This increase may have implications for drought in the future.

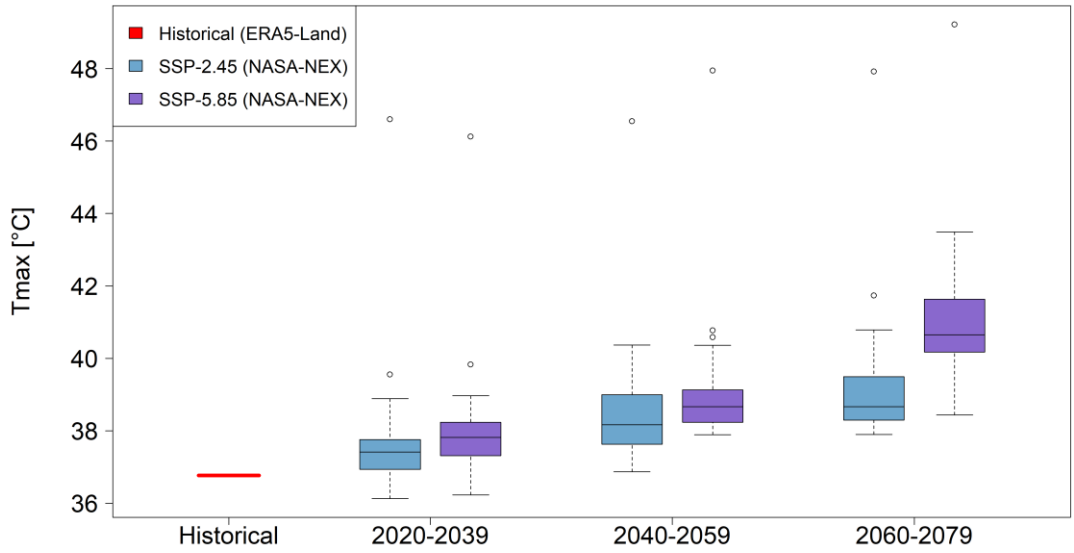

Figure 16. Boxplots indicating the spread in climate model predictions of maximum daily temperature per year (TXx) for the historical (1995–2014) and future time horizons under the two SSP scenarios for the box FerAndNam.

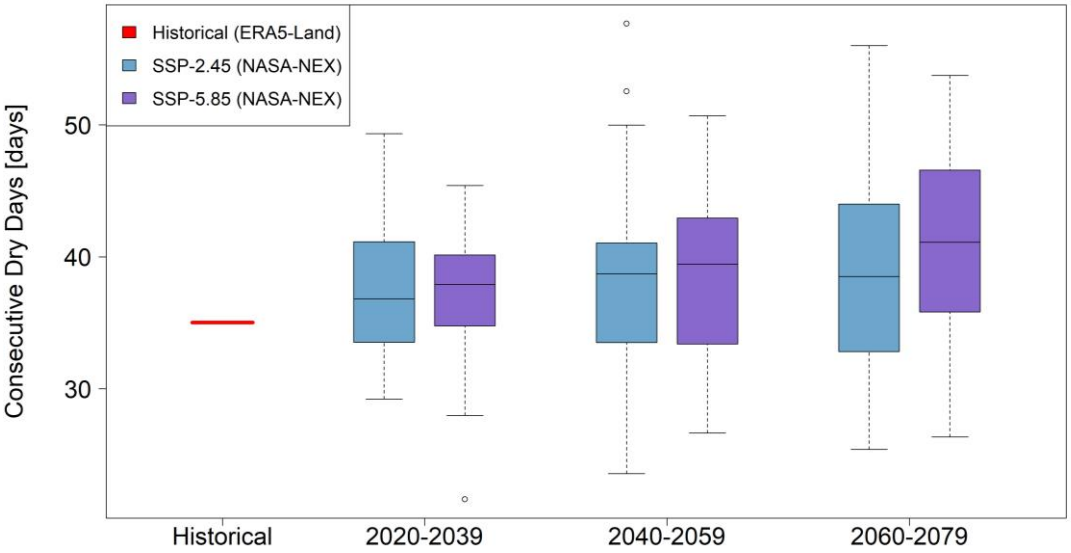

Figure 17. Boxplots indicating the spread in climate model predictions of average consecutive dry days per year (CDD) for the historical (1995–2014) and future time horizons under the two SSP scenarios for the box FerAndNam.

Precipitation-related extremes

The climate model ensemble shows a clear trend of increasing extreme 1-day precipitation events under both SSP scenarios and time horizons for all the boxes, suggesting an increase in intense precipitation-associated hazards (flash flooding and soil erosion) in the future for the project area (Figure 18 and Figure A35-Figure A38). Similarly, the consecutive 5-day episodes of precipitation increase in the future

for all boxes implying that associated hazards such as river floods, landslides, and mudflow may increase in the future (Figure 19 and Figure A39 to Figure A42).

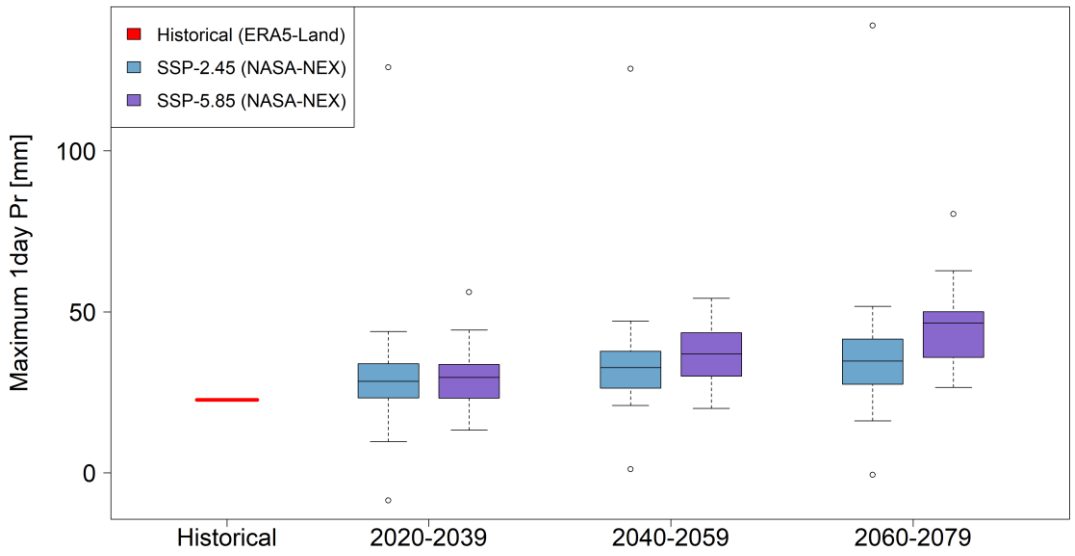

Figure 18. Boxplots indicating the spread in climate model predictions of yearly maximum 1-day precipitation sum (Rx1day, in mm/day) for the historical and future time periods under two SSP scenarios for the box FerAndNam.

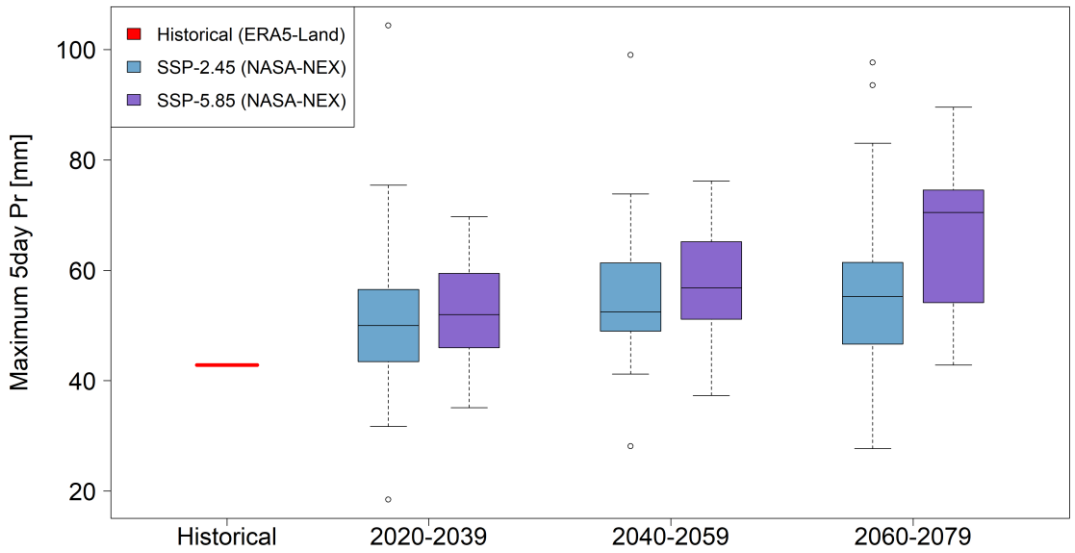

Figure 19. Boxplots indicating the spread in climate model predictions of yearly maximum 5-day precipitation sum (Rx5day, in mm/day) for the historical and future time periods under two SSP scenarios for the box FerAndNam.

4.3 Summary tables

The combination of 35 GCMs, two SSPs, and three time-horizons leads to a total of 210 (35 x 2 x 3) projections for the future. Table 8 and Table 9 show detailed results for all projections of changes in mean annual temperature and total annual precipitation for the box FerAndNam. Delta values (% change for precipitation and °C for temperature) indicate the difference between historical and future (T1, T2,

and T3) time horizons for the two SSP scenarios (for other boxes check Table A1 to Table A8). These tables show consistency between GCMs in terms of projecting a warmer future climate in the project area (especially for the longer-term horizon) but indicate the large uncertainty in the future precipitation. The main statistics (median, 25th percentile, and 75th percentile) of the changes in precipitation and temperature, respectively. It also includes the number of GCMs that are showing a positive versus negative change for precipitation, and the number of GCMs that are predicting a change above 2ºC and 4ºC. In summary, all GCMs predict a hotter future, with most predictions lying between 2 and 4ºC. All climate models predicted a hotter future for all the clusters, with most of the models predicting an increase of more than 4ºC for the 2070 horizon (Table 9 and Table A1 to Table A8). There is no clear consensus in precipitation predictions, but a slight majority of GCMs predict a wetter future for the SSP scenario. Considering the 75th percentile value of the projections as a benchmark for robust climate change adaptation, the statement can be made that wetter conditions should be anticipated in the future for all the boxes in the project area.

Similarly, Table 10 are Table 11 show that the extremes are going to exacerbate in the future. While the extreme temperature changes remain relatively similar for all the boxes, the CDD changes in the future are higher in magnitude for box FerAndNam compared to the other boxes. This may have serious implications for the heat wave and drought hazards in the future. The RX1 is expected to increase by more than 50% for SSP2-4.5 and double for SSP5-8.5 by the end of the century. The increase in the occurrence and magnitude of such extreme events in the future may increase the likelihood of hazards, for instance, erosion, floods, and sedimentation.

Table 8. Summary table showing statistics regarding spread in CMIP6 ensemble predictions for future changes in mean annual precipitation for the FerAndNam box.

Scenarios	Average (%)	25th Perc. (%)	75th Perc. (%)	GCMs Dryer	GCMs Wetter
2030_SSP245	6%	-1%	13%	10	24
2050_SSP245	10%	3%	17%	3	31
2070_SSP245	12%	5%	5%	3	31
2030_SSP585	5%	1%	1%	6	29
2050_SSP585	12%	5%	5%	4	31
2070_SSP585	17%	9%	26%	5	30

Table 9. Summary table showing statistics regarding spread in CMIP6 ensemble predictions for future changes in mean temperature for the FerAndNam box.

Scenarios	Average (°C)	25th Perc. (°C)	75th Perc. (%)	GCMs >2°C	GCMs >4°C
2030_SSP245	+0.8	+0.8	+1.2	0	0
2050_SSP245	+1.6	+1.5	+2.1	10	0
2070_SSP245	+2.4	+2.3	+2.3	24	24
2030_SSP585	+1.0	+1.0	+1.0	2	2
2050_SSP585	+2.3	+2.3	+2.3	23	23
2070_SSP585	+3.9	+3.9	+3.9	31	31

Table 10. Summary table (mean values) for the historical extremes.

Regions	Rx1day (mm)	Rx5day (mm)	CDD (days)	TXx (°C)
FerAndNam	22.7	42.8	35.0	36.8
BuKaSa	20.2	32.5	102.4	41.0
KarKho	12.4	16.3	101.1	42.2
Sur	15.2	27.0	138.3	43.7

TasSyrDhz	22.6	39.7	63.1	39.8

Table 11. Percentage change in climate extremes for the SSP scenarios and time horizons compared to the historical extremes

Horizon	Scenarios	Box	Rx1day (Δ%)	Rx5day (Δ%)	CDD (Δ%)	TXX (Δ%)
T1	SSP2-4.5	FerAndNam	35	19	7	2
		BuKaSa	39	27	1	4
		KarKho	77	61	1	3
		Sur	38	15	1	3
		TasSyrDhz	42	21	0	3
	SSP5-8.5	FerAndNam	32	22	6	3
		BuKaSa	37	25	1	4
		KarKho	42	44	0	4
		Sur	32	13	0	4
		TasSyrDhz	38	23	-1	4
T2	SSP2-4.5	FerAndNam	50	29	7	5
		BuKaSa	52	36	0	6
		KarKho	69	55	0	6
		Sur	59	27	0	5
		TasSyrDhz	56	29	1	6
	SSP5-8.5	FerAndNam	62	35	10	6
		BuKaSa	62	39	1	7
		KarKho	57	56	0	7
		Sur	87	32	1	7
		TasSyrDhz	70	34	2	7
T3	SSP2-4.5	FerAndNam	59	32	11	7
		BuKaSa	61	41	0	8
		KarKho	103	93	-1	7
		Sur	74	33	1	7
		TasSyrDhz	71	35	3	7
	SSP5-8.5	FerAndNam	97	55	17	12
		BuKaSa	95	62	2	12
		KarKho	116	94	2	11
		Sur	127	57	2	11
		TasSyrDhz	107	59	7	12

Table 12. Average percentage change in climate extreme across all the scenarios and time horizons compared to the historical extremes (i.e., summary of Table 11).

	Rx1day (Δ%)	Rx5day (Δ%)	CDD (Δ%)	TXX (Δ%)
Related hazard	Floods, landslides, erosion, mudflows		Droughts, dust storms, wildfire	Heatwaves, dust storms, wildfire
FerAndNam	55.8	31.9	9.6	5.9
BuKaSa	57.5	38.4	0.9	6.7
KarKho	77.5	67.1	0.3	6.5
Sur	69.4	29.4	1.1	6.3
TasSyrDhz	63.8	33.7	2.2	6.6

5 Climate Risks and Vulnerabilities

Uzbekistan is becoming increasingly vulnerable to the impacts of climate change. Frequent and intense floods, heatwaves, droughts, and dust storms continue to threaten the accelerating socioeconomic development in the country. An efficient, adequate, and uninterrupted power supply is critical to sustain and improve Uzbekistan's growing economy; however, the aging electric grid infrastructure is now experiencing significant power losses, especially under climate change. Additionally, the rapidly increasing population has also put immense pressure on the existing infrastructure to meet the swelling energy demands. Therefore, it is crucial to not only enhance the capacity and efficiency of the existing system through modern engineering solutions but also gain a clear understanding of how the electric power system is vulnerable to the different impacts of climate change. An improved understanding of climate risks will lead to the identification and implementation of the most effective mitigation and adaptation measures. This chapter identifies the sensitivities and vulnerability of the electricity transmission and distribution network to different climate risks and assesses the risk levels.

5.1 Sensitivity to project-relevant hazards

Power transmission and distribution systems are sensitive to climate factors in various ways. How climate change and increased severity and occurrence of climate-related hazards will impact the project will depend on how sensitive the infrastructural components (i.e. substations) are to climate variables. The sensitivity to project-relevant hazards is summarized in Table 13.

Table 13. Sensitivity of power distribution systems to climate hazards

Hazard	Substations
Floods	-Floods can damage the structures (civil, mechanical, and electrical) by erosion and when water comes into contact with electrical control systems causing short circuits
Droughts and Heatwaves	-Increased strain on substations due to high demands during warm periods -High temperatures can impair the operation of substations -Drought can increase dust damage
Dust storms and Wind Erosion	-Dust storms and high-speed winds can cause damage (corrosion etc.) to the infrastructure
Landslides and mudflows	-Landslides and mudflows can damage the substation infrastructure
Wildfire	-Wildfires can damage different components within the substation, particularly the sensitive electrical circuits

5.2 Adaptive capacity

The socio-economic context of the project influences the project´s capacity to cope with climate hazards and climate change. For this multi-regional energy project, this context is predominantly influenced by national-level adaptation planning and the national socio-economic resilience level.

According to the national-level Notre Dame Global Adaptation Index (ND-GAIN)[1], which indicates a country's climate vulnerability with respect to its readiness for enhanced resilience, Uzbekistan has a

[1] https://gain-new.crc.nd.edu/country/uzbekistan

score of 49.4 and an overall country index rank of 83 (100 being the best). This shows that the country is well-positioned to tackle the impacts of climate change, even though adaptation will be a challenge.

Figure 20 shows the temporal variation in vulnerability and readiness over the last 25 years. Vulnerability considers six major sectors i.e., food, water, health, ecosystem service, human habitat, and infrastructure while readiness is assessed according to economic, governance, and social readiness.

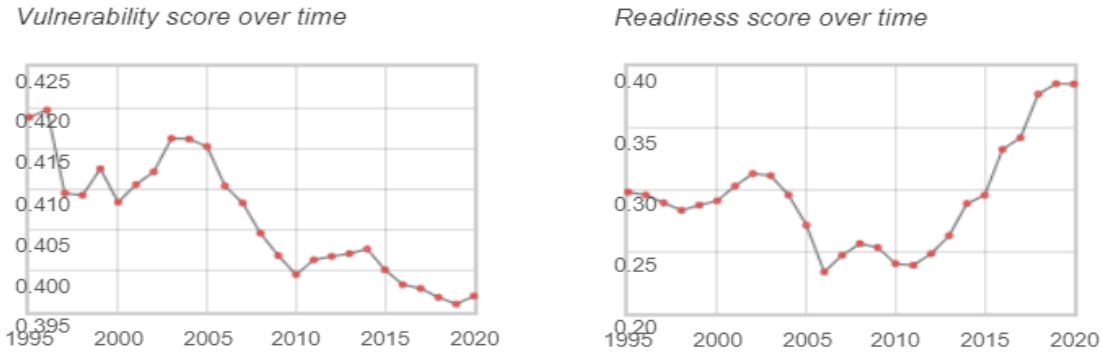

Figure 20. Temporal variation in Uzbekistan's vulnerability and readiness scores (1995 - 2020) (Source: GAIN-ND, University of Notre Dame).

Based on the ND-GAIN Index and the temporal changes in vulnerability and readiness scores, Uzbekistan has gained climate resilience over the years and has the potential to further enhance it. Figure 21 depicts the shift in Uzbekistan's position with respect to other countries on the vulnerability-readiness matrix (2010 vs 2020). The country has accelerated its efforts towards promoting climate mitigation and adaptation measures across all its sectoral strategies such as the National Development Goals, Green Economy Strategy, and Concept for the Development of Electric Power Industry. In its updated NDC, Uzbekistan has increased its commitments by more than 300 percent. The agenda includes increasing the share of renewable energy sources to 25 percent of total power generation, reducing the energy intensity of GDP by half, and doubling the energy-efficiency indicator relative to the level of 2018 – among others.

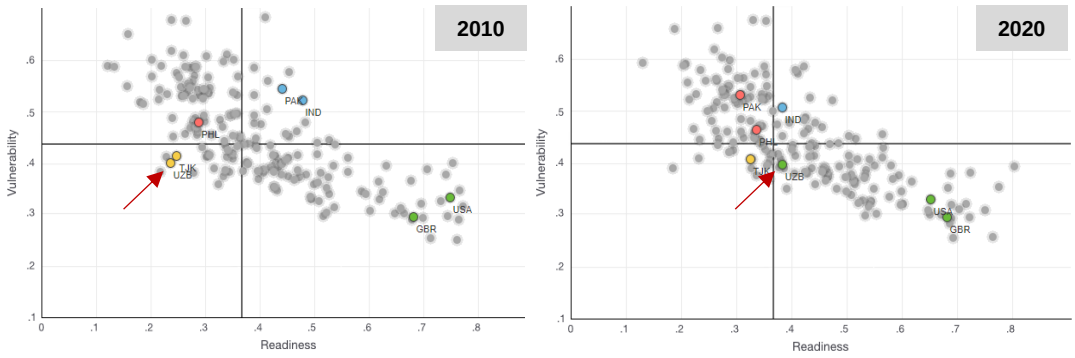

Figure 21. The shift in Uzbekistan's adaptive capacity in relation to other countries (2010 - 2020) (Source: GAIN-ND, University of Notre Dame).

With ADB's support, the country is committed to reforming its energy sector and transitioning into a green economy by 2030. Through Output 1 and 2 of the project, the growing issue of energy losses and insufficient capacity to meet future demands will be tackled while Output 3 will strengthen the technical and managerial capacity of JSC-REPN to ensure smooth operations. As adaptation priorities are already

reflected in almost all current and future socioeconomic development plans, Uzbekistan appears to be on track with effectual and timely implementation of these measures.

5.3 Climate risks

According to the GFDRR (Global Facility for Disaster Reduction and Recovery), over 9 percent of Uzbekistan's total land area is at risk from natural and man-made disaster, with nearly 66 percent of the population living in these areas and approximately the same percentage of the national GDP earned in them[1]. Among the natural hazards, earthquakes cause the largest economic losses, but also hydrometeorological extremes cause increasingly severe economic damage.

Due to variations in elevation, land use, and hydrology across the country, different regions of Uzbekistan are exposed to the different climate hazards. In April 2022, the country suffered from extreme floods and mudflows after torrential rain – making it the worst flood event in 80 years. The floods were followed by extreme heatwaves in July where temperatures rose to 42.6°C[2]. There were occasional blackouts due to a surge in energy demand because of increased air conditioning and refrigeration needs. Such events are only going to become more frequent in the future; therefore, mapping hazards is crucial to minimize losses and ensure climate proof infrastructure development.

5.3.1 Flooding

Overall, there is a medium to high flood hazard across the country except for the north and southeastern regions which show medium to high hazard (Figure 22). Three major flooding events have occurred in the last two decades. In 2005, a flash flood hit Boymurod (Kanimekh) and Qoshgudug (Nurata), affecting over 1,500 people. In 2020, a massive flood hit the Syrdarya region impacting more than 70,000 people[3]. Similarly, in April 2022, deadly floods and mudslides hit the Samarkand region along with parts of the Navoi and Qashqadarya regions. This disaster resulted in the death of four people, damaged over 260 farms and buildings, and left many displaced[4].

The study based on the global climate and hydrological model's (0.5° x 0.5° grid) reveals that the eastern part of Uzbekistan is exposed to floods compared to other regions (Figure 23)[5]. However, the models used for the global simulations were not tailored to the specifics of Uzbekistan (Lange et al., 2020). The glaciers and vegetation-related processes were strongly simplified in the global scale models so the exposure may increase in the future. Another global study estimated that more than 300 thousand people (Figure 24) will be affected by floods in the future in Uzbekistan (Ward et al., 2020). The total flood losses will increase from 850 million USD to about 20 trillion USD by 2080.

Based on Figure 22, the flood hazard exposure level is rated in Table 14 (low-medium-high) for each substation considered in the project, unless the flood hazard is not applicable (noted as n.a.). The substations most exposed to flood hazards are in the proximity of the high flood hazard areas in the Tashkent and Kashkadarya region, and it must be noted that SS Termez is directly exposed to high flood hazard levels. Extra measures need to be prioritized to decrease the vulnerability of these substations.

Considering the projected increases in extreme rainfall events, the present hazard level most likely will increase in the future and thus it is essential to design projects in these areas to be robust to river flood hazard in the long-term. The increase in precipitation in the future will have a significant impact on the

[1] https://www.gfdrr.org/en/publication/disaster-risk-profile-uzbekistan
[2] www.hydromet.uz
[3] Darthmouth Flood Observatory, https://floodobservatory.colorado.edu/Archives/index.html
[4] Ministry of Emergency Situations, https://floodlist.com/asia/uzbekistan-floods-april-2022
[5] https://www.isipedia.org/report/will-climate-change-increase-the-exposure-to-river-flooding/uzb/

floods in the region (see section 4.2). It is likely that flood-related hazards will increase for the regions in the east compared to the west of Uzbekistan in the future. The clusters FerAndNam, TasSyrDhz and Sur will be higher compared to the other regions. Thus, the additional risk due to climate change for floods related hazards is estimated to be **medium to high**.

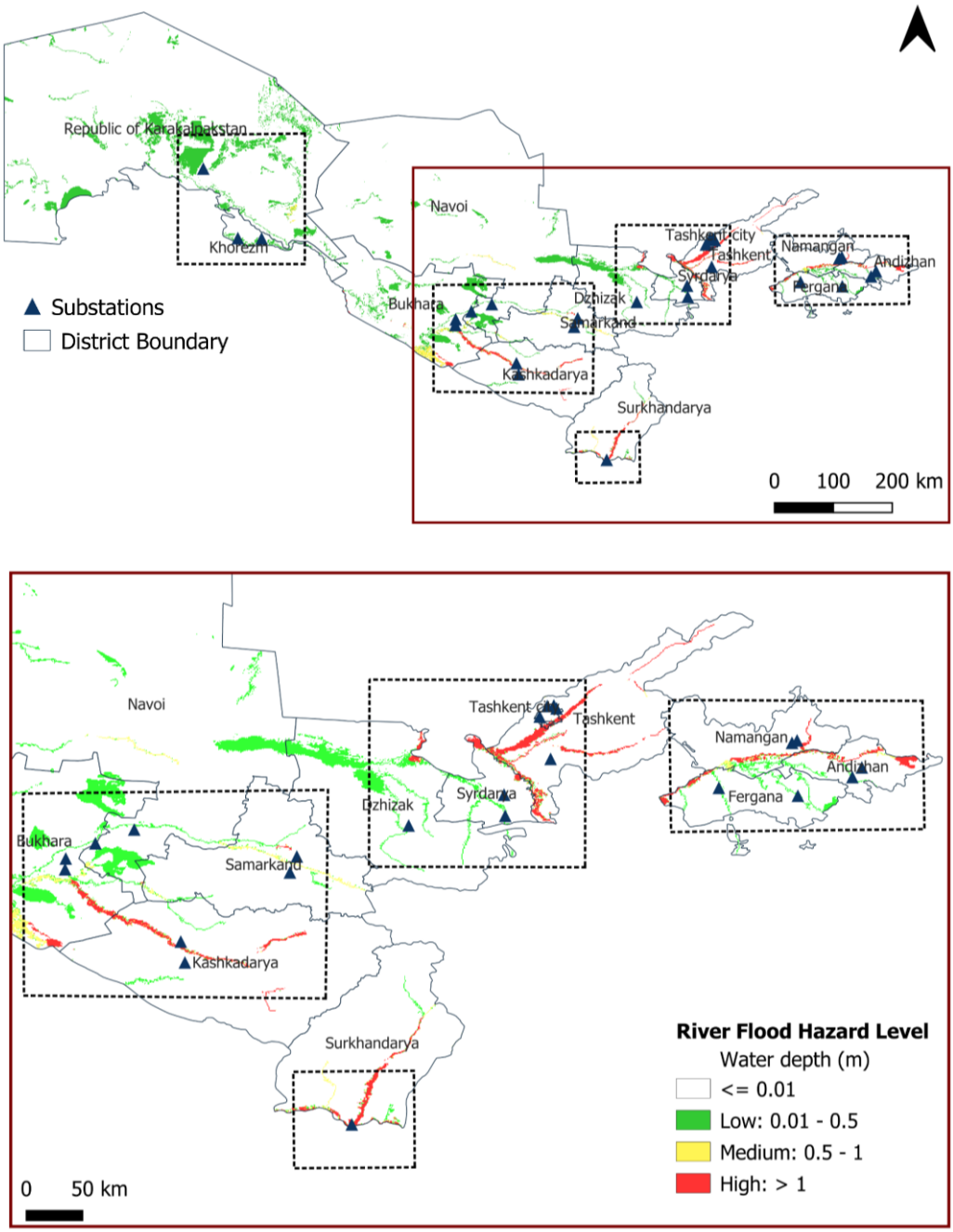

Figure 22. Flood hazard across Uzbekistan (Source: WRI Global Flood Model. Return Period 100 years - water depth).

Table 14. Flood hazard exposure level of the substations. Note n.a. denotes not applicable or very low hazard levels.

Name ID of the boxes	Regions	Project components	Flood hazard exposure
FerAndNam	Fergana, Andizhan Namangan	SS Yayilma (Andizhan) SS Asaka (Andizhan) SS Charkhi (Fergana) SS Atlas (Fergana) SS Namangan (Namangan) SS Vokzal (Namangan)	**n.a.** **Low** **Low** **Low** **High** **High**
TasSyrDhz	Tashkent Syrdarya Dzhizak	SS Eshonguzar (Tashkent) SS Sagban (Tashkent) SS Botanicheskaya (Tashkent) SS Yunusabad (Tashkent) SS Dungkurgon (Tashkent) SS Yangier (Syrdarya) SS Markaz (Syrdarya) SS Zilol (Dzhizak)	**High** **High** **High** **High** **n.a.** **Low** **Low** **Low**
Sur	Surkhandarya	SS Termez (Surkhandarya)	**High**
BukSamKas	Bukhara, Samarkand, Kashkadarya, Navoi	SS Strelkova (Bukhara) SS Galaosiyo (Bukhara) SS Malikchul (Bukhara) SS Karmana (Navoi) SS Loish (Samarkand) SS Juma (Samarkand) SS Beshkent (Kashkadarya) SS Koson (Kashkadarya)	**Medium** **Low** **Low** **Low** **Medium** **Medium** **High** **High**
KarKho	Karakalpakstan Khorezm	SS Khalkabad (Karakalpakstan) SS Bagat (Khorezm) SS Gilamchi (Khorezm)	**Low** **Low** **Low**

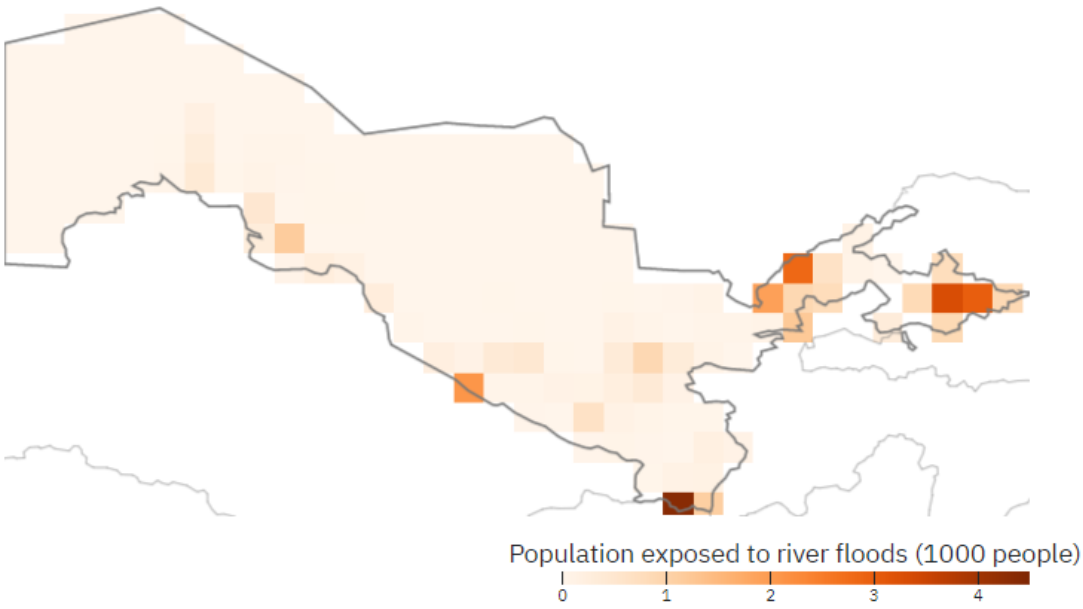

Figure 23. Population exposure to river flooding at 2°C global warming varies within Uzbekistan[1].

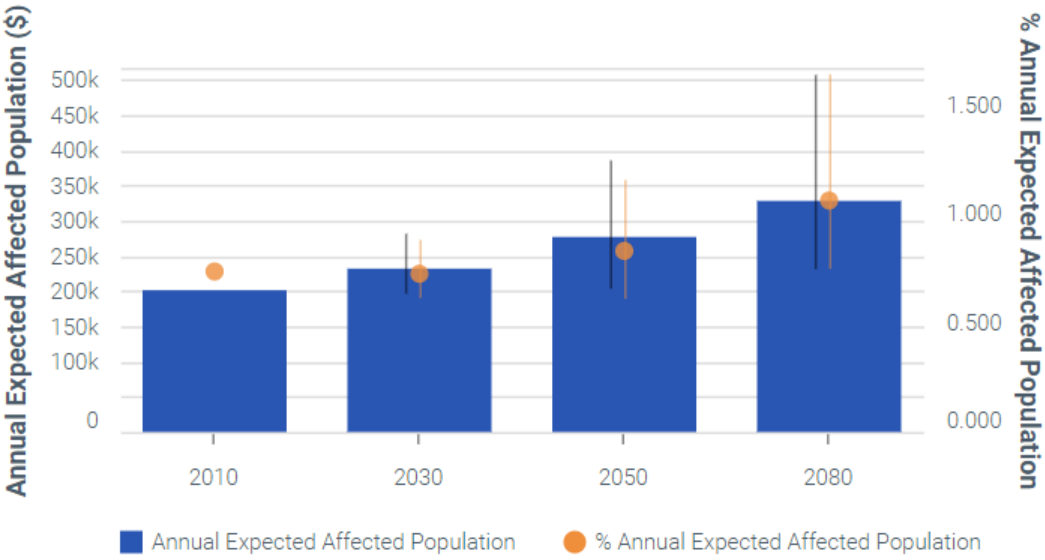

Figure 24. The expected annual damage to be incurred and the relative amount of damage for the Uzbekistan in the future. Error bars are bound by the minimum and maximum damage estimates from the different climate models[2].

5.3.2 Droughts and Heatwaves

The intensity and frequency of droughts and heatwaves are increasing in the country, with extreme heat levels being reported in the Samarkand region. In 2021, the Centre of Hydrometeorological Service of Uzbekistan (UZHYDROMET) identified early June as the hottest early summer since the end of the 19th century, with air temperatures 7-10°C higher than the climatic norm. Temperatures in Tashkent, during this period, rose to 42.6°C, which exceeded the peak values observed in the 19th and 20th centuries.

Given its geographic location and terrain, most of the country is already classified as semi-arid to arid. The rising temperatures have increased Uzbekistan's vulnerability to droughts. In 2000, an extreme drought event caused significant economic damages equivalent to USD 79,000, affecting more than 600,000 people over an area of 860 km^2.

Figure 25 shows the heat wave hazard across the country. Apart from two substations in the Samarkand province (SS Loish and SS Juma), all locations of the substations coincide with the extent of high-hazard zones, thus making the infrastructure vulnerable to the adverse impacts of heatwaves. Moreover, an alarming increase in average and extreme temperature-related indices (see section 4.2 and Table 12) will further exacerbate the frequency and intensity of drought and heatwaves in the future. Thus, the climate risk due to droughts and heat wave is estimated to be **high**.

[1] https://www.isipedia.org/report/will-climate-change-increase-the-exposure-to-river-flooding/uzb/
[2] https://www.wri.org/applications/aqueduct/floods/#/risk

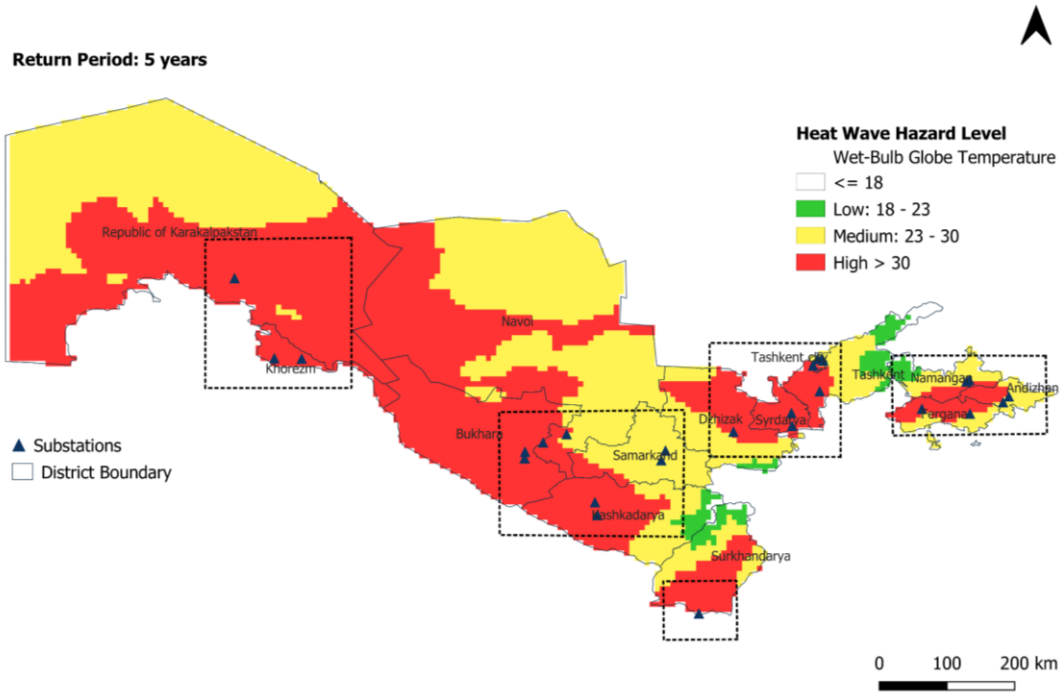

Figure 25. Heat wave hazard across Uzbekistan (Source: VITO Global Heat Model, 5 years RP hazard Map).

5.3.3 Dust storms and wind erosion

Increasing desertification because of aridity and land degradation has amplified the number of dust storm events in Uzbekistan. Water shortages and increasing aridity caused by climatic changes coupled with land degradation problems have aggravated the desertification processes. As a result, a desert expanding over 60,000 km^2, has formed at the bottom of the former Aal Sea and is now an additional source of sand and dust storms in the country[1]. As a major consequence, this has resulted in an increased number of dust storm events.

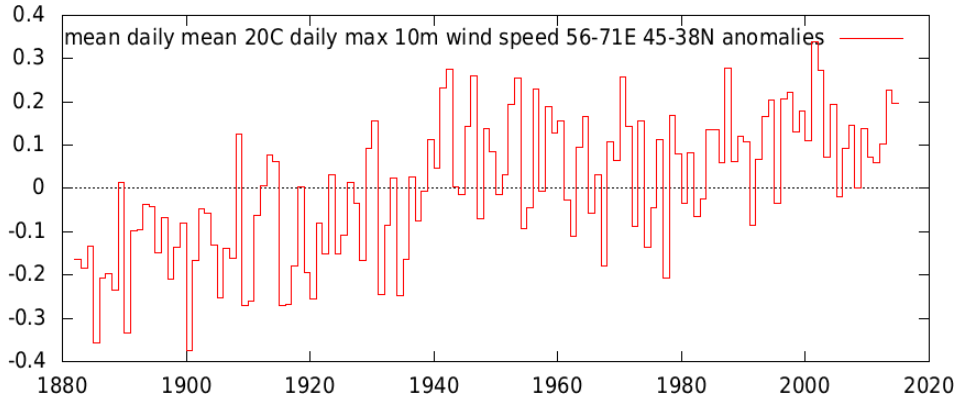

Figure 26. Wind speed anomaly for Uzbekistan (1880-2014) (Source: NOAA-CIRES).

The western part of Uzbekistan is susceptible to dust storms, as Figure 27 illustrates. The map shows the wind erosion risk for Uzbekistan, based on the erosivity of the wind and the erodibility of the surface.

[1] https://kun.uz/en/news/2022/02/05/sand-and-dust-storms-of-aralkum-yearly-carry-out-up-to-75-million-tons-of-sand-dust-and-salt

Erosivity is expressed by max wind speeds at 10m heights measured[1], while erodibility is expressed as a combination of land cover[2] and soil type[3] (and texture). The expected substantial increase in air temperatures across Uzbekistan is expected to lead to more prolonged periods of drought conditions. This is likely to contribute to increased aridity and desertification in the country, which may also increase the occurrence of dust storms.

For the most part, the considered substations in the project lie within a low wind erosion hazard zone, as per Figure 27, but energy distribution infrastructure in Karakalpakstan, Khorezm and Bukhara, Kashkadarya provinces are exposed to locally high wind erosion / dust storm risks. The increased hazard level may adversely affect energy transmission performance, as dust storms are known to cause corrosion and transmission losses from overhead power lines and can cause damage to pole mounted transformers and energy distribution systems. More powerful dust storms due to stronger wind may also develop, causing damage to overhead transmission lines and poles. Finally, dust particles hitting power lines can cause sparks, so dust storms could potentially start wildfires which may damage the energy network and cause power outages. These dust storms are not only harming human health but also damaging development infrastructure.

Based on the trends observed in the wind speed anomalies in Uzbekistan (Figure 26) and the increase in temperature-related extremes in the future, more frequent and intense dust storms are likely to follow in the future (see section 4.2 and Table 12). Overall, the climate risk for dust storms and wind-related erosion is **medium to high**.

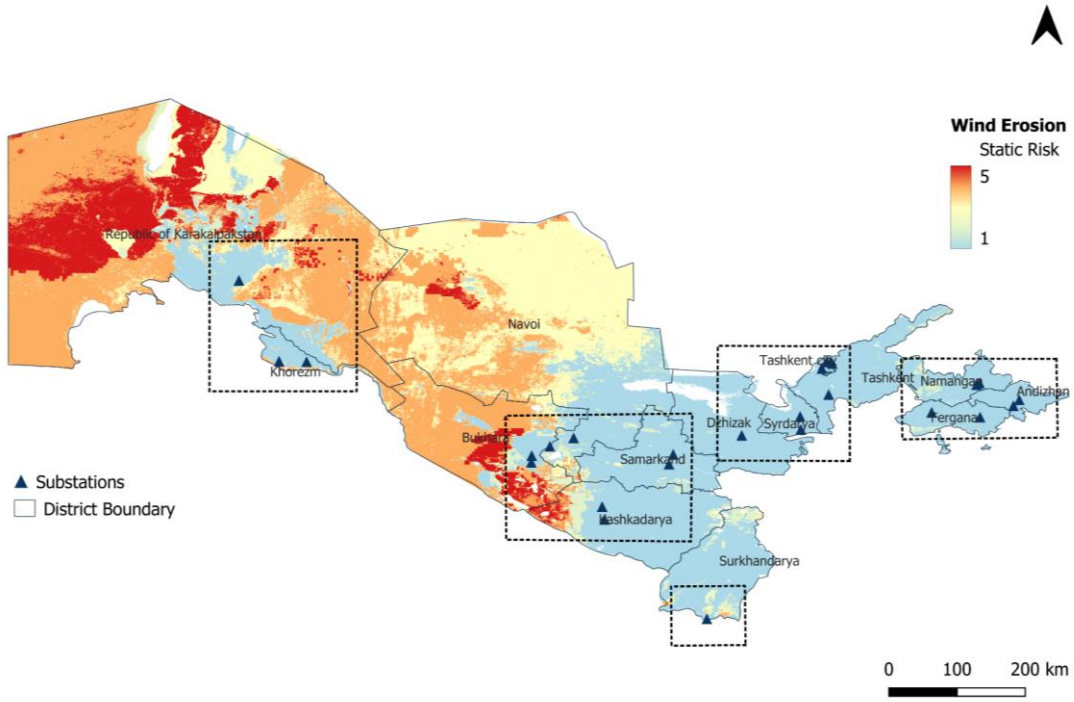

Figure 27. Wind Erosion risk (Low-1 to High-5) for Uzbekistan, based on historical wind records, land cover and soil texture.

[1] Abatzoglou, J.T., S.Z. Dobrowski, S.A. Parks, K.C. Hegewisch, 2018, Terraclimate, a high-resolution global dataset of monthly climate and climatic water balance from 1958-2015, Scientific Data 5:170191, doi:10.1038/sdata.2017.191

[2] Buchhorn, M. ; Lesiv, M. ; Tsendbazar, N. - E. ; Herold, M. ; Bertels, L. ; Smets, B. Copernicus Global Land Cover Layers-Collection 2. Remote Sensing 2020, 12Volume 108, 1044. doi:10.3390/rs12061044

[3] Tomislav Hengl. (2018). Soil texture classes (USDA system) for 6 soil depths (0, 10, 30, 60, 100 and 200 cm) at 250 m (Version v02) [Data set]. Zenodo. 10.5281/zenodo.1475451

5.3.4 Landslides, water-related erosion, and mudflows

More than 3,300 mudflows of which 85% are associated with storm activity has been registered in Uzbekistan between 1900-2013. Approximately 83% of the mudflow occurred in the months between March to July.[1] Fergana valley alone has experienced more than 44% of such mudflow events in the past. More than 90 % of all recorded mudflows were associated with extreme precipitation events, hail, and sleet, whereas 6 % of mudflow episodes were observed during intensive snowmelt events induced by respective temperature and precipitation changes.[2]

Climate model projections (CMIP5-based) revealed that mudflow generating large-scale circulation flows will increase by up to 5% by the end of the century for Uzbekistan (Mamadjanova & Leckebusch, 2022). Moreover, the third UNFCCC national report of Uzbekistan[3] have also confirmed the increase of precipitation-induced natural hazards such as mudflows to be 4 times more in the country by 2080. Two significant mudslide events have been reported, one in the Fergana Valley in the Namangan Region in 2021 and the other earlier this year in Samarkand, Navoi and Qashgadarya regions.

As shown in Figure 28, most substations are situated in either none or low rainfall-induced landslide hazard zones. The spatial pattern for this landslide dataset resembles very much the spatial pattern of the recorded mudflow events in Uzbekistan (Mamadjanova et al., 2018). However, substations in the Fergana, Andizhan, Samarkand and Surkhadarya provinces could potentially be impacted by landslides in the future – depending on the extent and magnitude of the landslide. Projected increases in temperature are likely to increase the liquid fraction of precipitation; given the high mountainous region in the northeast and southeast part of the country, there is a **medium to high** rainfall-induced landslide hazard.

[1] Mamadjanova, Gavkhar, et al. "The role of synoptic processes in mudflow formation in the piedmont areas of Uzbekistan." Natural Hazards and Earth System Sciences 18.11 (2018): 2893-2919.
[2] Ibis
[3] https://unfccc.int/sites/default/files/resource/TNC%20of%20Uzbekistan%20under%20UNFCCC_english_n.pdf

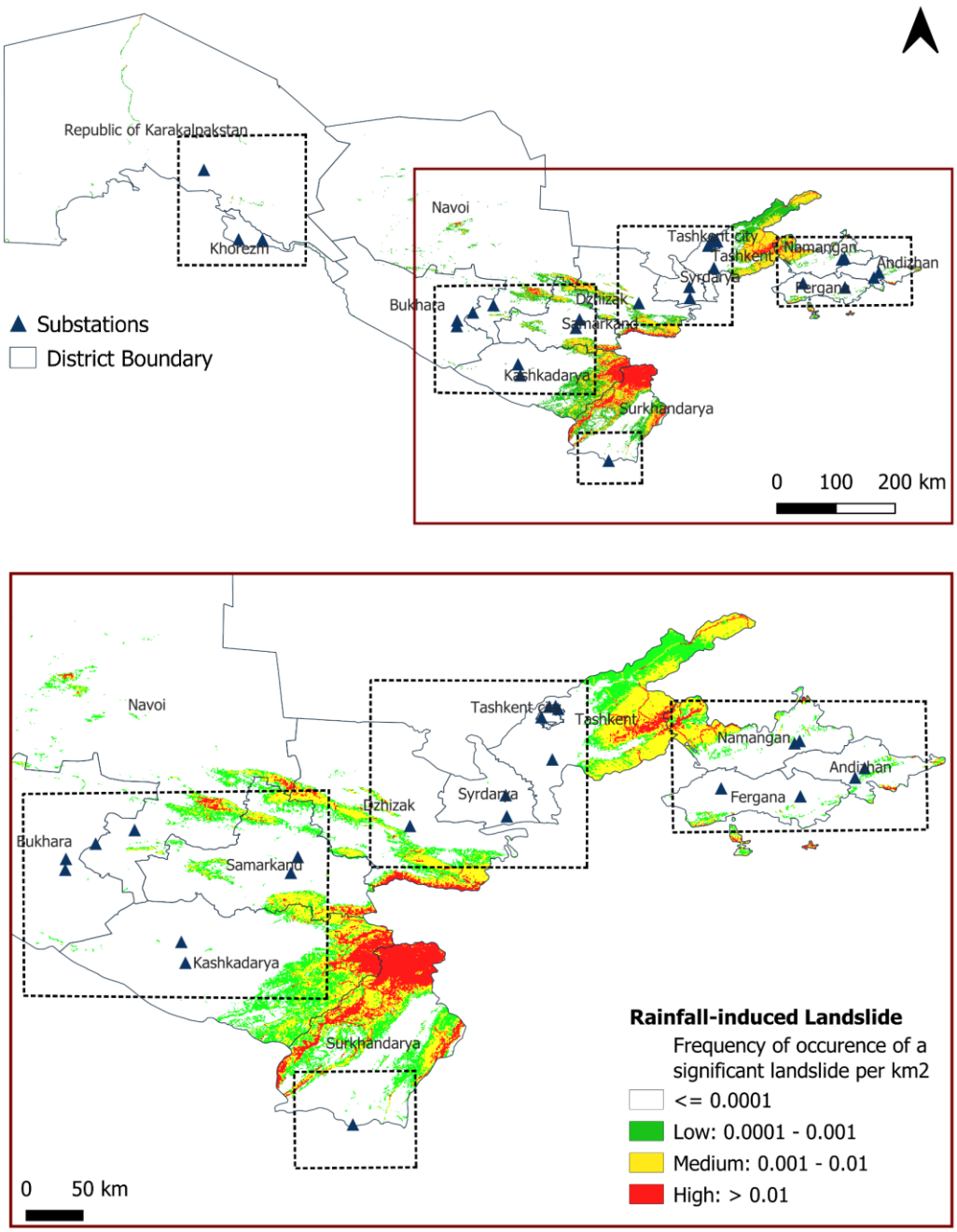

Figure 28. Rainfall-induced landslide hazard across Uzbekistan (Source: Global Landslide Hazard Map: Rainfall trigger, The World Bank).

5.3.5 Wildfire

The wildfire hazard across Uzbekistan is classified as **high**, indicating that there is a greater than 50% probability of weather conditions causing a significant wildfire[1]. The extent of the wildfire hazard zone is also likely to increase in the future, posing a serious risk for major infrastructure developments.

[1] https://thinkhazard.org/en/report/261-uzbekistan/WF

Like the map depicting heat wave hazards across the country (Figure 25), the wildfire hazard (Figure 29) is also categorized as high in areas where the transmission lines and substations are located. The highest hazard is in the regions of Samarkand and Kashkadarya followed by Andizhan. Therefore, extra protection measures need to be in place to minimize damage caused by wildfires.

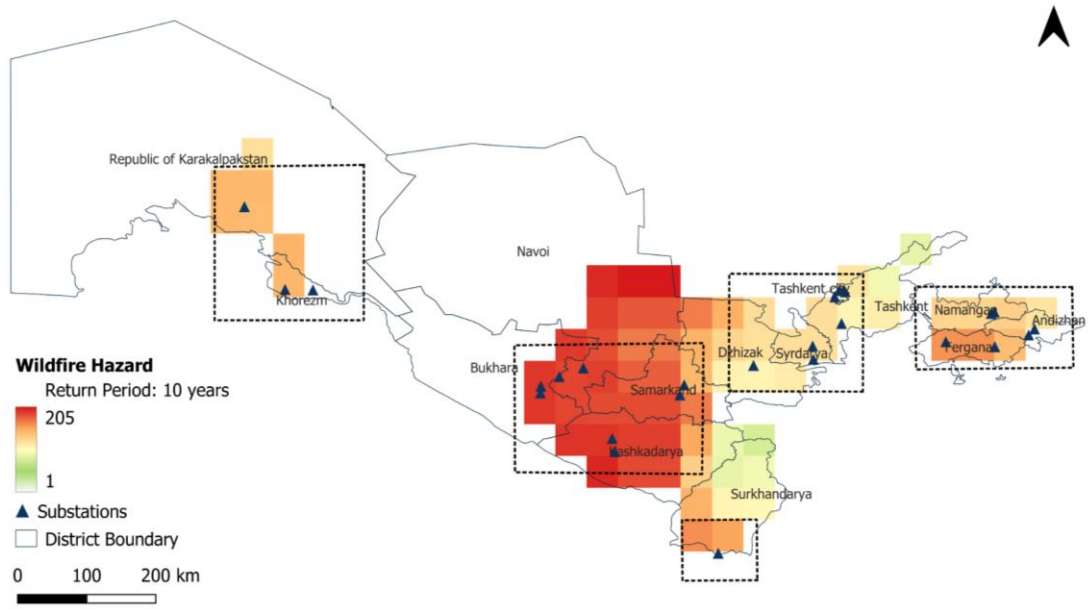

Figure 29. Wildfire hazard across Uzbekistan (Source: Global Facility for Disaster Reduction and Recovery, GeoNode).

5.4 Risk summary table

The climate vulnerability and risk analysis process has gathered several datasets in the public domain, together with local information, associated with each risk to determine the most important risks associated with the project area. Table 15 summarizes this and provides an expert judgement of the risk for the project components.

Table 15. Climate risk assessment of the project outputs.

Hazard	Expected Change in related climate indices	Exposed Project Output	Risk	Detailed comments
Floods	Increase in maximum 5-day rainfall and precipitation intensity predicted by climate model ensemble	All subsations *FerAndNam* *TasSyrDhz* *Sur* *BukSamKas* *KarKho*	**Medium to High** **M** **H** **H** **H** **L**	The substations in the boxes TasSyrDhz, BukSamKas and Sur face the highest risk (>30% of RX5 day) of floods in the future (see Table 12). For these infrastructures, heavy rains and flooding can undermine tower structures through erosion, as well as damage underground cables and infrastructure when moisture comes into contact with the equipment and leads to short-circuiting.
Droughts and heatwaves	Moderate increase in CDD and high increase in extreme temperature predicted by climate model ensemble	All substations *FerAndNam* *TasSyrDhz* *Sur* *BukSamKas* *KarKho*	**High** **H** **H** **H** **M to H** **H**	Across the country, the substations are all at high risk of droughts and heat waves in the future. This is mainly due to a large increase in the average temperature and TXx (~7%) in the future for all the boxes (see section 4.2 and Table 12). High temperatures can damage control systems through loss of information and communications technology service or reduce the quality of service. Drought may also cause additional risk for damage from dust.
Dust storms and wind erosion	Increase in maximum temperature predicted by climate model ensemble	All subsations *FerAndNam* *TasSyrDhz* *Sur* *BukSamKas* *KarKho*	**Medium to High** **M** **M** **M** **H** **H**	The substations in the boxes BukSamKas and KarKho are at high risk of dust storms and wind erosion hazards in the future. The consistent increase in average temperature and TXx (~7%) in the future will likely increase the frequency and magnitude of wind-related hazards (see section 4.2 and Table 12). The increased hazard level may adversely affect energy transmission performance, as dust storms are known to cause corrosion and transmission losses from overhead power lines and can cause damage to pole-mounted transformers and energy distribution systems.
Landslides, water-related erosion, and mudflows	Increase in maximum 1-day and 5-day precipitation predicted by climate model ensemble	All subsations *FerAndNam* *TasSyrDhz*	**Medium** **H** **M**	The consistent increase in the precipitation-related extremes RX1 and RX5 in the future will likely increase the risk of landslide and erosion activity in the region. Moreover,

		Sur *BukSamKas* *KarKho*	**M** **M** **L**	the mountainous part in the east and south are highly vulnerable to landslide hazards.
Wildfire	Increase in maximum temperature predicted by climate model ensemble	All subsations *FerAndNam* *TasSyrDhz* *Sur* *BukSamKas* *KarKho*	**Low** **L** **L** **L** **L** **L**	The project has a low exposure to wildfires, and thus a low-risk level

6 Climate Adaptation Options

The climate risks assessed in the previous chapter urge the adoption of effective adaptation measures to ensure that the project development objectives are not compromised by climatic changes. This chapter presents potential adaptation measures that address both the medium (next decades) and long-term (second half of the century) impacts of climate change.

In general, robust design specifications could allow structures to withstand more extreme conditions (such as floods and dust storms). In some circumstances, it may also be necessary to consider redesigning extremely vulnerable existing infrastructure. The proposed adaptation measures address the following climate risks that were classified as “medium” or “high” in the climate risk assessment. These are:

- **Floods:** Due to the increased frequency and magnitude of rainfall, there is a higher probability of flooding in the region. Therefore, flood-prone areas should be avoided for project implementation and infrastructure solutions or Nature-based solutions should be adopted to further mitigate flood risk.

- **Droughts and heatwaves:** Higher temperatures and increased frequency and duration of heat waves can damage control systems of the transmission and distribution infrastructure.

- **Dust storms and wind erosion:** Strong winds and erosion have already increased the occurrence of dust storms in parts of Uzbekistan. High speed winds can weaken the stability of the transmission and distribution infrastructure; thus, the design should be able to endure extreme weather conditions.

- **Landslides and mudflows:** In areas of higher elevation, there is an increased risk of water-related erosion, landslides and mudflows which can tamper the transmission and distribution infrastructure. Therefore, added protection measures need to be in place to minimize damage and ensure uninterrupted transmission.

- **Wildfire:** Given the increasing number of days with high temperatures, the risk of wildfires erupting during the summer period will likely increase. Distribution substations and associated overhead lines in these areas will be susceptible to fires; therefore, it is crucial to implement mitigation and adaptation strategies to prevent such incidents.

6.1 Options for resilient design

The following adaptation measures comprise both engineering and non-engineering measures. Since Output 3 is related to improved project management and institutional development of JSC-REPN, they are identified as least sensitive to the above-mentioned climate risks.

Optional adaptation measures to be included in the project design have been identified in Table 16 along with the relative cost estimates derived from the relative change in the related climate index. This cost estimate is based on a combination of expert judgement and the projected changes in the climate indices as presented in Table 12. The absolute estimates of the costs and the total adaptation cost can be estimated from these relative figures as soon as the project design with component-specific cost estimates is available.

Table 16. Potential adaptation options for enhanced climate resilience.

Climate Risk	Adaptation Options	Justification for adaptation finance
Floods	Design and construct flood protection measures such as high retaining walls to keep the equipment that is mounted at ground level in substations safe Increase the plinth height of the substation as well as the equipment installed in the substation Expand hydrological monitoring to identify the level of risk and develop an early warning system Develop contingency funds for post-disaster rehabilitation and restoration Substation footings should be located above the highest recorded flood levels Increase drainage facilities in both capacity and number	Implementation of these adaptation options would reduce potential infrastructure damage as well as assist the JSC REPN to forecast climate-induced disasters and better manage the impacts to ensure quick recovery.
Drought and heatwaves	Install more efficient cooling systems for substations Recruit and train staff on fire early response to prevent infrastructure damage Ensure that ICT components and electricity metering systems are certified for higher temperatures	Design and material modifications can enhance the tolerance of the system to high temperatures. Investments should be directed toward installing cooling systems to prevent the substations from malfunctioning due to excessive heat.
Dust storms and Erosion	Ensure that the area in the proximity of the substation infrastructure is free of trees to avoid damages caused by the uprooting trees	Effective planning with respect to the location of substations can significantly minimize the exposure of the infrastructure to high-speed winds.
Landslides and mudflows	Build retaining walls to protect the substation infrastructure	An in-depth assessment of parameters such as slope, and drainage can strengthen the stability of the structures.
Wildfire	Ensure the area is clear of trees and vegetation to minimize the risk of wildfires reaching the substation infrastructure Recruit and train staff on fire early response to prevent infrastructure damage	No/low cost assuming these adaptations are not implemented, given wildfire risk level is low
All risks	Adopt digital solutions and capacity-building measures (described in the following section)	Through a dense hydrometeorological monitoring network, the JSC REPN can

	Expand the meteorological monitoring network to gain a better understanding of variations in climatic conditions and climate-induced disasters	develop a comprehensive database consisting of measurements for different climate variables. These ground observations, in combination with modern tools and technology, can enable JSC REPN to conduct quantitative assessments of climate risks and forecast disasters. Such analyses can lead to the design and implementation of robust adaptation strategies.

6.2 Digital solutions

In addition to the adaptation options above, supervisory control and data acquisition (SCADA) system must be installed in the substations to avoid regional blackouts. Such digital protection relays improve the transmission operation reliability. In particular, SCADA enables the operation dispatch center to gain remote access to real-time data and historical data. Therefore, the use of modern tools would allow JSC REPN to effectively manage critical situations and support the contribution of renewable energy to the national grid.

Moreover, as per United Nations Office for Disaster Risk Reduction (UNDRR) early warning system (EWS) is an integrated part of hazard monitoring forecasting, prediction, assessment, and communication (Meechaiya et al., 2019). Dissemination and communication of flood risk, landslide and dust storm information and early warnings to the operators and managers of JSC REPN could help in improved risk management and adaptation.

6.3 Capacity building measures

Adaptation measures are not limited to engineering interventions but also include capacity building. Output 3 of the project focuses on enhancing the JSC REPN's project management expertise. By establishing a designated risk management unit at JSC REPN, the officials will be able to effectively analyse and manage climate risks. The unit can also be responsible for the timely implementation of the abovementioned adaptation options to minimize the electric system's vulnerability. Without a specialized institution and a well-defined strategy, implementation of adaptation measures becomes a challenge. Additionally, through improved project management skills, JSC REPN can increase the scope, impact, and reach of its activities. Capacity building should enable JSC REPN's staff to analyze climate data, forecast disasters such as floods, explore more climate-resilient materials for substation and transmission operations, and design mitigation and adaptation plans accordingly.

It is equally important for the JSC REPN staff to track the reliability of the electric grid through indices such as System Average Interruption Duration Index (SAIDI) and System Average Interruption Frequency Index (SAIFI)[1]. Through this, JSC REPN can measure its performance and identify areas for improvement.

[1] https://www.ensto.com/company/newsroom/articles/saidi-and-saifi-indices-guiding-towards-more-reliable-distribution-network/

6.4 Strengthening meteorological monitoring capacity

A universal methodology for sensor network design is not available and this is mainly attributed to the diversity of cases, criteria, assumptions, and limitations. The scale of the processes to be monitored and the objectives to be addressed drive the design of meteorological sensors (Chacon-Hurtado et al., 2017). According to the information available for this study, which was taken from the website of the Uzbekistan Hydrometeorological Service[1], the existing meteorological monitoring network consists of one weather station per province, as shown in Figure 30. The density of meteorological sensors in Uzbekistan is about 32,000 Km^2 per station. This number is significantly higher compared to the WMO recommendation as shown in Table 17. Almost 21% (96000 Km^2) of the area of Uzbekistan is covered by mountains. This number suggests almost 38 stations (based on recording type precipitation stations in Table 17) in the mountain and 61 stations in the interior plain regions of Uzbekistan.

Table 17. Recommended minimum densities of stations (area in km^2 per station) as per WMO[2].

Physiographic unit	*Precipitation*		*Evaporation*	*Streamflow*	*Sediments*	*Water quality*
	Non-recording	*Recording*				
Coastal	900	9000	50000	2750	18300	55000
Mountains	250	2500	50000	1000	6700	20000
Interior plains	575	5750	5000	1875	12500	37500
Hilly/undulating	575	5750	50000	1875	12500	47500
Small islands	25	250	50000	300	2000	6000
Urban areas	–	10–20	–	–	–	–
Polar/arid	10000	100000	100000	20000	200000	200000

Figure 30. Meteorological monitoring network of Uzbekistan (Source: Uzhydromet).

Given the topographic variation in Uzbekistan, shown in Figure 31, the existing network does not spatially capture the local weather and climatic conditions adequately. The elevation reaches up to 4,400 meters in northeastern and southeastern provinces, namely Tashkent, Namangan, Surkhdarya and Kashkadarya. The location of the stations in these provinces does not account for weather conditions in the mountainous regions which makes glacial/snow monitoring a challenge. This is crucial to analyse

[1] https://hydromet.uz/
[2] Guide to Hydrological Practices, Volume I: Hydrology – From Measurement to Hydrological Information,WMO

trends and forecast risks relevant to the energy transmission project, especially to monitor temperature and better anticipate heatwaves. Also, extreme rainfall leading to flood risk to the project can be monitored better with a denser network around the project infrastructure. Therefore, it is strongly recommended to install additional hydrometeorological stations in the mountainous regions of these provinces.

Moreover, with respect to historic trends, climate projections and the areal extents of the provinces, the coverage of the existing hydrometeorological monitoring network is considered sparse. As summarized in Table 12, the average percentage change in climate extremes compared to historic extremes is quite significant. Therefore, the density of the network needs to be increased to better monitor the climatic variations and enhance the climate preparedness of the vulnerable regions.

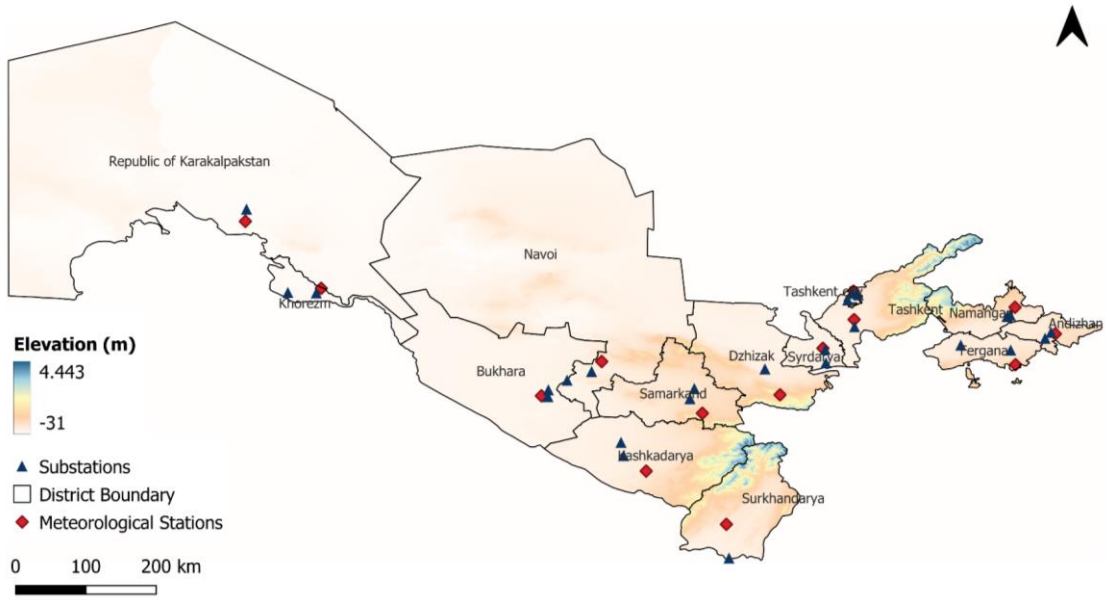

Figure 31. Location of meteorological stations with respect to substations.

As shown in Table 18, the largest distance identified between a substation and the nearest meteorological station is approximately 80 kilometers in Fergana. Assessing climate risks as well as forecasting climate-induced disasters can become a challenge when the monitoring network is limited. Similarly, adaptation options for increasing the climate resilience of project infrastructure can only be effective when the climate risk assessment is data-driven. Through a larger number of hydrometeorological stations, more ground observations can enhance the reliability and accuracy of such analyses.

Table 18. Shortest approximate distance to the nearest meteorological station.

Substation	Region	Shortest distance (km)
SS Yangier	Sirdarya	26.0
SS Galaosiyo	Bukhara	14.0
SS Strelkova	Bukhara	9.0
SS Sagban	Tashkent	4.5
SS Dungkurgon	Tashkent	13.0
SS Charkhi	Fergana	80.0
SS Khalkabad	Karakalpakstan	23.0
SS Namangan	Namangan	15.0

SS Malikchul	Navoi	56.5
SS Beshkent	Kashkadarya	41.0
SS Vokzal	Namangan	19.0
SS Yunusabad	Tashkent	6.0
SS Zilol	Dzhizak	49.0
SS Atlas	Fergana	26.0
SS Yayilma	Andizhan	6.5
SS Botanicheskaya	Tashkent	9.0
SS Koson	Kashkadarya	60.0
SS Markaz	Sirdarya	4.0
SS Juma	Samarkand	30.0
SS Gilamchi	Khorezm	44.0
SS Loish	Samarkand	44.0
SS Bagat	Khorezm	11.0
SS Termez	Surkhandarya	59.0
SS Asaka	Andizhan	16.0
SS Eshonguzaar	Tashkent	18.0
SS Karmana	Navoi	22.0

More generally, beyond this specific project, the map showing the population density by province (Figure 32) also indicates that the majority of the population is concentrated in eastern parts of Uzbekistan, starting from the province of Bukhara. This means that the large population in these areas is vulnerable to risks associated with high elevation such as landslides and floods. Thus, for improved climate-induced disaster mitigation and preparedness, improved surveillance is required in this region.

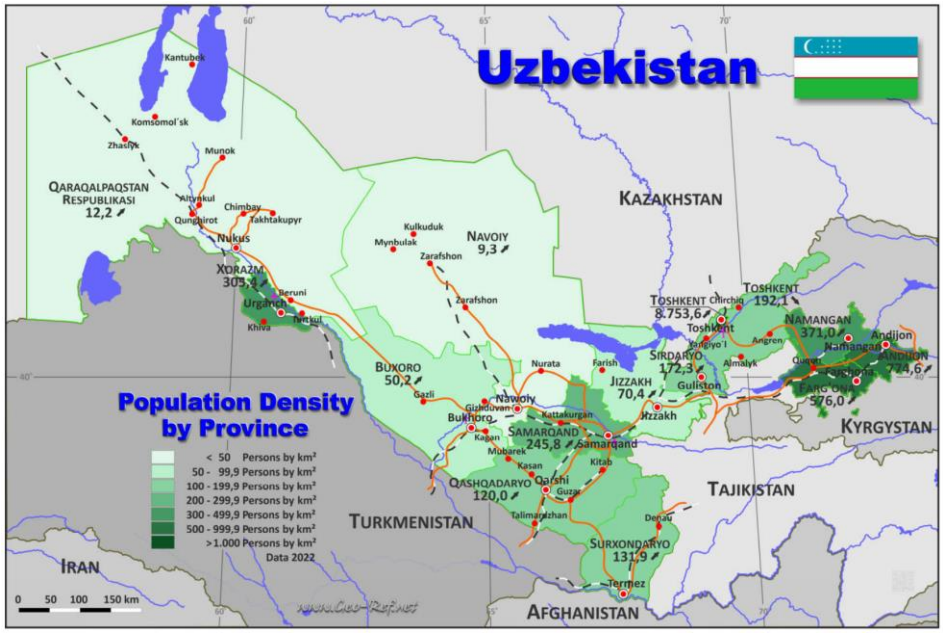

Figure 32. Population density by province (Source: Geo-ref.net).

7 Climate Mitigation

This CRA focuses on climate change risks to the projects and possible adaptation measures to be included in the project to respond and reduce those risks to an acceptable level. Projects however may also have the potential to contribute to climate mitigation, i.e. have a positive impact through the reduction of greenhouse gas (GHG) emissions. Due to increasing annual emission rates of carbon dioxide and methane (Smith et al., 2015), global temperature is rising rapidly, but even more in some areas of the world, as also in Uzbekistan. Since the early 1950s, the average rate of increase in air temperature in Uzbekistan has been 0.29°C for every ten years[1], which is twice the rate of global warming.

Despite being relatively minimal contributors to the overall greenhouse gas emissions, developing countries can have a crucial role to play in order to limit their emissions. As per Uzbekistan's revised Nationally Determined Contribution (NDC, 2021), the country has committed to reducing its specific greenhouse gas emissions per unit of GDP by 35% (compared to the level in 2010), by the year 2030. The previously intended goal was set at 10%. This means that Uzbekistan must accelerate its efforts on multiple fronts in order to fulfil its commitment. Higher energy efficiency and a diverse energy mix are essential to significantly reduce GHG emissions as this sector currently accounts for approximately 76% of the national GHG emissions[2] (Figure 33).

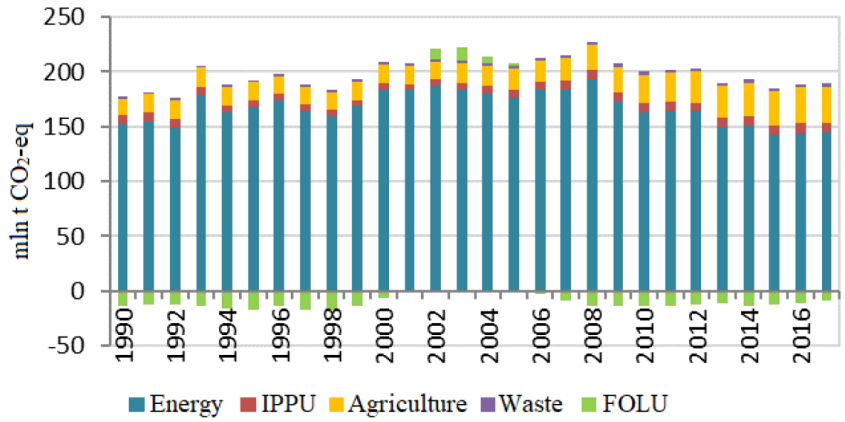

Figure 33. Dynamics of greenhouse gas emissions for 1990-2017 by sectors (Source: Updated NDC, 2021).

Uzbekistan is one of the world's largest producers of natural gas, annually producing approximately 60 billion cubic metres[3]. As shown in Table 16, extraction, processing, transportation of natural gas accounts for 22.6 percent of the total GHG emissions, followed by combustion of fuels for power generation (15.2 percent). Compared to 2010, the percentage of GHGs emitted from the fuel combustion for power generation increased by almost 2 percent in 2017 despite the pledge to cut down emissions. An aging power transmission system means higher transmission and distribution losses which leads to increased combustion of fuels to meet the swelling energy demands.

[1] Updated Nationally Determined Contribution, 2021. https://unfccc.int/sites/default/files/NDC/202206/Uzbekistan_Updated%20NDC_2021_EN.pdf
[2] Nationally Determined Contribution, 2017.
[3] https://www.iea.org/reports/uzbekistan-energy-profile

Table 19. Greenhouse gas emissions and removals in 2010-2017 (Source: Updated NDC, 2021).

Sector	IPCC category	2010 GHG emissions / removals (Gg of CO_2-eq)	Share of the source in the total emission, %	2017 GHG emissions / removals (Gg of CO_2-eq)	Share of the source in the total emission, %
		A	B	C	D
Energy	Extraction, processing, transportation of natural gas	63,783.31	27.1	47,370.58	22.6
	Fuel combustion. Residential sector	32,170.63	13.7	19,627.03	9.4
	Fuel combustion. Power generation	31,611.01	13.4	31,933.28	15.2
	Fuel combustion. Commercial sector	10,519.01	4.5	6,113.32	2.9
	Fuel combustion. Processing industry and construction	7,580.12	3.2	21,214.68	10.1
	Road transport	7,465.28	3.2	11,900.08	5.7
	Other means of transport	5,375.21	2.3	3,781.49	1.8
	Oil production and refining	2,732.12	1.2	1,872.12	1.7
	Fuel combustion. Agriculture	1,435.73	0.6	54.72	0.0
	Railway transport	498.63	0.2	354.26	0.2
	Solid fuels	109.24	<0.1	127.66	0.1
	Civil aviation	100.62	<0.1	58.46	<0.1
	Total for sector	**163,380.91**		**144,407.83**	

Therefore, it is critical to not only upgrade the existing infrastructure to minimize losses but also diversify the energy mix and promote the development of renewable energy to sustainably meet the growing demands. The updated NDC (2021) recognizes the importance of structural reforms and prioritizes energy efficiency measures and expansion of renewable energy sources. However, such development agendas require investment. As part of this project, ADB has agreed to fund the implementation of climate mitigation and adaptation measures. To secure climate financing, it is important to provide an estimate of the GHG emission reduction attributable to the proposed project interventions. Therefore, ADB has developed two harmonized guidance documents on GHG accounting: one for energy efficient projects and another for renewable energy projects (ADB, 2017).

7.1 Methods

The GHG emissions are typically calculated as per the methodology outlined in the guidelines for *Energy Efficiency Projects (Improvement of Existing Electricity Transmission and Distribution System)*[1] specifically. This methodology is applicable for projects that aim to reduce electricity losses by improving the existing transmission and distribution system by either reconductoring, controlling power flow, optimizing transformer locations etc. The key components are:

Emission Reduction (*ER*)
Emission reduction is the difference between baseline and project emissions when the T&D system delivers the same amount of electrical power or energy.

$ER = BE - PE$

where:
BE = baseline emission
PE = project emission

Baseline Emission (*BE*)
BE is the amount of emissions generated by the existing T&D when delivering the same amount of electricity as the project.

[1] Guidelines for Estimating Greenhouse Gas Emissions of ADB project, April 2017. http://dx.doi.org/10.22617/TIM178659-2

BEe = ECb × EFgrid/(1-%Lb)

where:
BEe = Baseline emission for the T&D system, tCO_2/year
ECb = annual electricity delivered by the existing T&D system, MWh/year
%Lb = baseline T&D losses expressed as decimal equivalent (i.e. 20% loss is expressed as 0.20)
EFgrid = combined emission factor for the grid, tCO_2/MWh

Project emission (*PE*)
Project emission is the amount of emissions generated by the project activity.

PEe = ECp × EFgrid/(1-%Lp)

where:
PEe = Project emission from the project activity, tCO_2/year
ECp = annual electricity delivered by the project activity, MWh/year;
%*Lp* = project T&D losses expressed as decimal equivalent (i.e. 20% loss is expressed as 0.20)
EFgrid = combined emission factor for the grid, tCO_2/MWh

However, for this project, the engineering team at ADB adopted the following approach to quantify the reduction in greenhouse gas emissions:

*GHG emission reduction (tCO_2e/year) = Energy savings (per year) * grid emission factor*

where:
Energy savings = Reduction in power loss as a result of modernization and increased efficiency (MWh/year)
Grid emission factor = A country-specific factor that represents the average GHG emissions intensity of the electricity grid (tCO_2/MWh)

7.2 Results

By modernizing 26 substations, the reduction in losses is estimated to be 33,316 MWh per year. Using this energy saving as well as Uzbekistan's grid emission factor (0.533 tCO2e/MWh), the reduction in greenhouse gas emissions is calculated to be 17,757 tCO_2e/year[1].

Table 20. Reduction in greenhouse gas emissions

Mitigation Activity	Estimated GHG Emissions Reduction (tCO_2e/yr)	Estimated Mitigation Costs ($ million)	Mitigation Finance Justification
Retrofit of distribution systems to reduce technical losses including improving grid reliability	17,757	124.3	The project will rehabilitate the old and inefficient substations to improve grid reliability while reducing technical losses in the system. For T&D projects, 40% factor is applied following the Guidance Note on Counting Climate Finance in Energy[2]

[1] Calculated by the engineering team at ADB
[2] ADB (Sustainable Development and Climate Change Department; Strategy and Policy Department). 2017. Guidance Note on Counting Climate Finance in Energy. Memorandum. 5 January (internal).

8 References

ADB. (2012). *Climate Risk and Adaptation in the Electric Power Sector*. Manila, Philippines.

ADB. (2013). *Guidelines for climate proofing investment in the energy sector*. Manila, Philippines.

ADB. (2014). *Climate Risk Management in ADB projects*. Manila.

ADB. (2016). *Guidelines for Climate Proofing Investment in the Water Sector - Water Supply and Sanitation*. Manila.

Chacon-Hurtado, J. C., Alfonso, L., & Solomatine, D. P. (2017). Rainfall and streamflow sensor network design: A review of applications, classification, and a proposed framework. *Hydrology and Earth System Sciences*, *21*(6), 3071–3091. https://doi.org/10.5194/hess-21-3071-2017

FutureWater. (2020). Draft Final Report for the Detailed Risk and Vulnerability Assessment for preparing ADB's Climate Adaptive Water Resources Management in the Aral Sea Basin Project, (August).

Immerzeel, W.W., Wanders, N., Lutz, A. F., Shea, J. M., & Bierkens, M. F. P. (2015). Reconciling high altitude precipitation with glacier mass balances and runoff. *Hydrology and Earth System Sciences*, *12*, 4755–4784. https://doi.org/10.5194/hessd-12-4755-2015

Immerzeel, W W, Wanders, N., Lutz, A. F., Shea, J. M., & Bierkens, M. F. P. (2015). Reconciling high-altitude precipitation in the upper Indus basin with glacier mass balances and runoff. *Hydrology and Earth System Sciences*, *19*(11), 4673–4687. https://doi.org/10.5194/hess-19-4673-2015

Immerzeel, Walter Willem, Pellicciotti, F., & Shrestha, A. B. (2012). Glaciers as a Proxy to Quantify the Spatial Distribution of Precipitation in the Hunza Basin. *Mountain Research and Development*, *32*(1), 30–38. https://doi.org/10.1659/MRD-JOURNAL-D-11-00097.1

Khanal, S., Lutz, A. F., Kraaijenbrink, P. D. A., van den Hurk, B., Yao, T., & Immerzeel, W. W. (2021). Variable 21st Century Climate Change Response for Rivers in High Mountain Asia at Seasonal to Decadal Time Scales. *Water Resources Research*, *57*(5), e2020WR029266. https://doi.org/10.1029/2020wr029266

Khanal, S., Tiwari, S., Lutz, A. F., Hurk, B. V. D., & Immerzeel, W. W. (2023). Historical Climate Trends over High Mountain Asia Derived from ERA5 Reanalysis Data, 263–288. https://doi.org/10.1175/JAMC-D-21-0045.1

Lange, S., Volkholz, J., Geiger, T., Zhao, F., Vega, I., Veldkamp, T., et al. (2020). Projecting Exposure to Extreme Climate Impact Events Across Six Event Categories and Three Spatial Scales. *Earth's Future*, *8*(12), 1–22. https://doi.org/10.1029/2020EF001616

Mamadjanova, G., & Leckebusch, G. C. (2022). Assessment of mudflow risk in Uzbekistan using CMIP5 models. *Weather and Climate Extremes*, *35*(March), 100403. https://doi.org/10.1016/j.wace.2021.100403

Meechaiya, C., Wilkinson, E., Lovell, E., Brown, S., & Budimir, M. (2019). the Governance of Warning System Opportunities Under Federalism, 48.

Thrasher, B., Wang, W., Michaelis, A., Melton, F., Lee, T., & Nemani, R. (2022). NASA Global Daily Downscaled Projections, CMIP6. *Scientific Data 2022 9:1*, *9*(1), 1–6. https://doi.org/10.1038/s41597-022-01393-4

Ward, P. J., Winsemius, H. C., Kuzma, S., Bierkens, M. F. P., Bouwman, A., Moel, H. DE, et al. (2020). Aqueduct Floods Methodology. *World Resources Institute*, (January), 1–28. Retrieved from www.wri.org/publication/aqueduct-floods-methodology

WB, & ADB. (2020). Climate risk country profile - Uzbekistan, 32. Retrieved from www.worldbank.org

Appendix A: Past and Future Climate trends

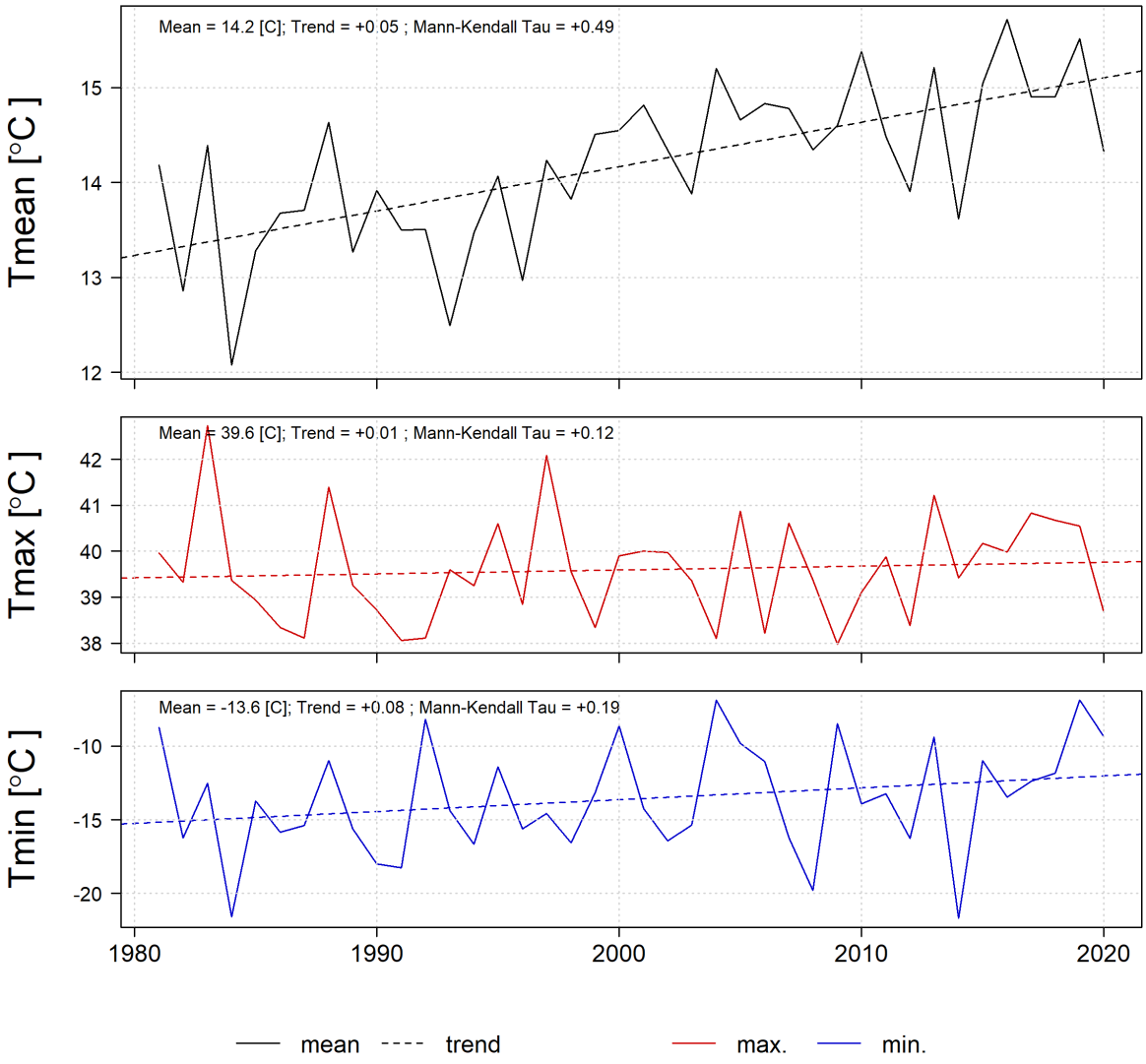

Figure A1: Average, maximum and minimum yearly temperatures from ERA5-Land dataset with trendline for box TasSyrDhz as shown in Figure 5.

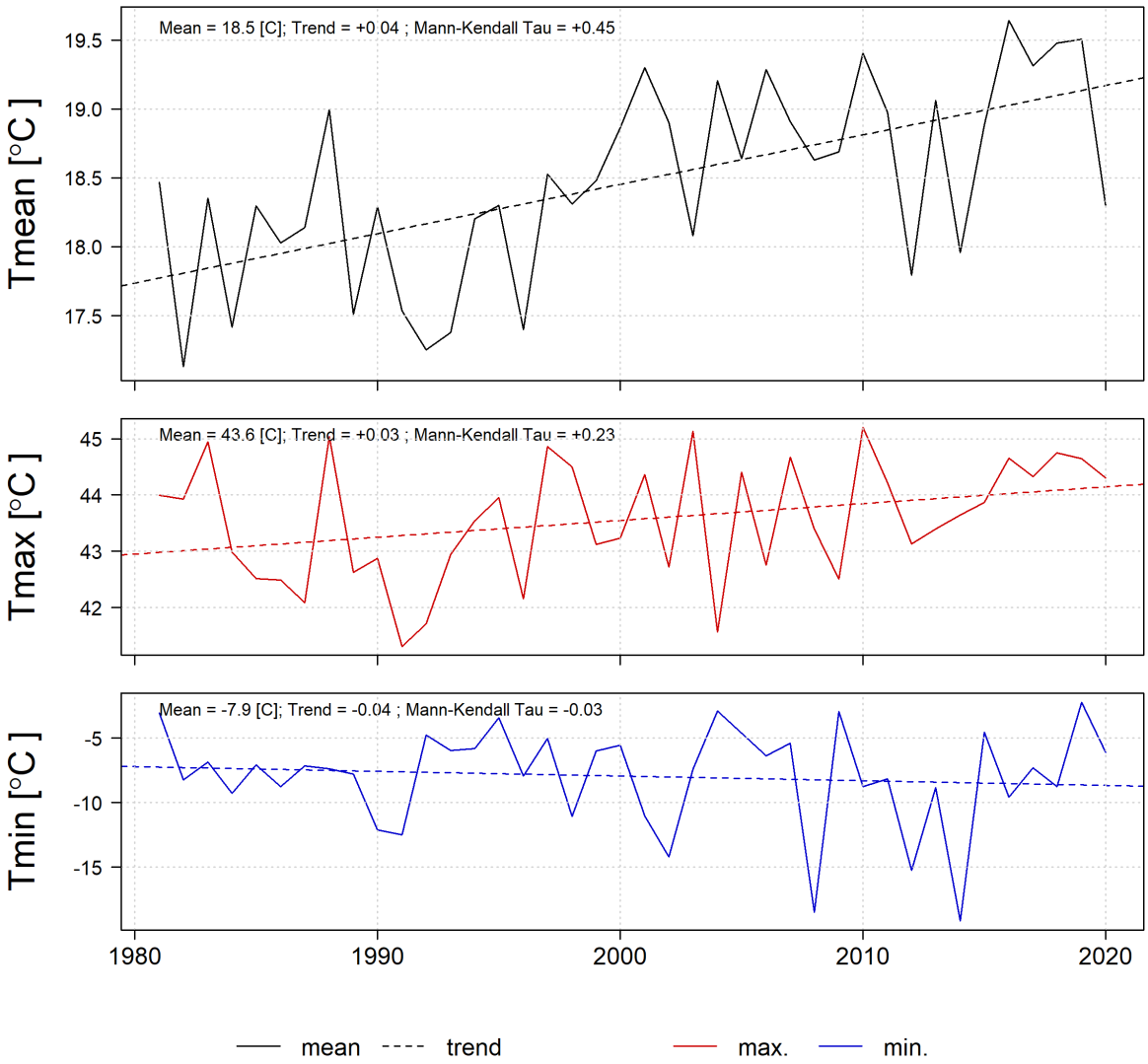

Figure A2: Average, maximum and minimum yearly temperatures from ERA5-Land dataset with trendline for box Sur as shown in Figure 5.

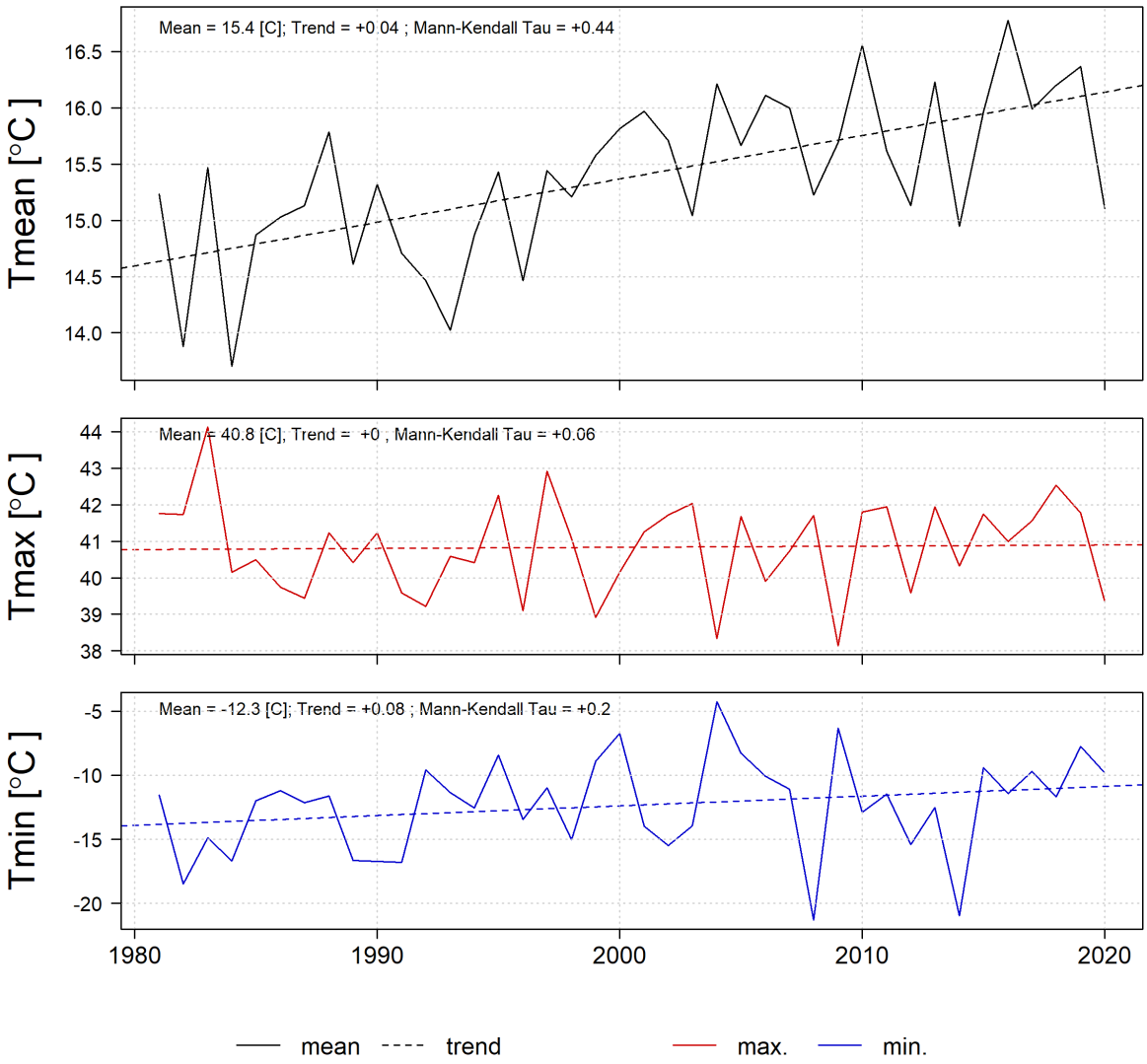

Figure A3: Average, maximum and minimum yearly temperatures from ERA5-Land dataset with trendline for box BukSamKas as shown in Figure 5.

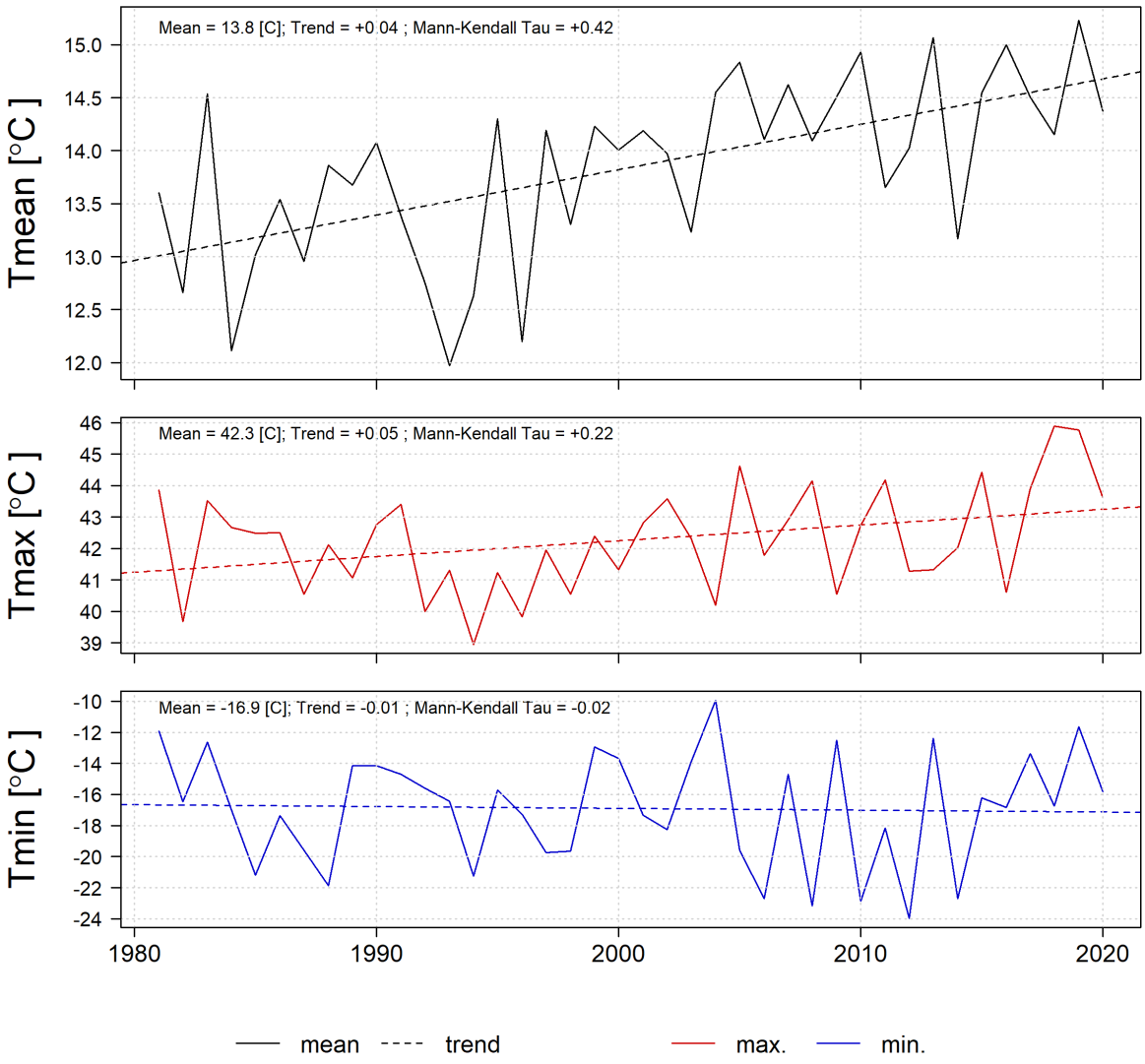

Figure A4: Average, maximum and minimum yearly temperatures from ERA5-Land dataset with trendline for box KarKho as shown in Figure 5.

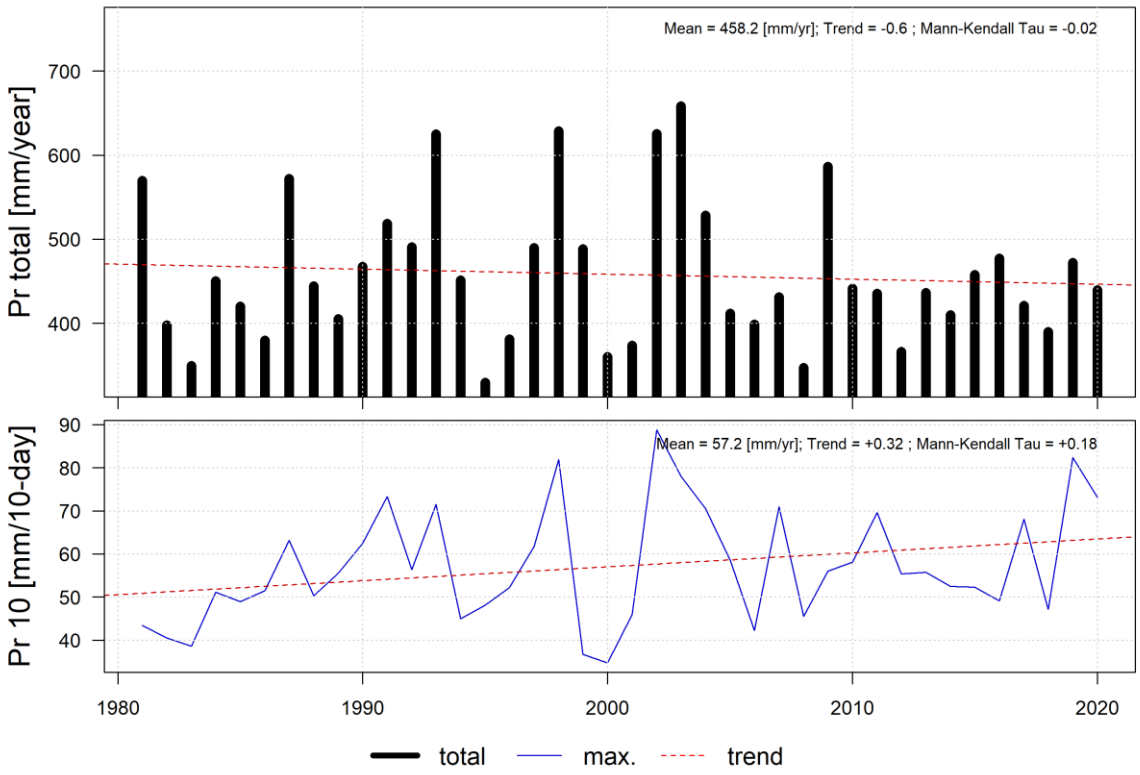

Figure A5: Total yearly and 10-day maximum cumulative precipitation with a trendline for box TasSyrDhz as shown in Figure 5. Mann Kendall Tau value indicates the strength of the monotonic trend of increase or decrease in a time series, with a value of 1 indicating a strong significant trend and -1 indicating no trend.

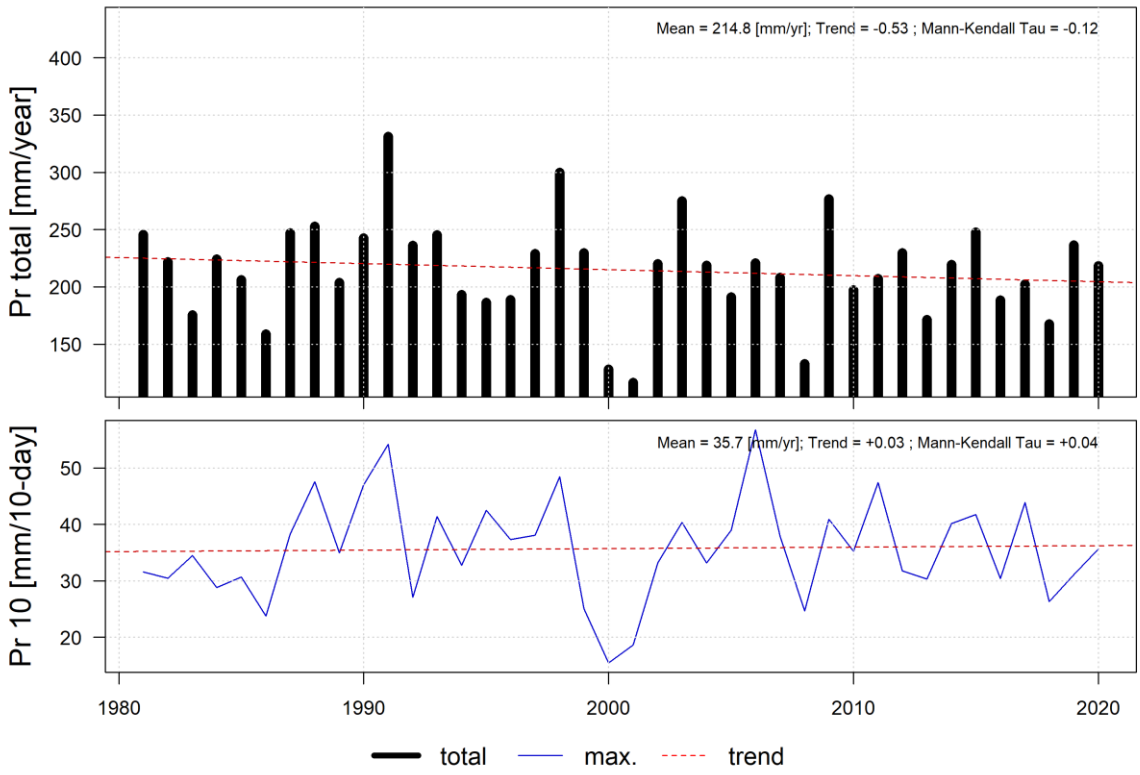

Figure A6: Total yearly and 10-day maximum cumulative precipitation with a trendline for box Sur as shown in Figure 5. Mann Kendall Tau value indicates the strength of the monotonic trend of increase or decrease in a time series, with a value of 1 indicating a strong significant trend and -1 indicating no trend.

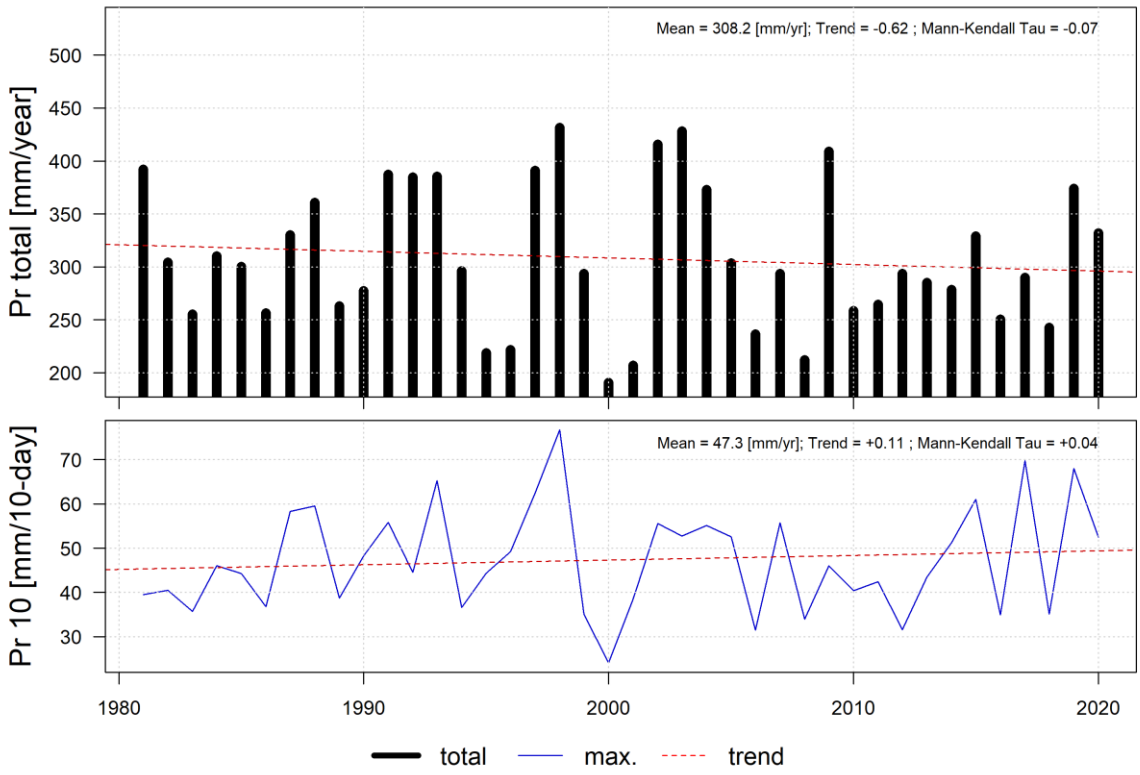

Figure A7: Total yearly and 10-day maximum cumulative precipitation with a trendline for box BukSamKas as shown in Figure 5. Mann Kendall Tau value indicates the strength of the monotonic trend of increase or decrease in a time series, with a value of 1 indicating a strong significant trend and -1 indicating no trend.

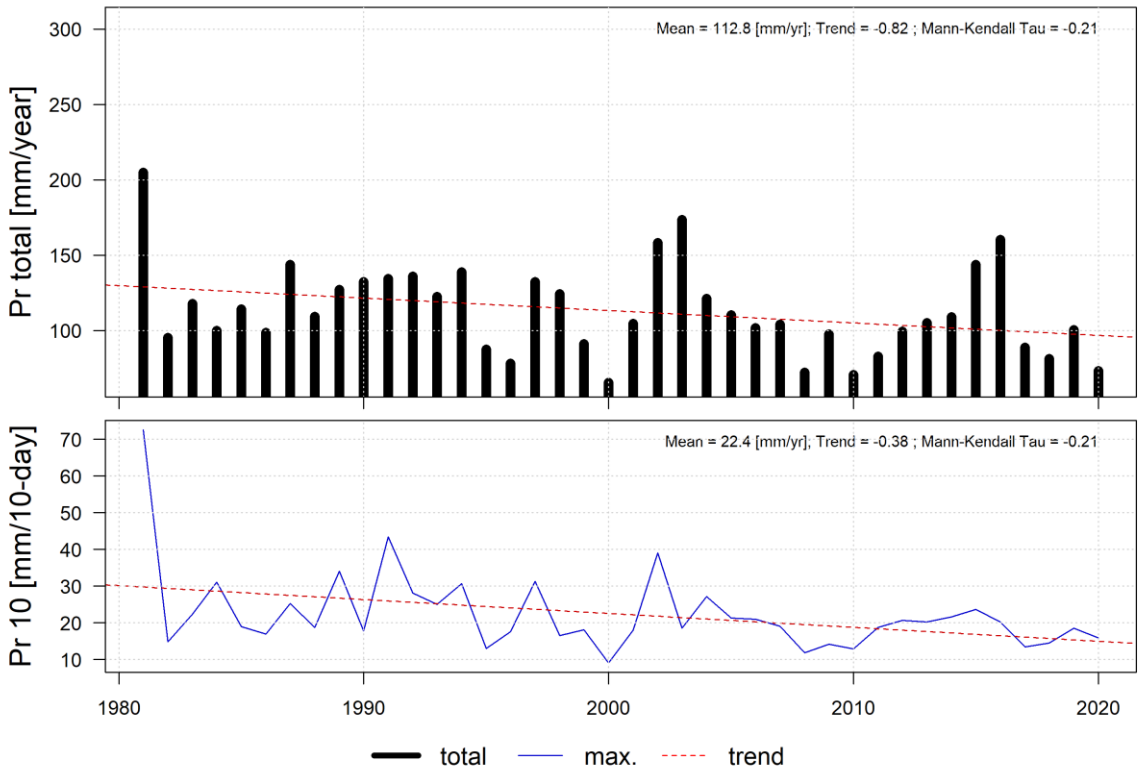

Figure A8: Total yearly and 10-day maximum cumulative precipitation with a trendline for box KarKho as shown in Figure 5. Mann Kendall Tau value indicates the strength of the monotonic trend of increase or decrease in a time series, with a value of 1 indicating a strong significant trend and -1 indicating no trend.

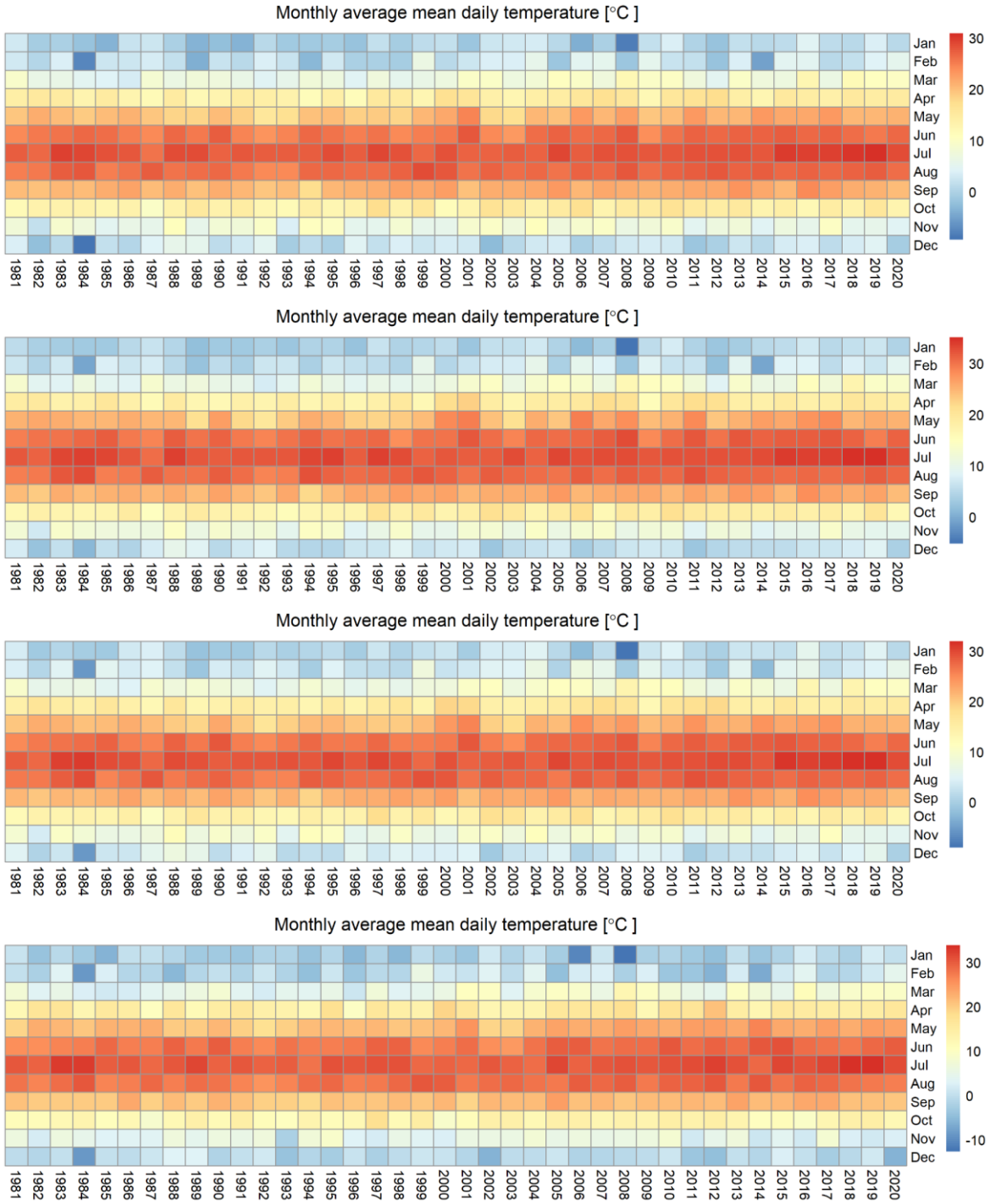

Figure A9: Seasonality in mean temperature from ERA5-Land dataset for box TasSyrDhz, Sur, BukSamKas and KarKho as shown in Figure 5.

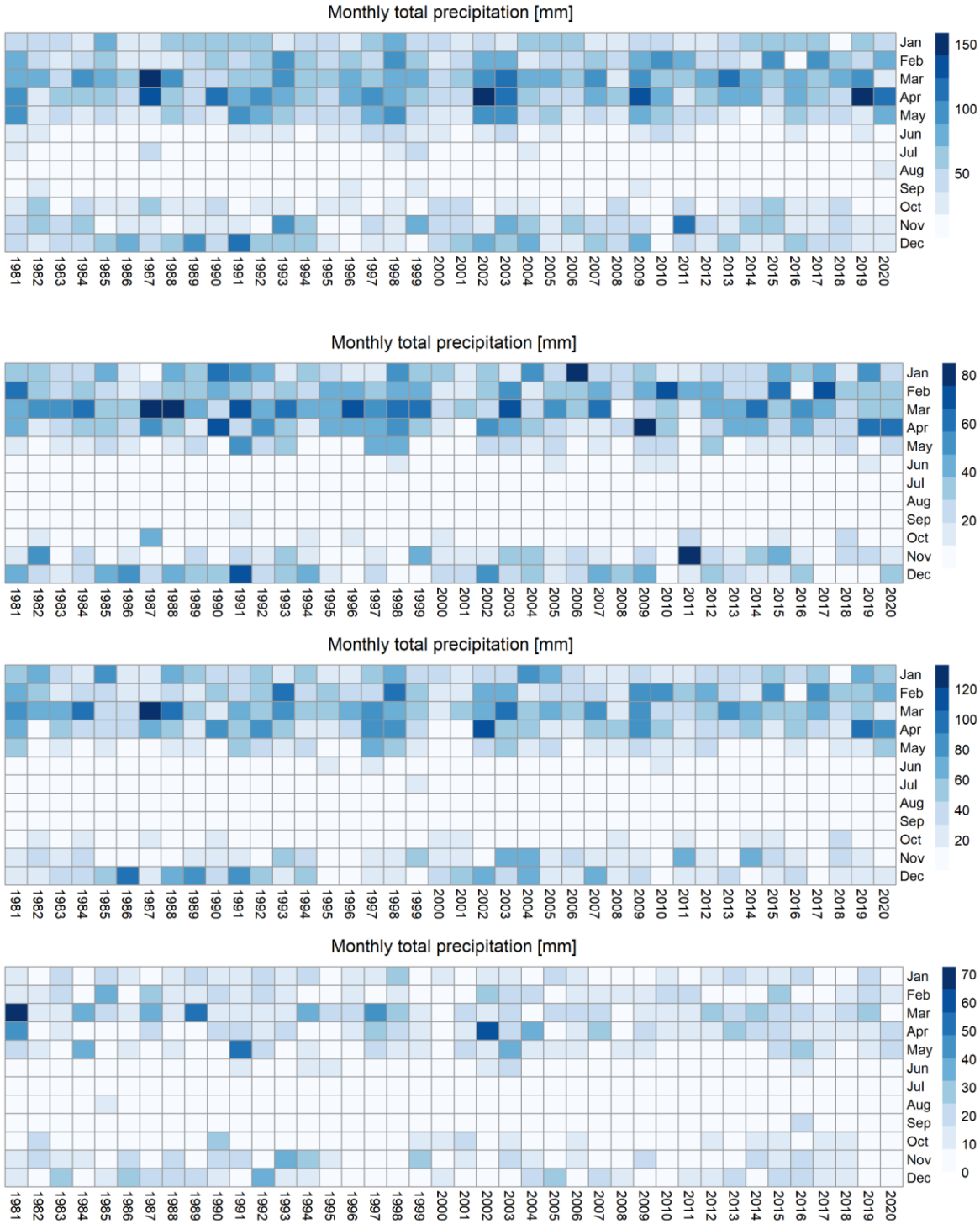

Figure A10: Seasonality in annual precipitation from ERA5-Land dataset for box TasSyrDhz, Sur, BukSamKas and KarKho as shown in Figure 5.

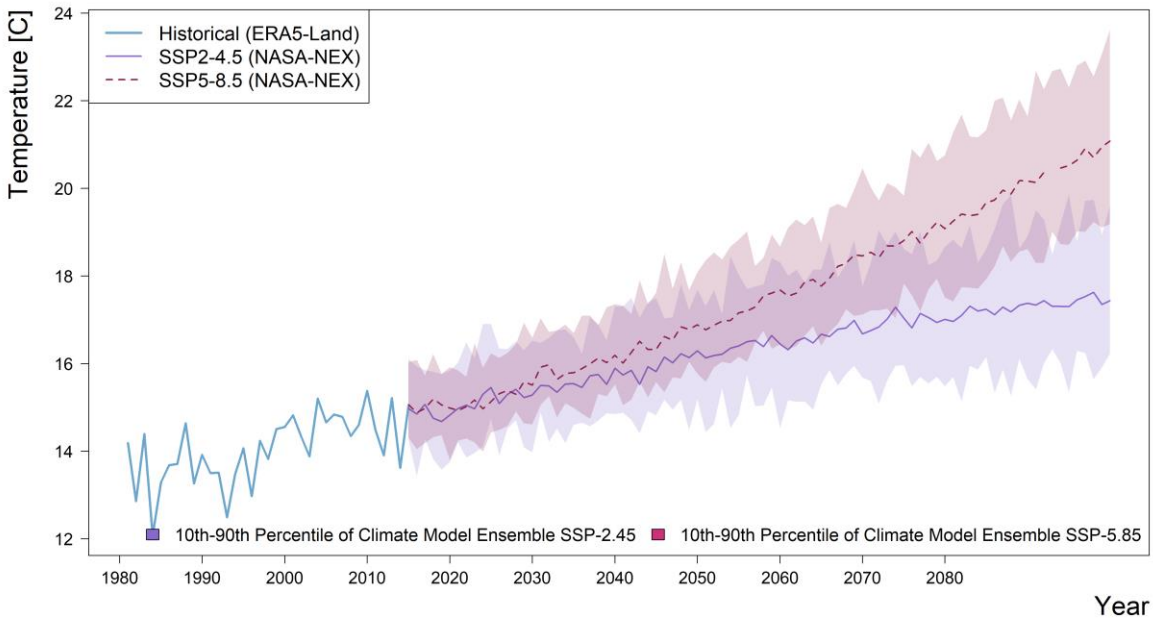

Figure A11: Time series of mean yearly ERA5-Land temperature for the box TasSyrDhz for the historical period (1981–2020), and NASA NEX (per model bias-corrected) for the future period. Shaded areas show the 10th and 90th percentiles in the spread of model predictions

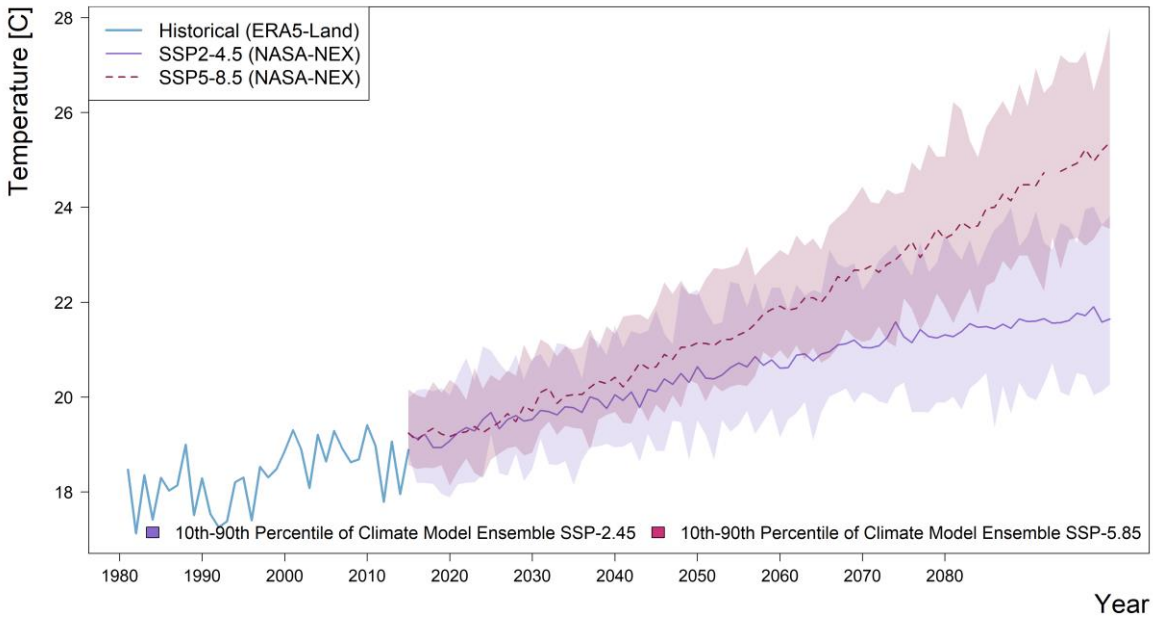

Figure A12: Time series of mean yearly ERA5-Land temperature for the box Sur for the historical period (1981–2020), and NASA NEX (per model bias-corrected) for the future period. Shaded areas show the 10th and 90th percentiles in the spread of model predictions.

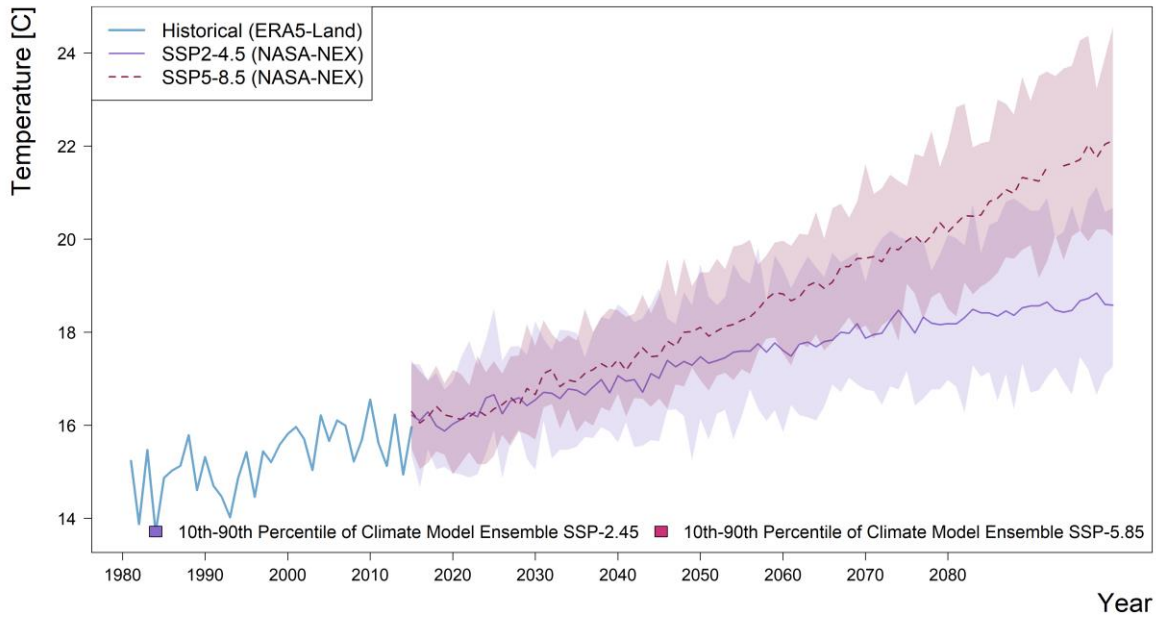

Figure A13: Time series of mean yearly ERA5-Land temperature for the box BukSamKas for the historical period (1981–2020), and NASA NEX (per model bias-corrected) for the future period. Shaded areas show the 10th and 90th percentiles in the spread of model predictions.

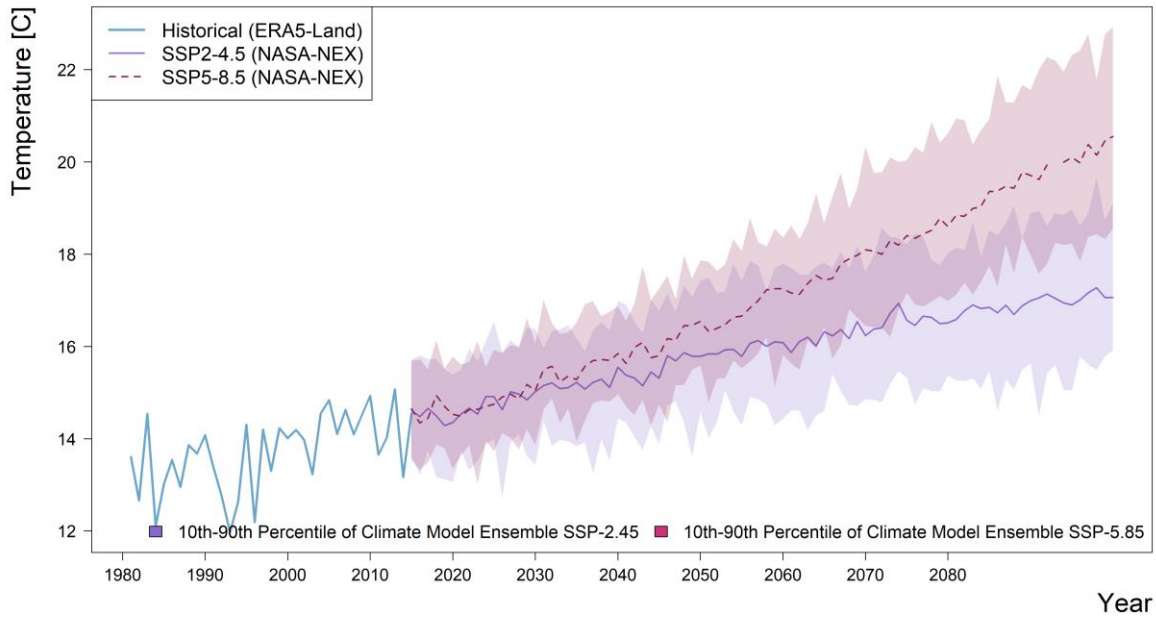

Figure A14: Time series of mean yearly ERA5-Land temperature for the box KarKho for the historical period (1981–2020), and NASA NEX (per model bias-corrected) for the future period. Shaded areas show the 10th and 90th percentiles in the spread of model predictions.

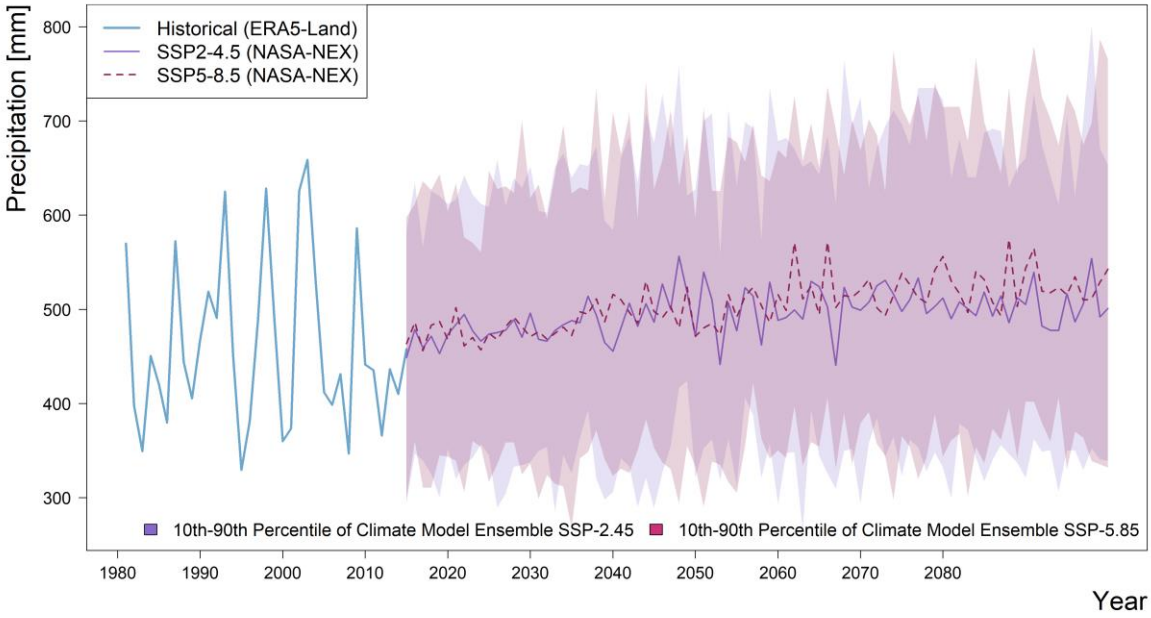

Figure A15: Time series of yearly ERA5-Land precipitation for the box TasSyrDhz for the historical period (1981–2020), and NASA NEX (per model bias-corrected) for the future period. Shaded areas show the 10th and 90th percentiles in the spread of model predictions.

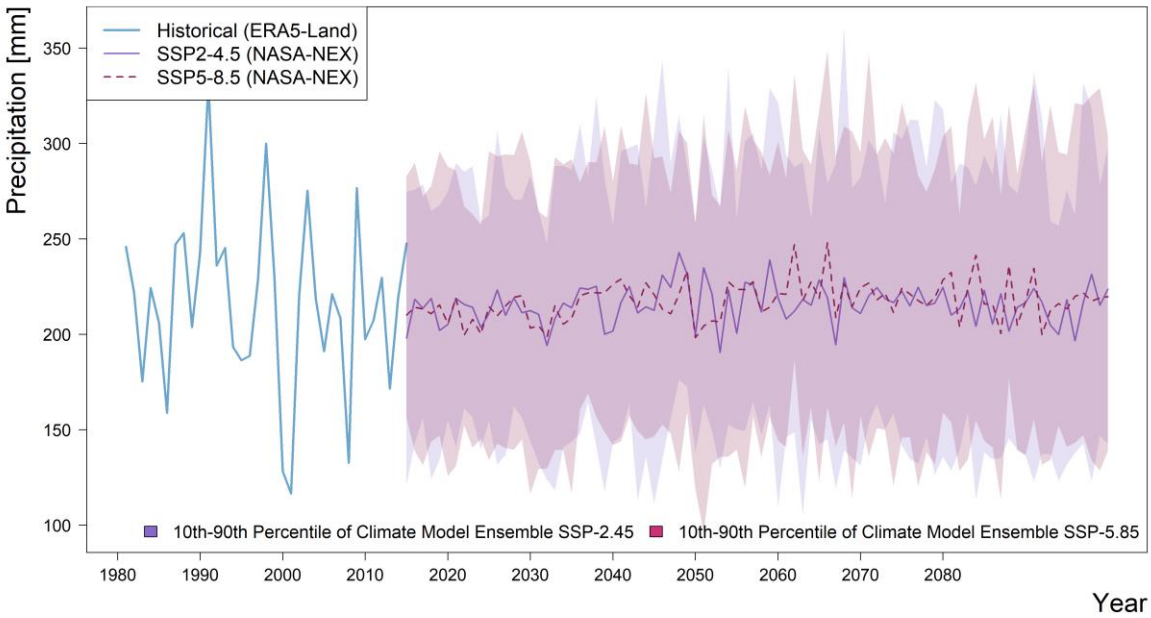

Figure A16: Time series of yearly ERA5-Land precipitation for the box Sur for the historical period (1981–2020), and NASA NEX (per model bias-corrected) for the future period. Shaded areas show the 10th and 90th percentiles in the spread of model predictions.

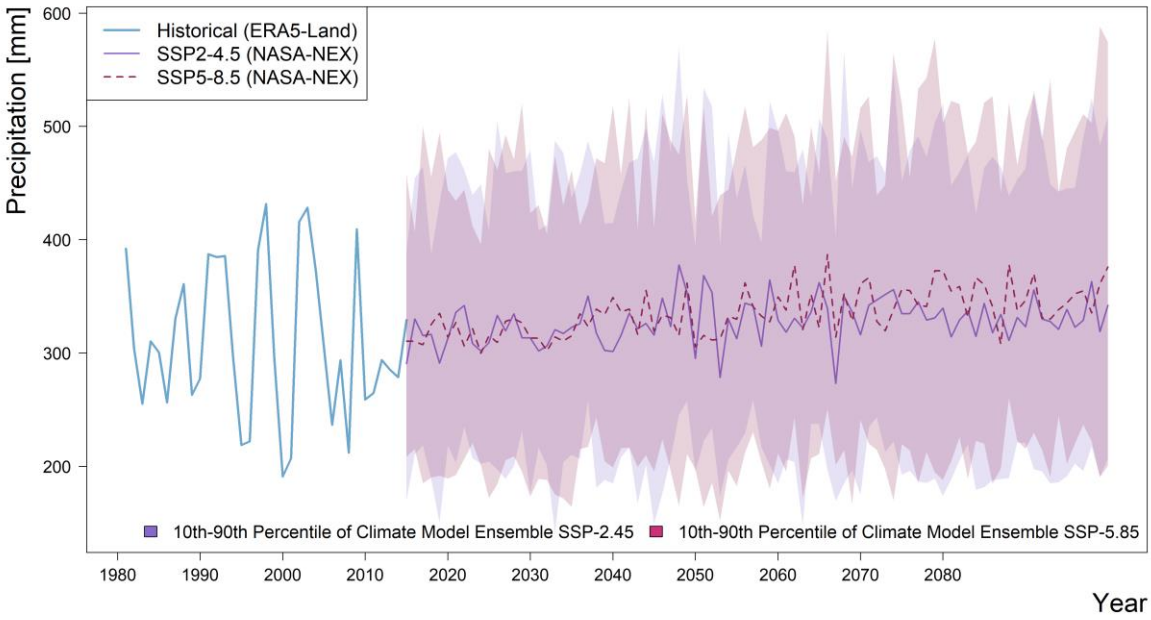

Figure A17: Time series of yearly ERA5-Land precipitation for the box BukSamKas for the historical period (1981–2020), and NASA NEX (per model bias-corrected) for the future period. Shaded areas show the 10th and 90th percentiles in the spread of model predictions.

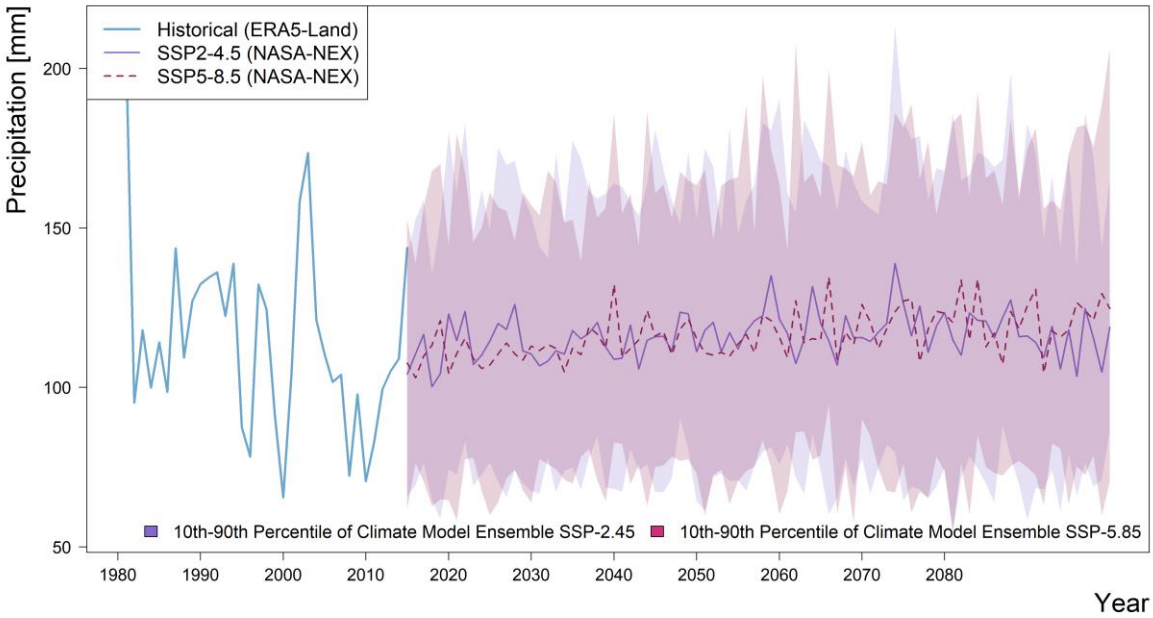

Figure A18: Time series of yearly ERA5-Land precipitation for the box KarKho for the historical period (1981–2020), and NASA NEX (per model bias-corrected) for the future period. Shaded areas show the 10th and 90th percentiles in the spread of model predictions.

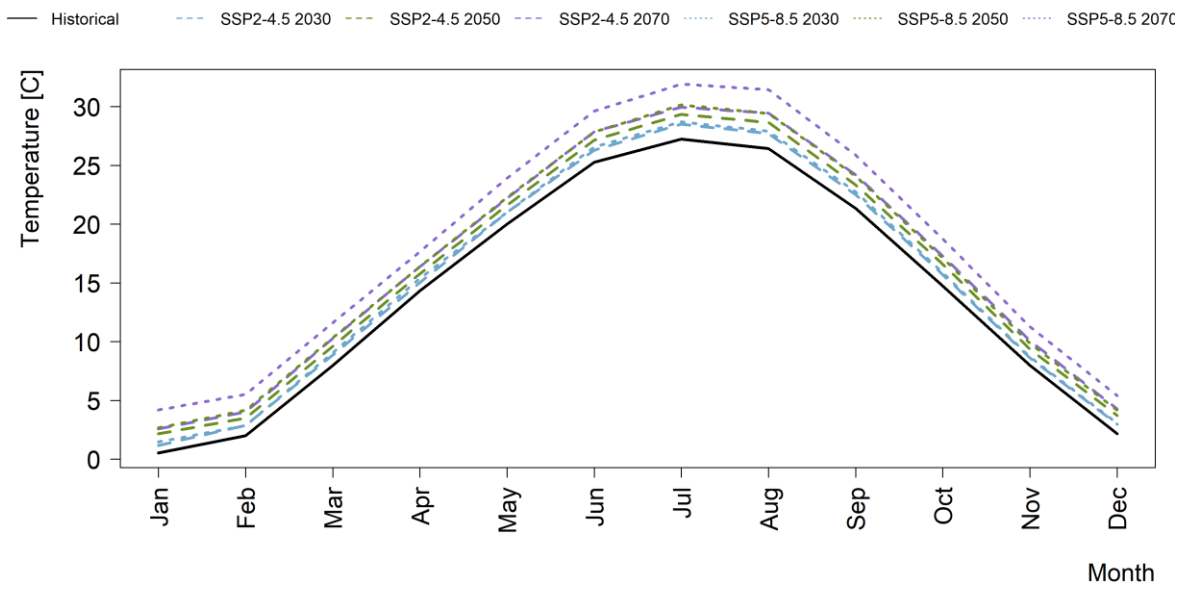

Figure A19: Average monthly temperature for historical (1995–2014) and future (time horizons under the two SSP scenarios for the box TasSyrDhz.

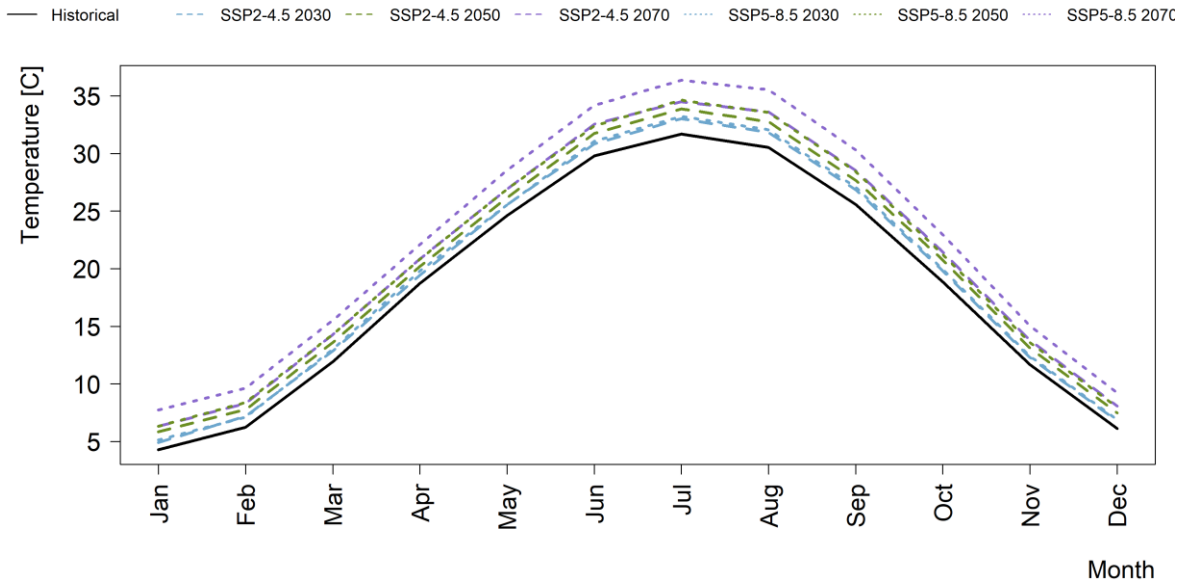

Figure A20: Average monthly temperature for historical (1995-2014) and future (time horizons under the two SSP scenarios for the box Sur.

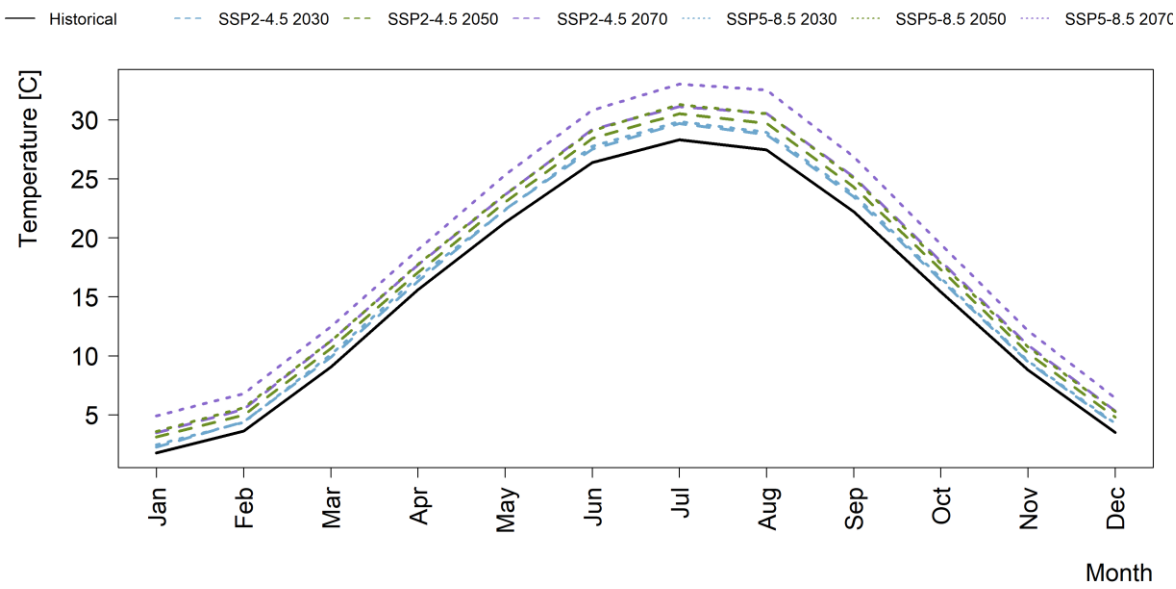

Figure A21: Average monthly temperature for historical (1995–2014) and future (time horizons under the two SSP scenarios for the box BukSamKas.

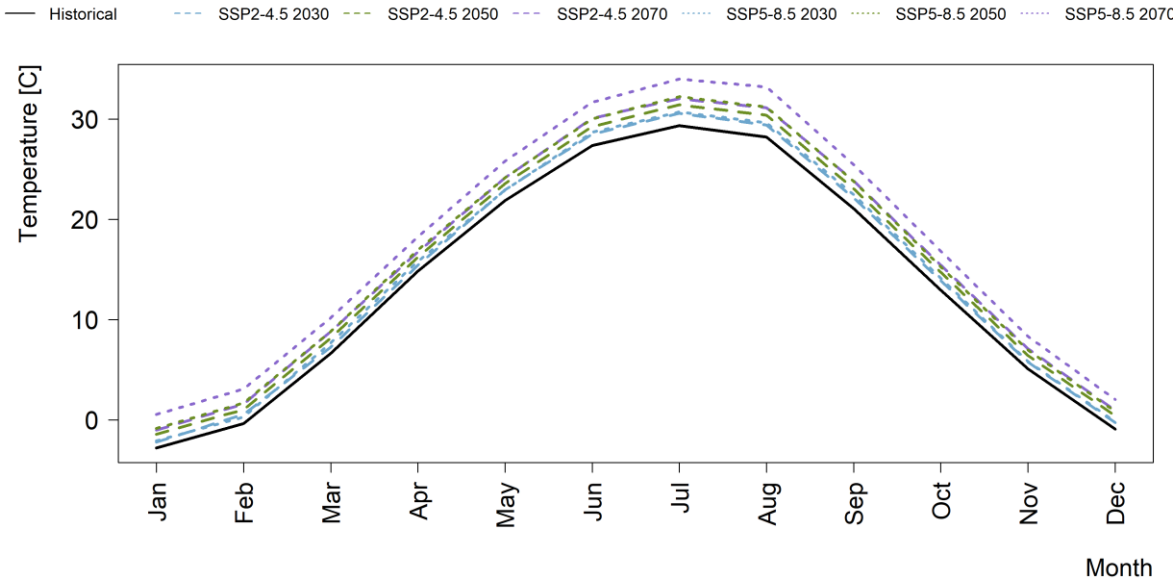

Figure A22: Average monthly temperature for historical (1995–2014) and future (time horizons under the two SSP scenarios for the box KarKho.

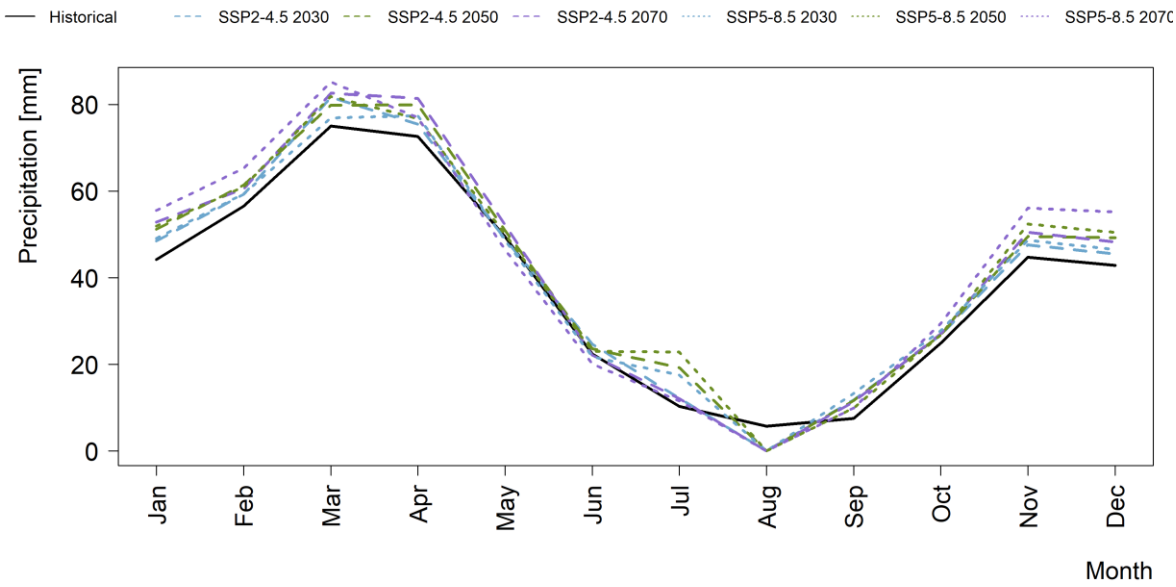

Figure A23: Average monthly precipitation for historical (1995–2014) and future (time horizons under the two SSP scenarios for the box TasSyrDhz.

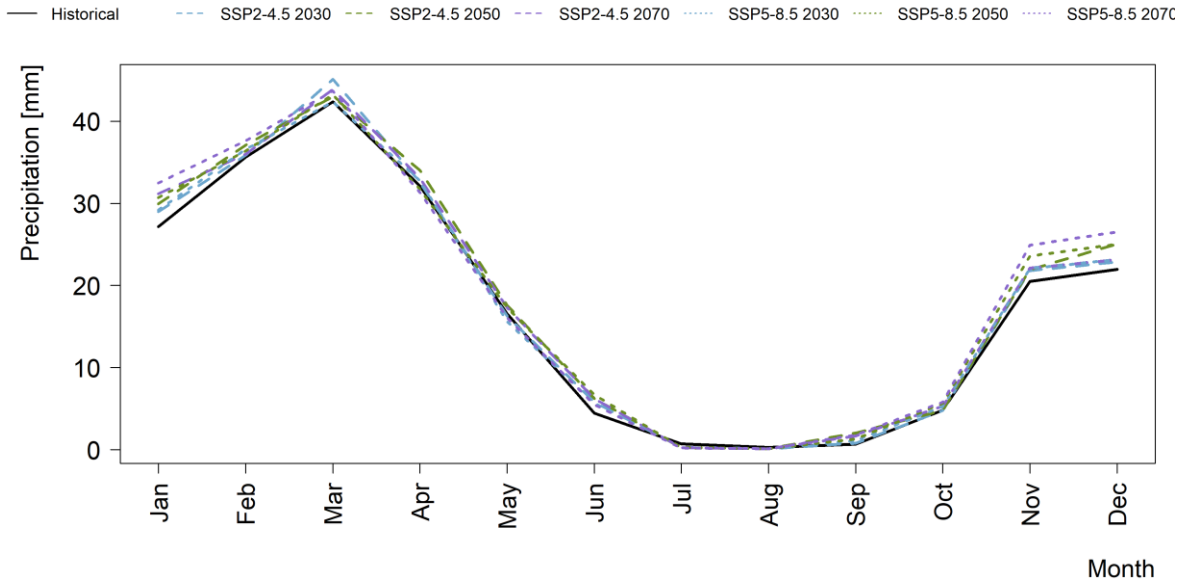

Figure A24: Average monthly precipitation for historical (1995–2014) and future (time horizons under the two SSP scenarios for the box Sur.

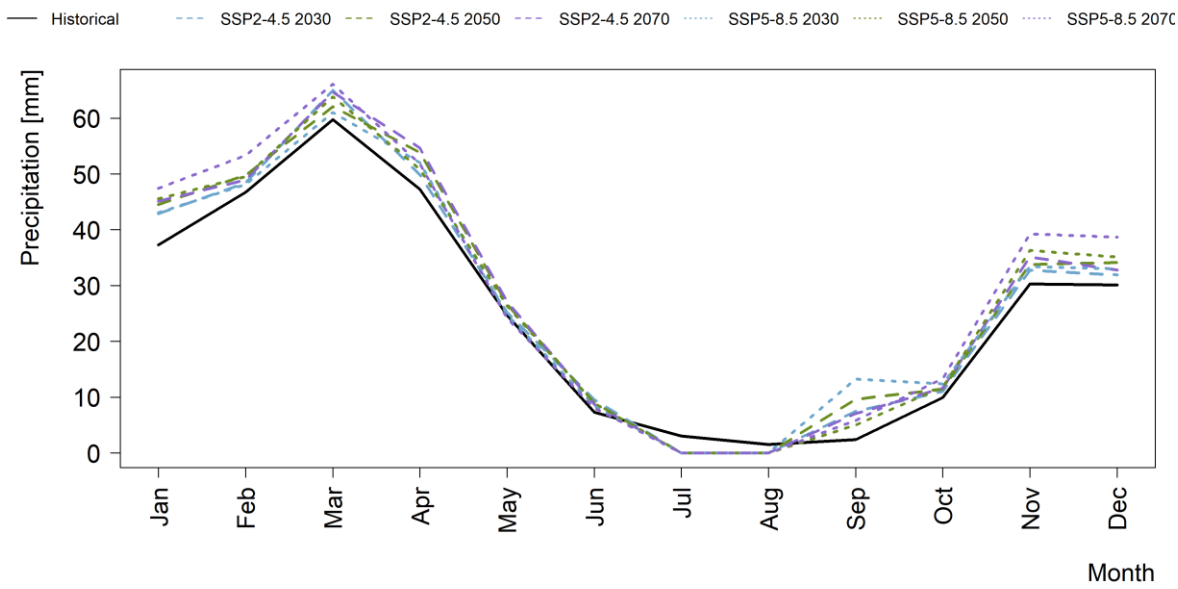

Figure A25: Average monthly precipitation for historical (1995–2014) and future (time horizons under the two SSP scenarios for the box BukSamKas.

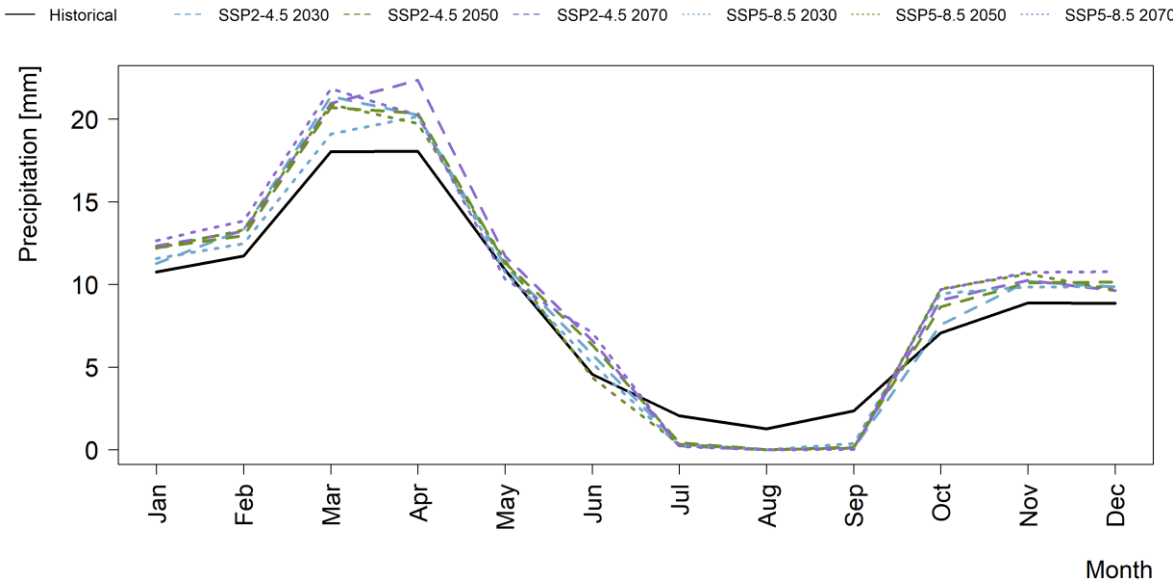

Figure A26: Average monthly precipitation for historical (1995–2014) and future (time horizons under the two SSP scenarios for the box KarKho

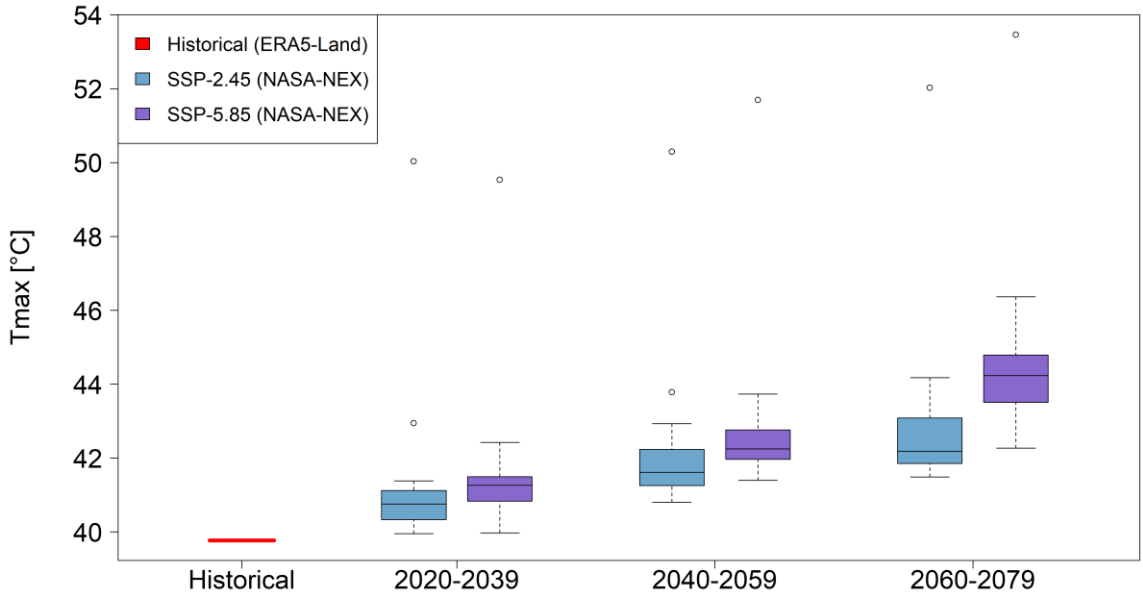

Figure A27: Boxplots indicating the spread in climate model predictions of maximum daily temperature per year (TXx) for the historical (1995–2014) and future time horizons under the two SSP scenarios for the box TasSyrDhz.

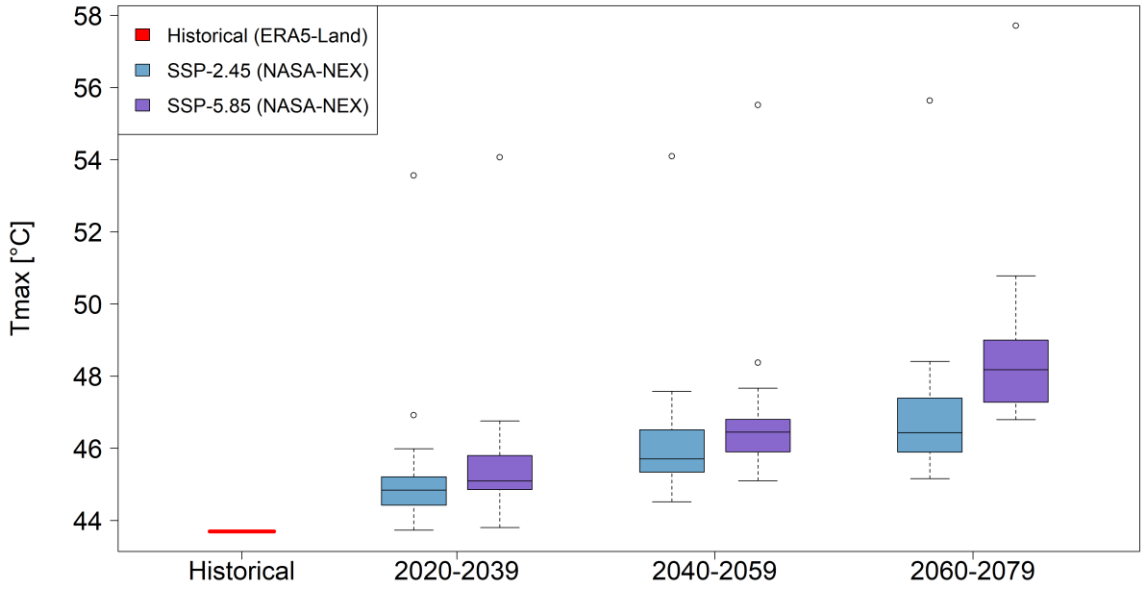

Figure A28: Boxplots indicating the spread in climate model predictions of maximum daily temperature per year (TXx) for the historical (1995–2014) and future time horizons under the two SSP scenarios for the box Sur

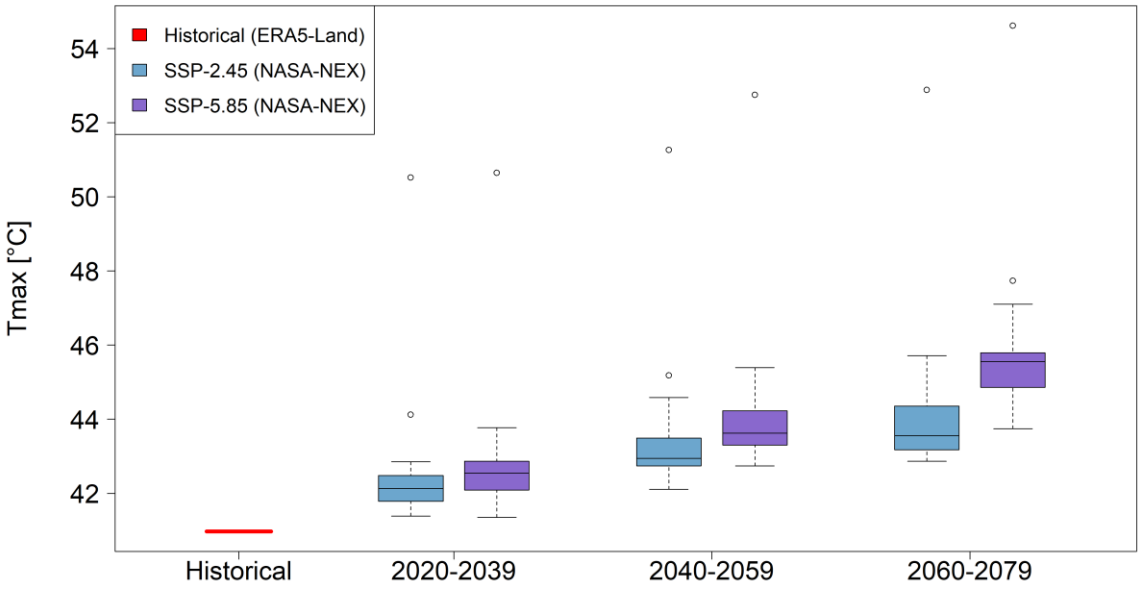

Figure A29: Boxplots indicating the spread in climate model predictions of maximum daily temperature per year (TXx) for the historical (1995–2014) and future time horizons under the two SSP scenarios for the box BukSamKas

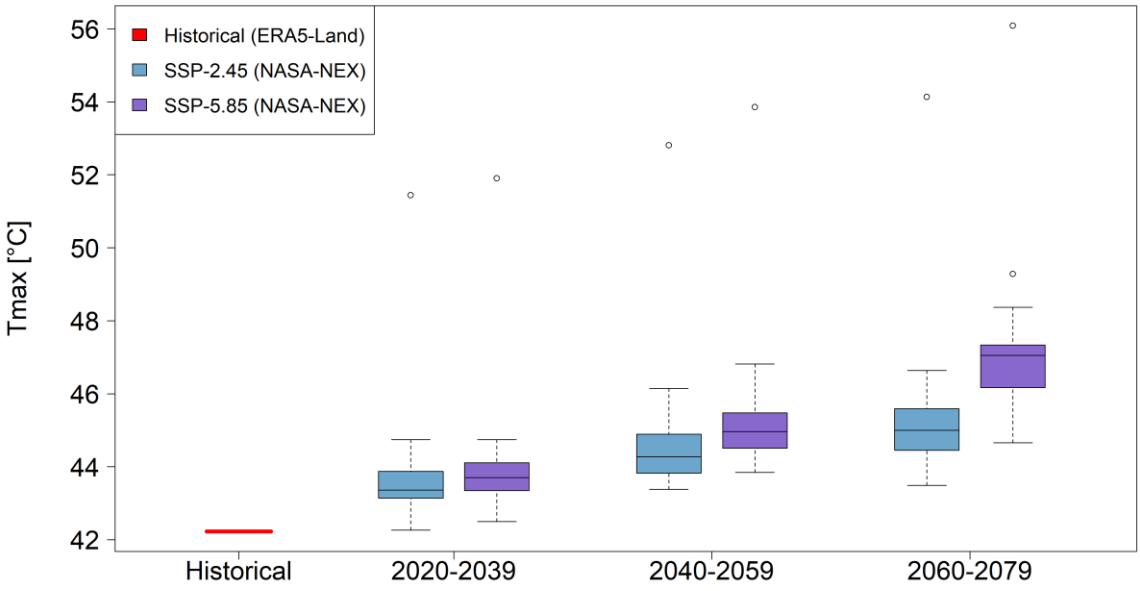

Figure A30: Boxplots indicating the spread in climate model predictions of maximum daily temperature per year (TXx) for the historical (1995–2014) and future time horizons under the two SSP scenarios for the box KarKho

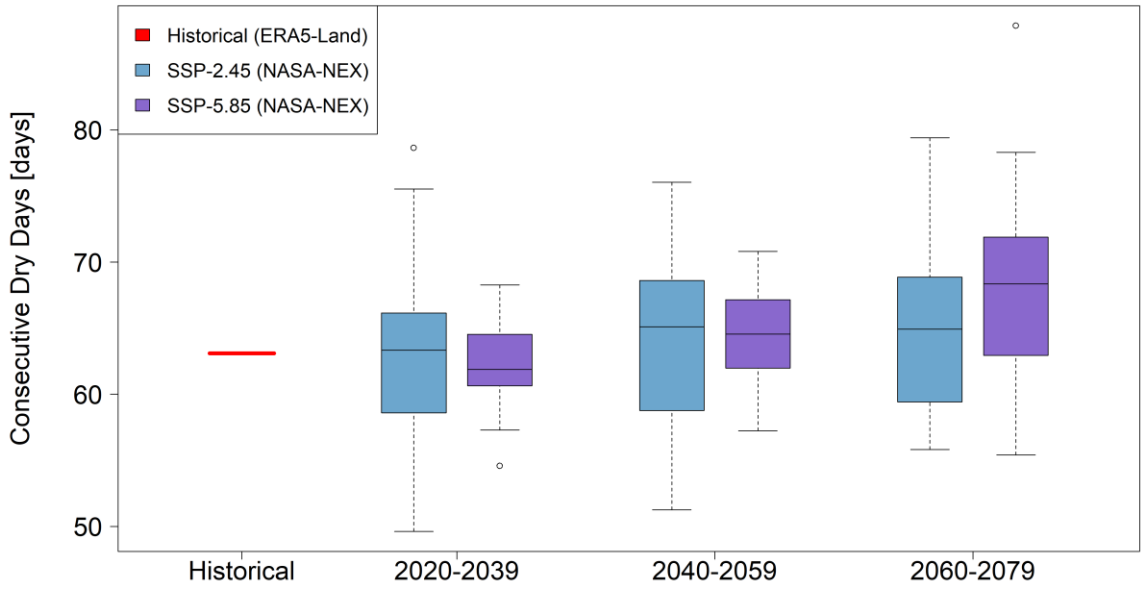

Figure A31: Boxplots indicating the spread in climate model predictions of average consecutive dry days per year (CDD) for the historical (1995–2014) and future time horizons under the two SSP scenarios for the box TasSyrDhz.

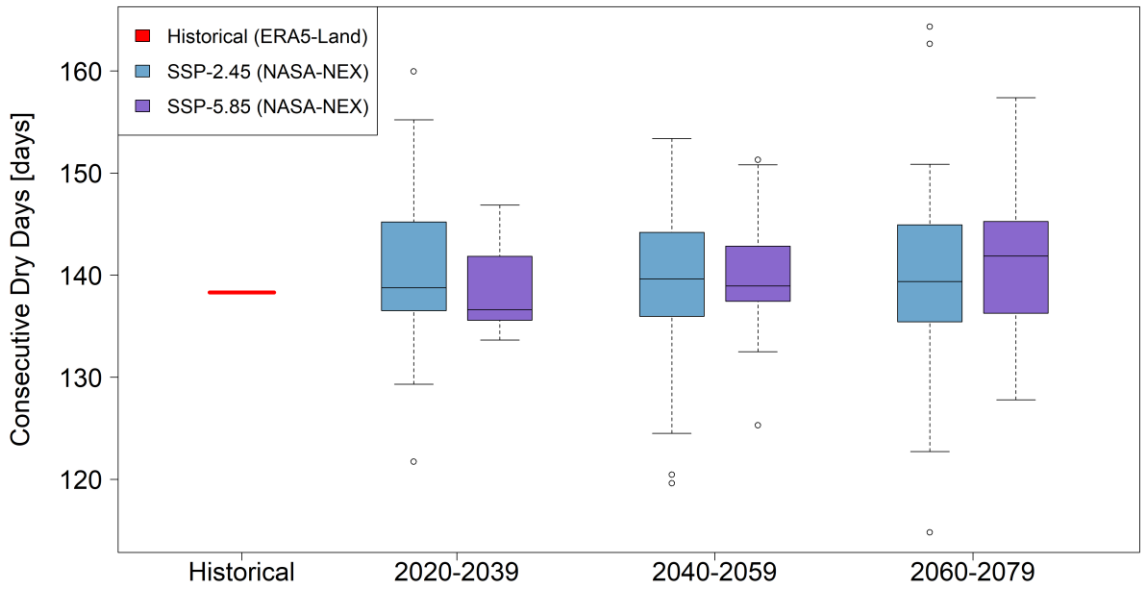

Figure A32: Boxplots indicating the spread in climate model predictions of average consecutive dry days per year (CDD) for the historical (1995–2014) and future time horizons under the two SSP scenarios for the box Sur.

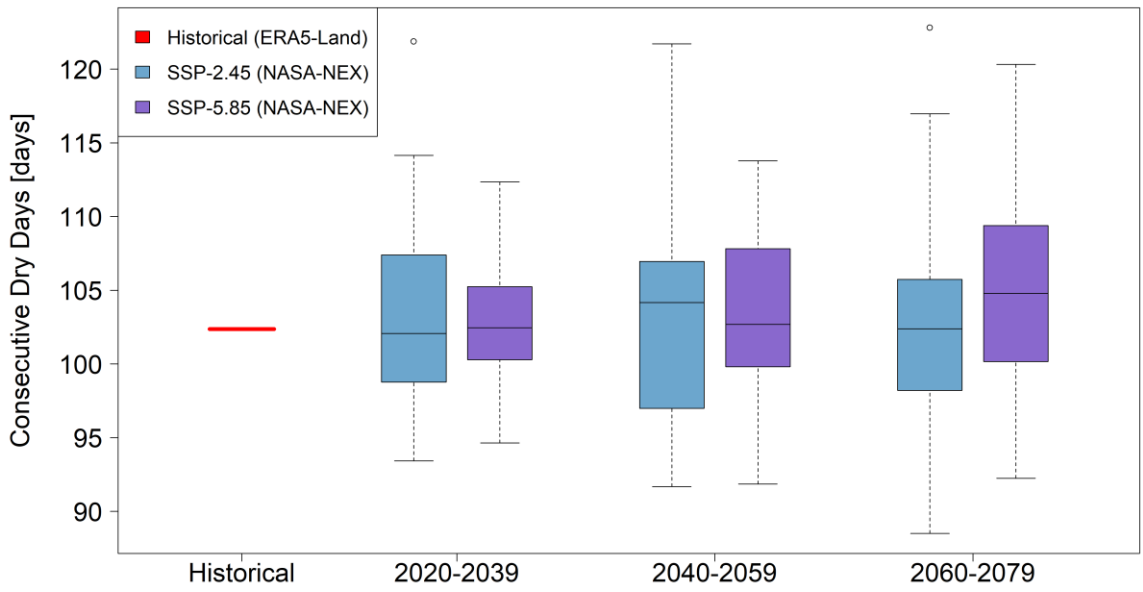

Figure A33: Boxplots indicating the spread in climate model predictions of average consecutive dry days per year (CDD) for the historical (1995–2014) and future time horizons under the two SSP scenarios for the box BukSamKas.

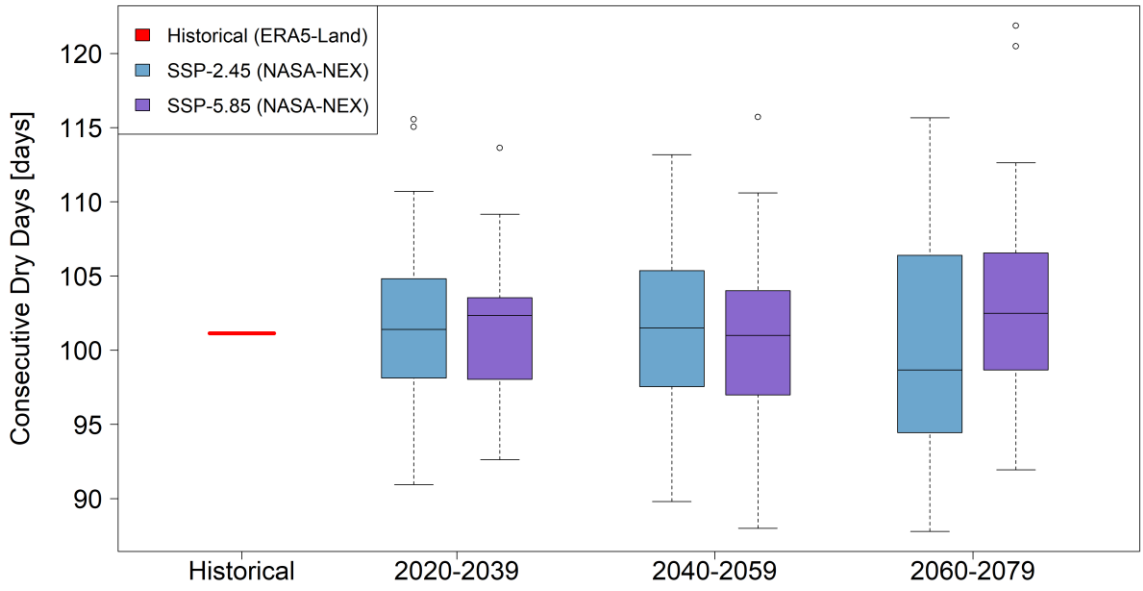

Figure A34: Boxplots indicating the spread in climate model predictions of average consecutive dry days per year (CDD) for the historical (1995–2014) and future time horizons under the two SSP scenarios for the box KarKho.

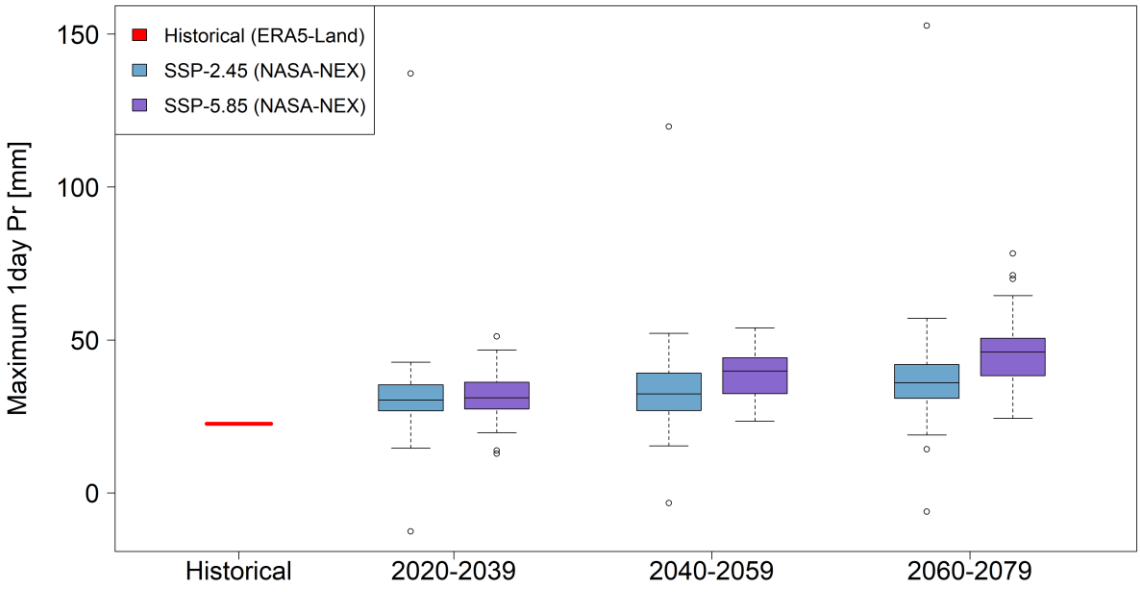

Figure A35: Boxplots indicating the spread in climate model predictions of yearly maximum 1-day precipitation sum (Rx1day, in mm/day) for the historical and future time periods under two SSP scenarios for the box TasSyrDhz.

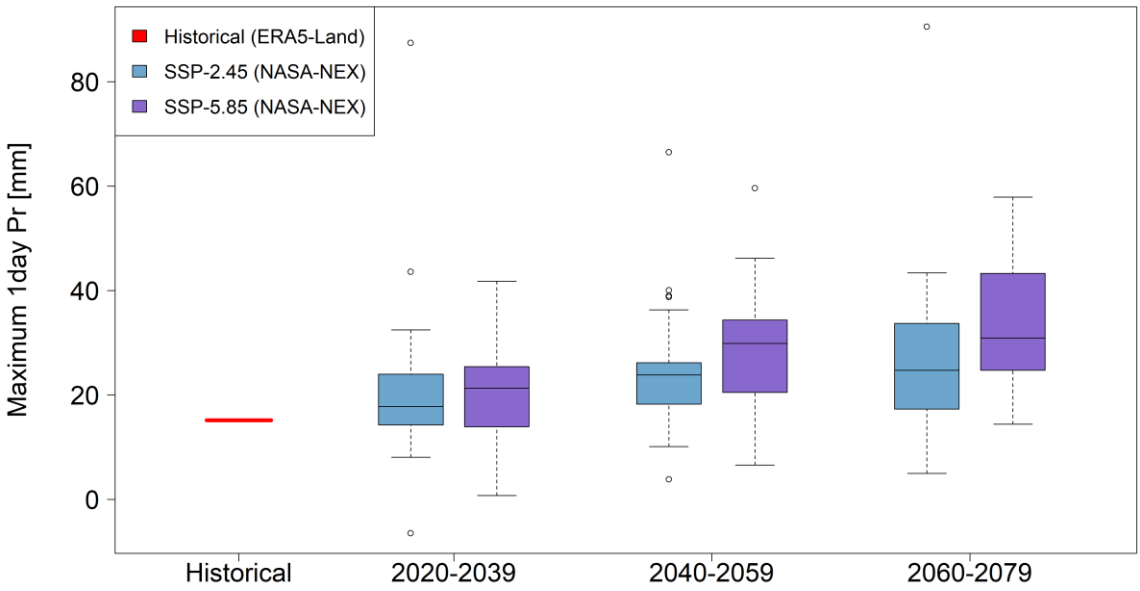

Figure A36: Boxplots indicating the spread in climate model predictions of yearly maximum 1-day precipitation sum (Rx1day, in mm/day) for the historical and future time periods under two SSP scenarios for the box Sur.

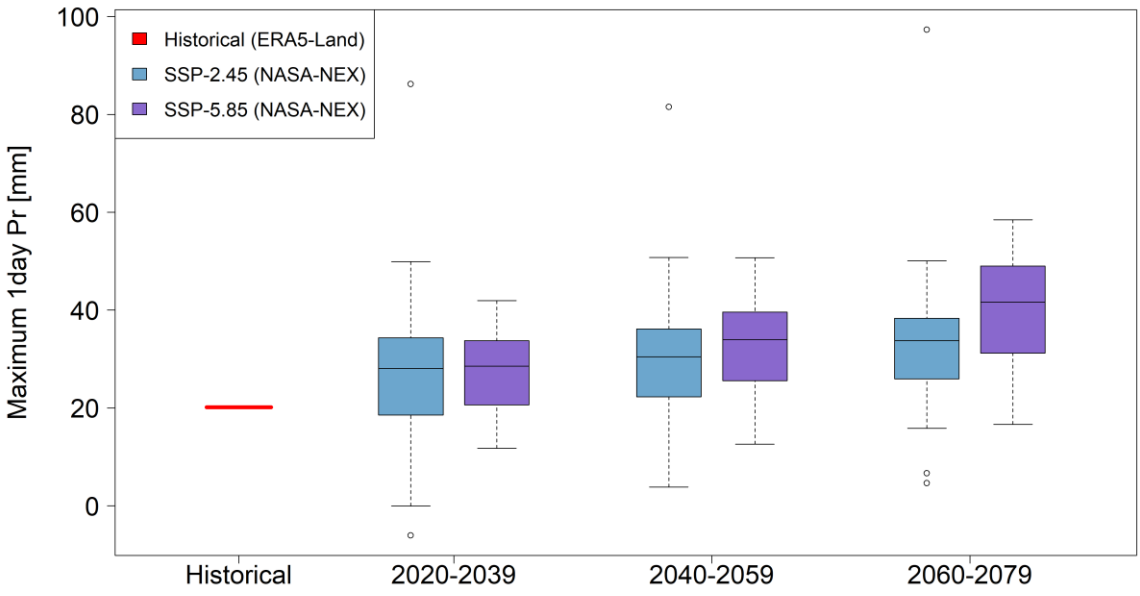

Figure A37: Boxplots indicating the spread in climate model predictions of yearly maximum 1-day precipitation sum (Rx1day, in mm/day) for the historical and future time periods under two SSP scenarios for the box BukSamKas.

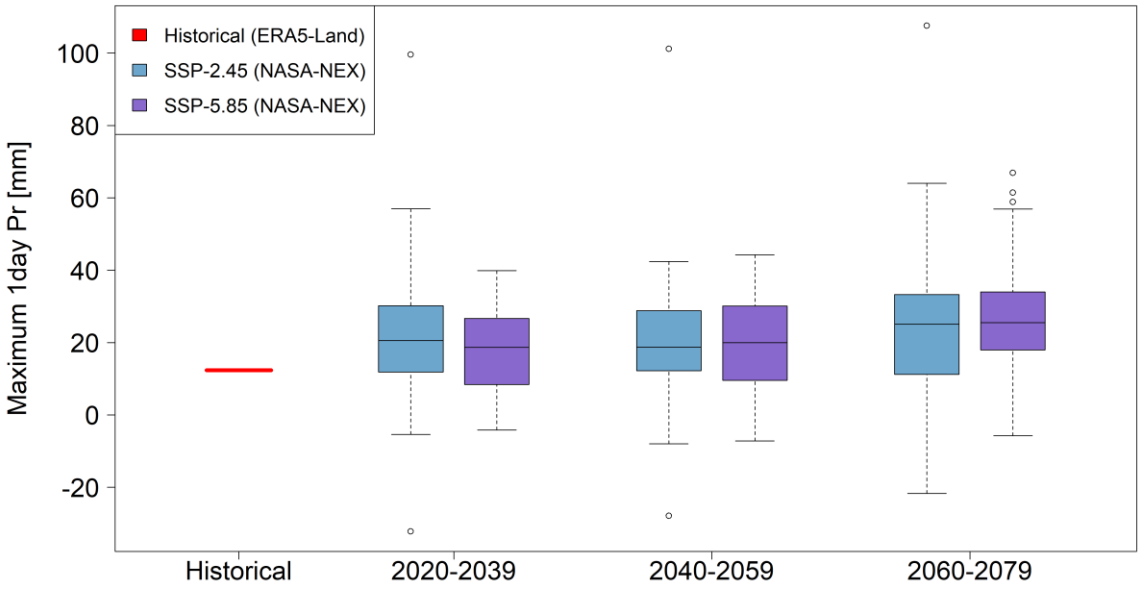

Figure A38: Boxplots indicating the spread in climate model predictions of yearly maximum 1-day precipitation sum (Rx1day, in mm/day) for the historical and future time periods under two SSP scenarios for the box KarKho.

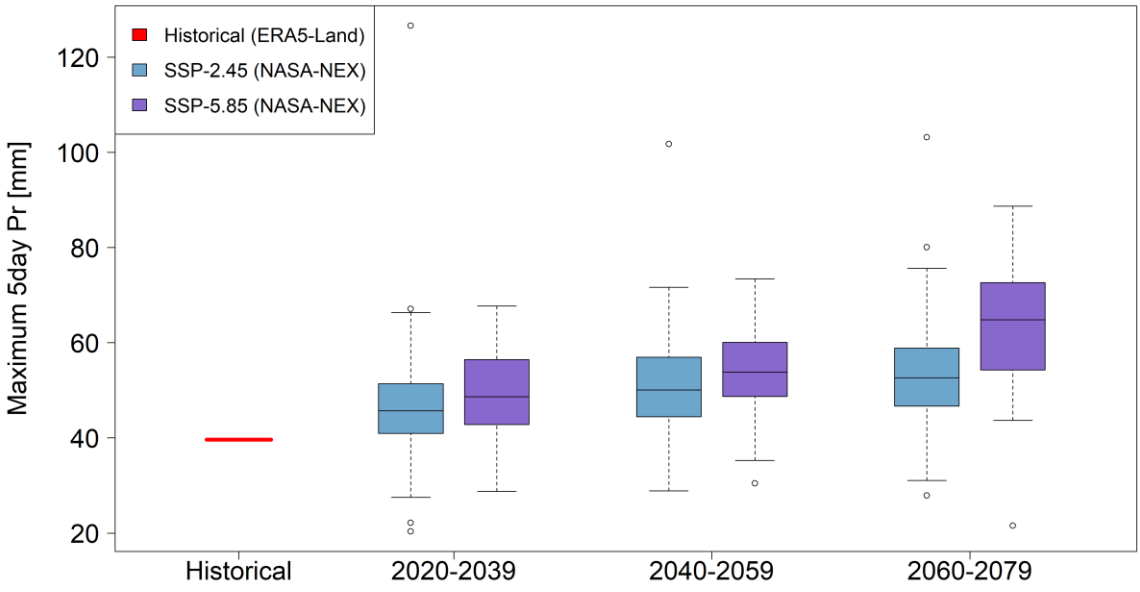

Figure A39: Boxplots indicating the spread in climate model predictions of yearly maximum 5-day precipitation sum (Rx5day, in mm/day) for the historical and future time periods under two SSP scenarios for the box TasSyrDhz.

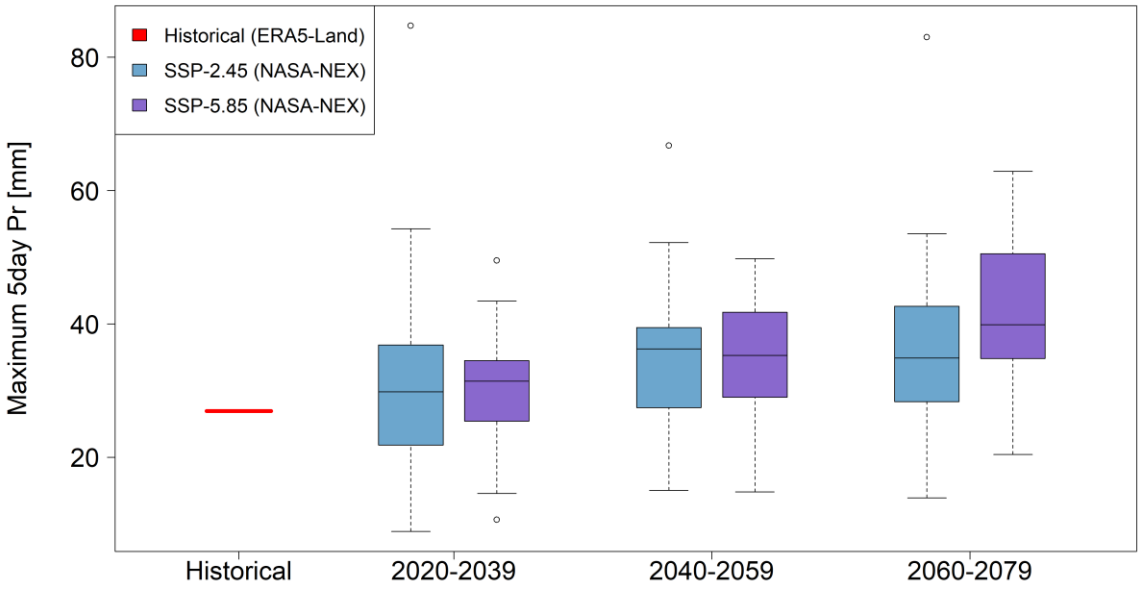

Figure A40: Boxplots indicating the spread in climate model predictions of yearly maximum 5-day precipitation sum (Rx5day, in mm/day) for the historical and future time periods under two SSP scenarios for the box Sur.

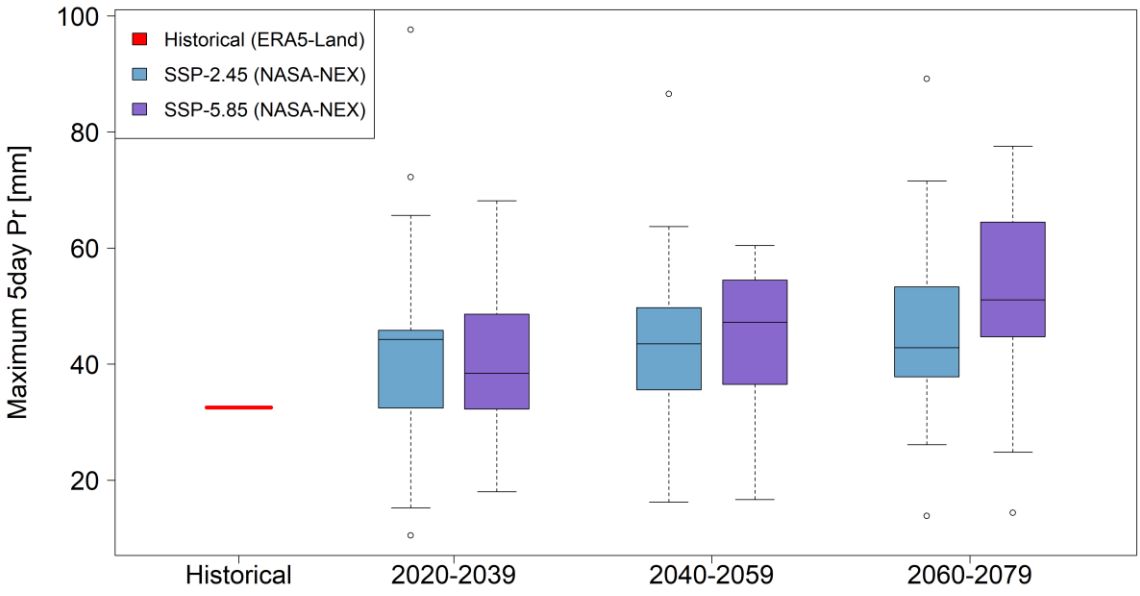

Figure A41: **Boxplots indicating the spread in climate model predictions of yearly maximum 5-day precipitation sum (Rx5day, in mm/day) for the historical and future time periods under two SSP scenarios for the box BukSamKas.**

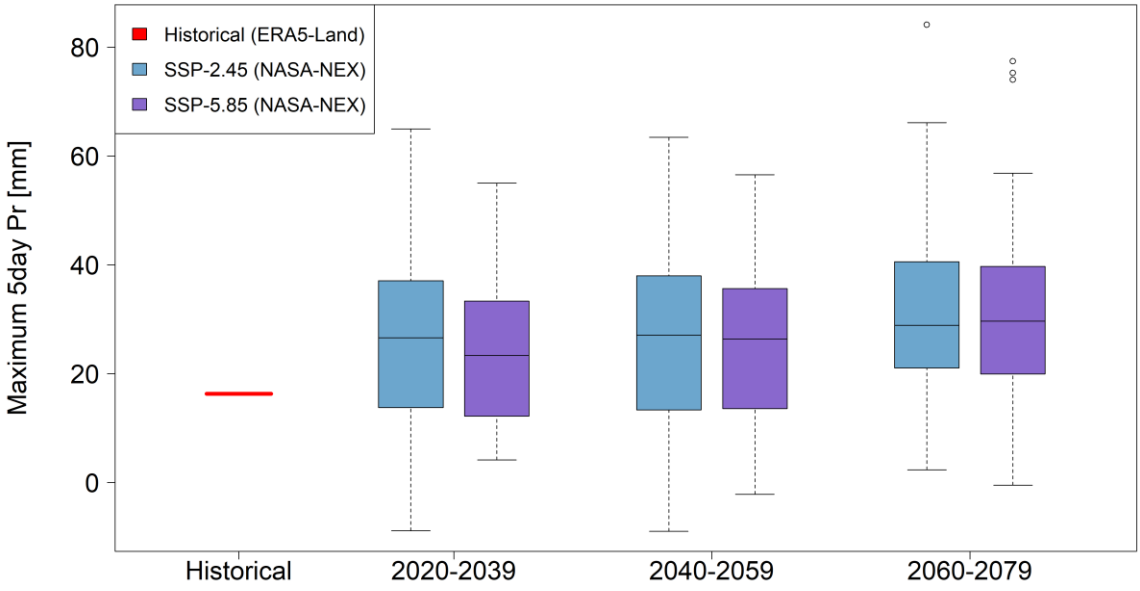

Figure A42: Boxplots indicating the spread in climate model predictions of yearly maximum 5-day precipitation sum (Rx5day, in mm/day) for the historical and future time periods under two SSP scenarios for the box KarKho.

Table A1: Summary table showing statistics regarding spread in CMIP6 ensemble predictions for future changes in annual precipitation for the box TasSyrDhz.

Scenarios	*Average (%)*	*25th Perc. (%)*	*75th Perc. (%)*	*GCMs Dryer*	*GCMs Wetter*
2030_SSP245	*5%*	*-2%*	*13%*	*10*	*24*
2050_SSP245	*9%*	*2%*	*18%*	*7*	*27*
2070_SSP245	*10%*	*4%*	*4%*	*5*	*29*
2030_SSP585	*5%*	*-2%*	*-2%*	*12*	*23*
2050_SSP585	*9%*	*0%*	*0%*	*8*	*27*
2070_SSP585	*14%*	*6%*	*22%*	*7*	*28*

Table A2: Summary table showing statistics regarding spread in CMIP6 ensemble predictions for future changes in mean temperature for the box TasSyrDhz.

Scenarios	*Average (%)*	*25th Perc. (%)*	*75th Perc. (%)*	*GCMs >2°C*	*GCMs >4°C*
2030_SSP245	*+1.0*	*+0.8*	*+1.1*	*1*	*0*
2050_SSP245	*+1.7*	*+1.5*	*+2.1*	*10*	*0*
2070_SSP245	*+2.4*	*+2.4*	*+2.4*	*24*	*24*
2030_SSP585	*+1.1*	*+1.1*	*+1.1*	*2*	*2*
2050_SSP585	*+2.4*	*+2.4*	*+2.4*	*25*	*25*
2070_SSP585	*+3.9*	*+3.9*	*+3.9*	*31*	*31*

Table A3: Summary table showing statistics regarding spread in CMIP6 ensemble predictions for future changes in annual precipitation for the box Sur.

Scenarios	*Average (%)*	*25th Perc. (%)*	*75th Perc. (%)*	*GCMs Dryer*	*GCMs Wetter*
2030_SSP245	*3%*	*-3%*	*11%*	*13*	*21*
2050_SSP245	*5%*	*-4%*	*12%*	*12*	*22*
2070_SSP245	*4%*	*-2%*	*-2%*	*10*	*24*
2030_SSP585	*2%*	*-5%*	*-5%*	*14*	*21*
2050_SSP585	*5%*	*-4%*	*-4%*	*10*	*25*
2070_SSP585	*7%*	*-6%*	*21%*	*12*	*23*

Table A4: Summary table showing statistics regarding spread in CMIP6 ensemble predictions for future changes in mean temperature for the box Sur.

Scenarios	*Average (%)*	*25th Perc. (%)*	*75th Perc. (%)*	*GCMs >2°C*	*GCMs >4°C*
2030_SSP245	*+1.0*	*+0.8*	*+1.3*	*2*	*0*
2050_SSP245	*+1.7*	*+1.5*	*+2.2*	*11*	*0*
2070_SSP245	*+2.5*	*+2.4*	*+2.4*	*23*	*23*
2030_SSP585	*+1.1*	*+1.1*	*+1.1*	*3*	*3*
2050_SSP585	*+2.4*	*+2.4*	*+2.4*	*24*	*24*
2070_SSP585	*+3.9*	*+3.9*	*+3.9*	*31*	*31*

Table A5: Summary table showing statistics regarding spread in CMIP6 ensemble predictions for future changes in annual precipitation for the box BukSamKas.

Scenarios	*Average (%)*	*25th Perc. (%)*	*75th Perc. (%)*	*GCMs Dryer*	*GCMs Wetter*
2030_SSP245	*7%*	*-3%*	*15%*	*11*	*23*
2050_SSP245	*9%*	*0%*	*20%*	*9*	*25*
2070_SSP245	*11%*	*4%*	*4%*	*6*	*28*
2030_SSP585	*6%*	*-3%*	*-3%*	*12*	*23*
2050_SSP585	*10%*	*-2%*	*-2%*	*10*	*25*
2070_SSP585	*15%*	*1%*	*27%*	*8*	*27*

Table A6: Summary table showing statistics regarding spread in CMIP6 ensemble predictions for future changes in mean temperature for the box TasSyrDhz.

Scenarios	*Average (%)*	*25th Perc. (%)*	*75th Perc. (%)*	*GCMs >2°C*	*GCMs >4°C*
2030_SSP245	*+1.0*	*+0.8*	*+1.2*	*0*	*0*
2050_SSP245	*+1.7*	*+1.4*	*+2.1*	*9*	*0*
2070_SSP245	*+2.4*	*+2.4*	*+2.4*	*20*	*20*
2030_SSP585	*+1.1*	*+1.1*	*+1.1*	*2*	*2*
2050_SSP585	*+2.3*	*+2.3*	*+2.3*	*21*	*21*
2070_SSP585	*+3.9*	*+3.8*	*+3.8*	*31*	*31*

Table A7: Summary table showing statistics regarding spread in CMIP6 ensemble predictions for future changes in annual precipitation for the box KarKho.

Scenarios	*Average (%)*	*25th Perc. (%)*	*75th Perc. (%)*	*GCMs Dryer*	*GCMs Wetter*
2030_SSP245	*9%*	*-1%*	*18%*	*9*	*25*
2050_SSP245	*11%*	*2%*	*20%*	*5*	*29*
2070_SSP245	*13%*	*6%*	*6%*	*4*	*30*
2030_SSP585	*7%*	*-1%*	*0%*	*11*	*24*
2050_SSP585	*10%*	*-1%*	*-1%*	*13*	*22*
2070_SSP585	*14%*	*4%*	*24%*	*6*	*29*

Table A8: Summary table showing statistics regarding spread in CMIP6 ensemble predictions for future changes in mean temperature for the box KarKho.

Scenarios	*Average (%)*	*25th Perc. (%)*	*75th Perc. (%)*	*GCMs >2°C*	*GCMs >4°C*
2030_SSP245	*+0.9*	*+0.8*	*+1.3*	*0*	*0*
2050_SSP245	*+1.7*	*+1.3*	*+2.2*	*9*	*0*
2070_SSP245	*+2.3*	*+2.3*	*+2.3*	*20*	*20*
2030_SSP585	*+1.1*	*+1.0*	*+1.0*	*1*	*1*
2050_SSP585	*+2.3*	*+2.3*	*+2.3*	*21*	*21*
2070_SSP585	*+3.8*	*+3.8*	*+3.8*	*31*	*31*

Appendix B: Detailed task and deliverables

The Specialist's tasks are expected to include but not be limited to:

1. Prepare Climate Risk and Adaptation assessment (CRA) and summarize it's results in the Climate Change Assessment (CCA). CCA preparation shall follow ADB guidance note on Climate Change Assessments.
2. Analyze climate model projections for the regions of interest.
3. Leading the detailed climate risk and adaptation assessment. The study is expected to assess the change and variability of key climate related parameters over the project lifetime to be used as inputs to the feasibility study among others.
4. Identify the uncertainties associated with the projections and provide guidance on how the results should be interpreted.
5. Review the existing meteorological monitoring network and propose additional weather stations and associated capacity requirements for proper monitoring and surveillance in the project areas.
6. Prepare GHG emissions reductions calculation.
7. Identify climate adaptation activities, calculate adaptation cost and provide justification for the climate financing.
8. Update Paris Agreement Alignment Assessment following Guidance Note on Implementing Operations' Alignment with the Paris Agreement at ADB

Deliverables:

a) Climate Risk and Adaptation assessment report
b) Climate Change Assessment Linked Document [using ADB Board Template]
c) Updated Paris Agreement Alignment Assessment [using ADB template]